Spatial and Temporal Population Genetics of Swiss Red Foxes (*Vulpes vulpes*) Following a Rabies Epizootic.

Peter Wandeler

Thesis is submitted for the degree of Doctor of Philosophy

Institute of Zoology
Zoological Society of London

Biodiversity and Ecological Process Research Group
School of Biosciences
Cardiff University

December 2004

ProQuest LLC
789 East Eisenhower Parkway
P.O. Box 1346
Ann Arbor, MI 48106-1346

SUMMARY

Infectious disease can affect the demography of natural populations and, as a consequence, can alter the genetic variation within and between those populations. This study investigated long-term effects of rabies-induced mortality on the demography and genetic variation in two Swiss red fox populations over ten to fourteen generations. In Switzerland, the last rabies epizootic persisted from 1967 to 1999 and was continuously monitored by collecting fox carcasses throughout the country. Alongside records of rabies tests and post-mortem data, tooth samples were systematically archived for ageing. In this study, DNA from 666 individual teeth was extracted. For 279 extracts, the concentration of nuclear DNA was estimated in a quantitative PCR and found to be negatively correlated with storage time. After excluding samples with insufficient DNA concentration for reliable genotyping, 382 samples were screened using between nine and seventeen canine and red fox specific microsatellites. Tooth samples were combined with 189 modern tissue samples. By assessing the age structure continuously throughout and after the rabies epizootic for the first population, population census size and age structure were found to be altered by the high rabies-induced mortality. In contrast, no long-term trends in genetic diversity were identified although a high variation of H_O, H_E, F_{IS} was discovered both in short-term and longer-term. A strong isolation-by-distance pattern was revealed for the second population by comparing individual pairwise genetic with spatial distances using modern samples. Furthermore, genetic data demonstrated that dispersal was sex-biased and diverted by the topography of the landscape. When investigating isolation-by-distance patterns within the same population in 1971-73 and 1982-84 at lower population densities, density-dependant dispersal was observed. In conclusion, this study revealed no loss of genetic diversity in red foxes following a rabies epizootic despite a population bottleneck, yet highlights population density as an important factor to determine local spatial genetic structure.

ACKNOWLEDGEMENTS

There are many people who have provided invaluable support on both a professional and a personal level and without whom this project would not have been possible.

First and foremost, I wish to thank Ruedi Wolf who, in spring 1999, drew my attention to some old card-boxes stacked with red fox tooth samples in the cellar of the Institute of Veterinary Virology, Bern. At this time, neither of us realised that less than two years later I would embark on an entire PhD project with these samples.

I would like to thank the past and present staff of the Swiss Rabies Centre, Reto Zanoni and Uli Mueller, but in particular Alexander Wandeler and Andreas Kappeler, who initiated, but more importantly, continued the systematic collection of these tooth samples a long time ago. A special thank goes to Matthias Ulrich for ageing a considerable number of teeth, and to Marcel Güntert, Christoph Meier, Peter Lüps and Beatrice Lüscher from the Natural History Museum in Bern, for logistic, methodological and mental support. I would also like to thank Mr Rudin from the Forensic Institute in Bern for introducing me into the technique of DNA extraction from hard tissues, and Mr Oetliker from the Technical Institute of the Kocher Institute, Bern, for manufacturing six simply undestroyable steel mortars.

Working for more than three years at the Institute of Zoology in London was, apart from some frenzy days of teeth smashing, PCR and fragment analyses, a wonderful experience. Listing all the people who directly contributed to this study or simply made life at the IOZ special to me would be too far-reaching. Nonetheless, I would like to mention and thank the following people: Sonia and Dada for always looking after me, and Oliver, Simon and Lizzie for peacefully sharing such a tiny office. Daisy, who by now would have got her own PhD and who I remember very fondly. I thank Seirian, Katrien and Kate for significantly improving the writing of this thesis, and Zjef, Christine and Helmut for their wonderful friendship. Much gratitude further goes to Bill, Simon and Mat,. but in particular to Jingliang for discussing and improving

some analyses of this study. Finally, I thank Richard for his statistical support of this study.

I am especially grateful to Steve Smith and Phil Morin from the Max Plank Institute of Evolutionary Anthropology, Leipzig whose support and generosity improved this study substantially. I further wish to thank Fridolin Zimmermann for his competent GIS computing and Gaby Obexer for saving hundreds of laboratory hours by drawing my attention to a magical PCR multiplex mix. Furthermore, I like to thank Lukas Keller and his group from the Zoological Museum in Zurich for their patience and support.

Although I could already depend upon a huge collection of historic tooth samples when I started this project, modern red fox samples were still needed. These were kindly provided by Peter Voser, Georg Brosi, Hannes Jenny and Georg Gerig from the hunting Authorities of the Canton Aargau, Grisons and Uri. I further would like to acknowledge Peter Deplazes and Daniel Hegglin from the Institute of Parasitology, Zürich for sharing their red fox samples.

I am very grateful to the Swiss Federal Offices for Education and Science, the Swiss Agency for the Environment, Forests and Landscape and Federal Veterinary Office of Switzerland for financial support of this project.

I would like to say special thanks to all of my three supervisors: Urs Breitenmoser from the Institute of Veterinary Virology, University of Bern for his encouragement since the very early days of this project but in particular for his trust. Mike Bruford from the Biodiversity and Ecological Process Research Group, Cardiff University for his supervision and valuable help throughout the course of this project. But especially I wish to thank Stephan Funk from the Institute of Zoology who had to deal with my questions, problems, but also with my ups and downs and my impatience on a daily bases. His support and his scientific enthusiasm were invaluable for this project.

Finally I am very grateful to my family and Leslie for all their support and love.

CONTENTS

GENERAL INTRODUCTION

The red fox is one of the best-studied wild carnivores worldwide. A large variety of literature describes the red fox's ecology and behaviour from the discovery of its occurrence in urban habitat (Teagle 1967) to its threat to native species in Australia (Dickman *et al.* 1993). Most research on the red fox, however, has considered its role as a potential carrier and vector for disease, particularly rabies. The impact of the last rabies epizootic on the abundance of red fox populations in Europe has been documented in several countries and, dependent on the initial density, was reported to reduce populations substantially (Macdonald 1980; Macdonald & Voigts 1985). To date, rabies has been eradicated in all Western European countries (*reviewed in* Vitasek 2004). Nonetheless, the potential of re-infection is high (Chautan *et al.* 2000) because most populations recovered from the rabies-induced mortality and have even reached higher densities than prior the epizootic. Furthermore, rabies has remained widespread in Eastern Europe (Vitasek 2004).

Rabies epidemiology is tightly associated with the social structure, population dynamics and ecology of the red fox (Steck & Wandeler 1980, Macdonald 1980). Fox dispersal is considered an important cause of the spread of rabies (*e.g.* Wandeler *et al.* 1974). Several studies have been carried out to describe fox density and social organization and with these findings obtained, models on fox contact rate and its implication for rabies control have been developed (*e.g.* Trewhella & Harris 1988, White *et al.* 1995). Infected foxes change their behaviour shortly after infection (Steck & Wandeler 1980, Artois *et al.* 1990). They become more active during daylight and lose their territoriality. By entering into neighbouring territories the disease can therefore be rapidly transmitted throughout the population (Artois *et al.* 1990). In general, the dynamics of rabies is a function of the density of foxes – or of the carrying capacity of the habitat type – and of their ability to disperse (Steck & Wandeler 1980, Macdonald 1980, Funk 1994). As a consequence, dispersal distances and directions have been the subject of several field (*reviewed in* Chautan *et al.* 2000) and simulation studies (*e.g.* Artois *et al.* 1997, Tischendorf *et al.* 1998). Dispersal in red foxes is thought to be male biased and negatively correlated with population density (Trewhella *et al.* 1988). Despite the importance of dispersal for the spread of rabies, so

far, no study has yet applied population genetic methods to improve knowledge of the rabies epizootiology in red foxes.

In a more general context, dispersal is central to our understanding of the ecology and evolution of species on a population and individual level (Clobert *et al.* 2001). Nonetheless gaining direct information about dispersal in the field is difficult (Koenig *et al.* 1996). As a consequence, population genetic methods based on Wright's *F*-statistics and neutral genetic markers have been widely used to infer the rate of migration between populations (Neigel 2002). However, these estimates of migration often reflect past rather than current levels of gene flow (Rousset 2001). Recently, Rousset (2000) developed a method to infer dispersal pattern on an individual level assuming isolation-by-distance (*IBD*, Wright 1943, 1946). By estimating dispersal at a local scale, this method is less sensitive to temporal and spatial heterogeneity (Leblois *et al.* 2004).

Infectious disease can threaten small and endangered populations by making them more vulnerable to stochastic factors and, as a consequence, reducing their viability (May 1988, Woodroffe 1999). In this context, disease might have a serious impact on the genetic structure of populations (O'Brien & Evermann 1988) by reducing the population size significantly (*i.e.* demographic bottleneck). The consequence of lower genetic variability can limit the adaptive potential of a population and increase the rate of inbreeding (*e.g.* Lande 1988). Despite the importance of infectious diseases in conservation, little is known about its potential influence on the genetic structure of natural population. Furthermore, our understanding of mechanics, dynamics and persistence of disease in natural systems remains poor (Funk *et al.* 2001).

Recent advances in molecular methods have revealed genetic information of historic samples by applying mitochondrial (Pichler & Baker 2000, Consuegra *et al.* 2002, Hadly *et al.* 2004) and nuclear genetic markers (*e.g.* Bouzat *et al.* 1998, Groombridge *et al.* 2000). Comparing the genetic structure of historic and recent samples not only permits an assessment of the level of genetic diversity for a given time period, but can also provide and estimate for the rate at which genetic diversity changes (Pichler &

Baker 2000). Furthermore, temporal changes in allele frequencies facilitate estimating variance effective population size (*e.g.* Berthier *et al.* 2002) and population growth or decline (Beaumont 2003). Nonetheless, as DNA degrades over time (*reviewed in* Lindahl 1993), it is difficult to gain reliable genotype data from historic samples. In addition, sample size and sampling information of museum collections are often limited (Nielsen *et al.* 1999a). So far, only a few studies (*e.g.* Queney *et al.* 2000) have estimated the impact of an infections disease on the genetic structure in natural populations. Finally, little is known about how changes in population size might affect the spatial genetic structure within and between populations over time.

The main objective of my thesis was to assess the population genetic structure within two red fox populations following a rabies epizootic. Red foxes are substantially hunted, providing easy access for post-mortem analyses and tissue for population genetic studies. The convenience of the latter is further facilitated by the red fox's relatedness to the domestic dog. Indirectly, this guarantees access to a large set of potential genetic markers (from the dog genome project). In Switzerland, monitoring of red foxes is unique since hunting statistics have been recorded since the early 20th century. Following the arrival of rabies in 1967, a long-term collection of foxes throughout Switzerland has been carried out to observe the ongoing rabies epizootic (Zanoni *et al.* 2000). As a result, a large number of historical tooth samples, individual rabies virus tests and post-mortem data have been continuously collected over 35 years. Using these canine teeth as a source for DNA and accurate ageing, it was possible to reconstruct past genetic and demographic population structure.

This thesis is subdivided into four independent chapters followed by a combined list of references. Contents and format of each chapter are expected to represent one scientific publication. The general aims and a brief summary for the four chapters are the following:

The objective of the first two chapters was to gain information on the quantity and quality of extracted DNA from historic tooth samples and subsequently to assess their feasibility for reliable genotyping. Moreover, patterns of DNA decay were investigated

by estimating the amount of nuclear DNA for samples collected continuously over 35 years. Methodological solutions were explored to facilitate consistent and efficient genotyping. The first chapter has already been published (Wandeler *et. al.* 2003a).

In the third chapter, the primary objective was to test for *IBD* within a continuous red fox population. Topographic effects on dispersal were inferred by comparing pairwise genetic with spatial distances in an *IBD* context. For this purpose, pairwise spatial distances between individuals were computed using a Geographic Information System (*GIS*). Based on the slope of the regression between relatedness and spatial distance, an estimate of average dispersal distance was inferred and compared with demographic data from the literature. In addition, sex-specific dispersal patterns were examined.

In chapter four, the effect of rabies-induced mortality was assessed for age structure, sex-ratio and genetic diversity of a local red fox population. Analyses were based on post-mortem data and historic and recent tooth samples, collected before, during and after a rabies epizootic and covering continuously 35 years.

The primary aim of the last chapter was to assess the spatial genetic structure within an growing and continuous red fox population. Individual based *IBD* was inferred for three distinct time periods representing three different population densities. Average gene dispersal distances were estimated for each period and temporal changes in allele frequencies and genetic diversity between time periods were assessed.

CHAPTER 1

Decay of Nuclear DNA in Historic Tooth Samples: Patterns, Methodological Constraints and Solutions.

Abstract

The amount of nuclear DNA extracted from teeth of 279 individual red foxes (*Vulpes vulpes)* collected the last three decades was determined by quantitative PCR. Although teeth were autoclaved during initial collection, 73.8% of extracts contained sufficient DNA concentration (> 5pg/μL) suitable for reliable microsatellite genotyping. However the quantity of nuclear DNA significantly decreased over time in a non-linear pattern. The success of PCR amplification using four examined canine microsatellites was dependent on fragment size and storage time. By including data from two different tests for human contamination and from frequencies of allelic dropout and false alleles, the methodological constraints of population genetic studies using microsatellite loci amplified from historic DNA are discussed.

Introduction

Historic samples of species are an important source for DNA in conservation and evolutionary studies. They allow us to reveal the evolutionary history of extinct species (*e.g.* Shapiro *et al.* 2002) and to address loss of genetic variation in species with declining populations (*e.g.* Bouzat *et al.* 1998, Pichler & Baker 2000, Pertoldi *et al.* 2001). Furthermore, samples collected over several generations from different populations allow us to identify temporal dynamics of gene flow, genetic drift and selection (Nielsen *et al.* 1999a).

Nucleic acids gradually degrade over time owing to the accumulation of hydrolytic and oxidative damage (*reviewed in* Lindahl 1993). Thus one of the main problems in using ancient and historic samples for genetic studies - apart from the frequently limited number of samples and sample information available (Nielsen *et al.* 1999a) - is related to problems arising from low concentrations of DNA (Taberlet *et al.* 1996) and degraded DNA (Nielsen *et al.* 1999b). Studies using ancient DNA preferentially utilise mitochondrial DNA markers, mainly because up to 1000 more DNA copies per cell are available compared to single-copy nuclear DNA (Höss 2000). Even so, small nuclear DNA sequences can be amplified in well-preserved specimens, as demonstrated in permafrost mammoth samples from the late Pleistocene (Greenwood *et al.* 1999). In fact, individual DNA profiles from human specimens up to 3,000-year-old were assessed by simultaneous amplification of microsatellite loci (Hummel *et al.* 1999). Using these polymorphic genetic markers to genotype historic samples allows the identification of spatial and temporal genetic structure of natural populations, especially when historic and recent samples can be combined (*e.g.* Nielsen *et al.* 1999a, Bouzat *et al.* 1998, Pertoldi *et al.* 2001). However, there may be a bias in genotyping results due to genotyping errors in samples with degraded DNA or very low amounts of DNA, and consequently special precautions are needed in order to ensure the accuracy of microsatellite data (*e.g.* Navidi *et al.* 1992, Taberlet *et al.* 1996, Morin *et al.* 2001).

One error that may occur is allelic dropout, which is though to be the stochastic amplification of only one of two alleles at a heterozygote locus. Allelic dropout is mainly explained by stochastic events when pipetting very diluted DNA (Taberlet *et*

al. 1996). The clear relationship between the initial amount of template DNA and the proportion of PCRs with allelic dropout in microsatellite markers was demonstrated by Morin *et al.* (2001) by initially quantifying the amount of extracted DNA from non-invasive samples using a quantitative PCR (qPCR) assay. Furthermore, low numbers of target molecules can also lead to PCR-generated false alleles, probably corresponding to slippage during the first few cycles of amplification (Taberlet *et al.* 1996, Goossens *et al.* 1998).

Although the decay of nuclear DNA over time has been demonstrated in a number of empirical studies (*e.g.* Nielsen *et al.* 1999b, Hummel *et al.* 1999), to the best of my knowledge it has not previously been quantified. The objective of this study was to quantify amplifiable amounts of nuclear DNA extracted from samples of red fox teeth collected and stored over a period of 30 years, to test their quality in relation to storage time and to discuss methodological limitations when using this DNA as a template for microsatellite amplification.

Methods

Historic tooth samples

Since 1967, hunters and game wardens provided red fox carcasses throughout Switzerland to the Swiss Rabies Centre at the University of Bern for the surveillance of rabies. Individual data were systematically recorded on date of delivery and included sex and site of origin. Age of individuals was initially estimated as either juvenile or adult by measuring the relative width of the pulp cavity of a canine tooth by X-ray (Kappeler 1985). In order to extract the caninus tooth, the lower jaw of each carcass was removed and autoclaved with the objectives of eradication of any rabies virus and facilitation of removal of the teeth. One tooth per individual was then fixed onto strong paper by adhesive tape and X-rayed. Subsequent storage of teeth was at room temperature in laboratories or cellars until 2000, when all teeth were moved to the Natural History Museum of Bern for archiving. A portion (10mm) of the root-tip of all adult individuals was removed and subsequently aged by counting annual

cementum lines (Kappeler 1985)[1]. Under the assumption that all animals were born on the 1st April, we estimated lifespan in months. Individual storage time of teeth was calculated as the number of days between delivery to the Swiss Rabies Centre and DNA extraction date.

DNA extraction from teeth

DNA from tooth samples was extracted following a revised protocol after Yang *et al.* (1998) using a PCR purification kit (QIAquick®, Qiagen). For juveniles the whole tooth, or for adults, the tooth crown remaining after ageing was sealed in a zip-bag and frozen for 20s in liquid nitrogen. After grinding the sample in a small steel mortar, the powder was transferred into a 2mL microcentrifuge tube and 1.1 – 1.7mL of EDTA buffer (0.5M, pH 8.0) was added. The mixture was incubated under agitation at room temperature for 72h. The samples were digested twice at 56°C under agitation over-night. For the first digestion, 60µL of 10% N-sarcosyl and 540µg of proteinase K were added. For the second digestion, an additional 260µg of proteinase K was used. After centrifugation, 1mL of supernatant was transferred in a 10mL tube containing 5mL PB Buffer (Qiagen) and mixed. The remaining supernatant was stored at –70°C for future DNA extractions. DNA was bound to the QIAquick silica membrane using a vacuum manifold (QIAvac24; Qiagen) at –400mmHg. Multiple loading was avoided by transferring the total solution into a small funnel (55mm disposable funnel; CAMLAB) resting on the QIAquick column. Silica membranes were washed twice with 500µL of PE Buffer (Qiagen) and then dried by centrifugation. DNA was eluted in 100µL of 10mM Tris-Cl (pH 8.5) and diluted to a final volume of 200µL with distilled water. Before each extraction mortars and disposable equipment were decontaminated by exposure to UV-light or by thoroughly rinsing with 4% bleach.

Quantification of nuclear DNA[2]

Total amount of extracted nuclear DNA was estimated by qPCR. A 5' exonuclease assay was used, which targets an 81bp portion of the highly conserved *c-myc* proto-oncogene (Morin *et al.* 2001). The assay was performed using an ABI Prism® 7700 Sequence Detector (ABI) in 20µL PCR reactions containing 5µL of DNA extract as

[1] All tooth samples were aged by Matthias Ulrich, Bern, CH.
[2] QPCR assay was developed by Phil Morin and Steve Smith, Leipzig, G. Quantification of nuclear DNA was performed by PW and Steve Smith.

described in Smith *et al.* (2002). A triplicate set of eight standards of known DNA quantity and no-template controls were included in the assay. A single preparation of the PCR reagent mix for all DNA extracts, standards and controls was applied. Amounts of nuclear DNA per PCR sample were estimated on the basis of the standards according to Morin *et al.* (2001). The total quantity of extractable DNA per tooth was then estimated taking into account the proportion of supernatant, which was not extracted after the digestion steps.

Human contamination tests[3]

The c-myc81 assay does not target exclusively the DNA of a species of interest, but also contaminant human or other DNA, if present. Consequently, we tested all extracts for contamination using two different methods. The first method is based on differences between red fox and human target sequences in 5' exonuclease assay efficiency caused by oligonucleotide mismatches (Smith *et al.* 2002). The efficiency of the *q*PCR amplification for all extracts was attained by using a 239bp assay targeting the *c-myc* proto-oncogene and by subsequent comparison of amplification plot slopes (APS; Smith *et al.* 2002*)*. Red fox template DNA does not perfectly match the 5' exonuclease assay probe in the c-myc239 assay (three mismatches, data not shown), leaving a less efficient template for cleavage of the probe. Dilution series of known levels of human and red fox DNA (percentage of human DNA were: 100, 75, 50, 40, 25, 15, 10, 5, 2.5, 1, 0.5 and 0; a constant total DNA concentration of 6ng/µL was maintained) were analyzed to define the threshold of APS value to detect human contamination. PCR conditions were identical with c-myc81 except that the annealing temperature was reduced from 59°C to 55°C and the subsequent ramp time to 95°C was slowed to 45s.

The second test for contamination with human DNA utilized a human microsatellite (HLABC-CA2; International Histocompatibility Working Group; www.ihwg.org) of small fragment-size (between 96 – 134bp). PCR was performed in a 10µL reaction volume containing 2µL of DNA extract, 0.5mM dNTPs, 3pmol primers, 2µg BSA, 0.4U HotStarTaq (Qiagen), PCR-buffer (Qiagen) and 2mM $MgCl_2$. PCR was carried out in a GeneAmp ® PCR System 9700 (ABI) using the following cycling parameters: 10mins of initial denaturation at 95°C, followed by 50 cycles of 25s at 94°C, 30s at

[3] APS – values were computed by Steve Smith and PW.

60°C annealing temperature and 40s extension at 72°C, finished by a final extension of 12mins at 72°C. All PCR products were electrophoretically separated using an ABI Prism® 377 DNA sequencer (ABI). Allele sizes were scored against the size standard GS350 Tamra™ (ABI) using GENESCAN™ Analysis and GENOTYPER™ software.

Canine microsatellite markers

All DNA extracts were genotyped twice for four canine microsatellites (AHT-130; Holmes *et al.* 1995; CXX-466, CXX-374 and CXX 436; all Ostrander *et al.* 1995), which amplify fragment sizes ranging from 118 to 246bp in red fox. PCR was carried out in a 6μL reaction volume containing 2μL of template DNA, 0.5mM of dNTPs, 2.5pmol primers, 1.2μg of BSA, 0.3U HotStarTaq® (Qiagen), PCR PARR™ Buffer (CAMBIO) and 1.5mM $MgCl_2$. Cycling conditions and genotyping procedure were identical with HLABC-CA2 apart from locus specific annealing temperatures (AHT-130: 56°C; CXX-466, CXX-374 and CXX-436: 60°C). The number of positive amplifications in two independent PCR reactions was recorded. Two subsets of samples collected before 1974 (n = 48) and after 1994 (n = 41), respectively, were genotyped a further three times to a total of five independent PCR amplifications for loci AHT-130, CXX-466 and CXX-374. For these two subsamples, the frequency of allelic dropout and false alleles across successful PCR amplifications was calculated only for extracts with three or more positive amplifications per locus.

The DNA extraction of the teeth and the PCR preparations for the human and canine microsatellite markers were performed within a spatially isolated laboratory dedicated for samples with low-copy DNA at the Institute of Zoology in London, UK. Throughout all procedures, special care was taken to avoid cross-contamination and contamination with contemporary DNA. Replicas of the canine microsatellite amplifications for all four polymorphic loci together with the sequential number and batch number of the DNA extraction allowed to detect contamination and hence to verify the viability of individual genotypes. Extraction and genotyping was not replicated in a second laboratory because no such evidence for contamination between extracts or contamination with contemporary fox DNA was obtained (Hofreiter *et al.* 2001). QPCR assays were carried out at the Laboratories for Conservation Genetics in Leipzig, Germany.

Statistics

The statistical significance of explanatory variables in relation to the amount of the quantified nuclear DNA per tooth extract was tested using generalized linear models (GLM's; Crawley 1993). The frequency distribution of the response variable (estimate of nuclear DNA present in each sample) was skewed; however, the log transformation of the values normalised the data and allowed a Gaussian error distribution to be fitted. All relevant explanatory variables were then added to the model, and non-significant variables sequentially removed in order of lowest explanatory power until only those terms that were significant remained in the model. The deleted terms were then reintroduced into the model to confirm their non-significance.

The relationship between the probability of successful PCR amplification at each locus and the storage time of each tooth sample was analysed using logistic regression within a generalized linear mixed model (GLMM) framework.[4] This mixed modelling is used specifically to account for the non-independence of data (Goldstein 1995; Longford 1993); in this instance, the four microsatellites amplified from each tooth sample were not independent of one another. For this approach, the relationship between the four outcomes (the success score for each microsatellite) for each tooth is explicitly coded as a random effect at the lowest level, 'nested' within the second random effect, namely tooth identity code (see Goldstein 1995; Rasbash *et al.* 2000). The fixed effects are then entered as explanatory variables as described for the GLM above. The GLMs and the logistic regression models were fitted using S-PLUS 2000 (MathSoft) and MLwiN (Rasbash *et al.* 2000) was used to fit the GLMMs.

Results

DNA was extracted from 279 tooth samples (0.72 ± 0.16g) collected between 1969 and 2000. Twenty (7.12%) extractions failed to amplify in the c-myc81 assay, of which 18 were stored for more than 10,000 days. The estimated nuclear DNA concentration ranged between 0.42pg/μL and 8,747pg/μL per extract. In 22 extracts (7.88%), a concentration higher than 1,000pg/μL was calculated. 73.8% of extracts contained

[4] GLMM analyses were performed by Richard Pettifor, London, UK in the presence of PW.

sufficient DNA concentration (> 5pg/μL) in 200μL volume suitable for microsatellite genotyping (Morin *et al.* 2001).

Statistical analyses showed that storage time was a highly significant explanatory variable (Figure 1; $p < 0.0001$), alongside tooth mass and the age of the individual (juvenile or adult; Table 1). The quantified amount of DNA extracted from each tooth sample decayed non-linearly with storage time (Figure 1). The presence of human contamination also significantly explained some of the total variance in the estimated amount of DNA extracted; however, this was only true for the microsatellite based (HLABC-CA2) method, and not for the qPCR (c-myc239) based approach (Table 1).

Across the series of twelve known contamination levels, the APS values for the c-myc239 assay varied between 0.030 for 100% fox DNA to 0.124 for 100% human DNA (data not shown). Based on these results, an APS value greater than 0.045 was taken to indicate human contamination level of at least 5% because smaller levels of human contamination could not be reliably distinguished from pure fox DNA. In total, 107 samples (38.9%) failed across all 275 tested extracts. Based on the predefined threshold APS value, 109 (64.9%) of the 168 remaining extracts indicated human contamination. Human contamination was detected in 110 (40.0%) of 279 tested samples by microsatellite typing (HLABC-CA2) and a total number of 13 different human alleles were revealed. The mean number of amplified alleles across contaminated extracts was 1.423 (range 1-3). Both test revealed human contamination in 72 (25.8%) samples, whilst one or the other test indicated contamination in a further 60 (21.5%) samples.

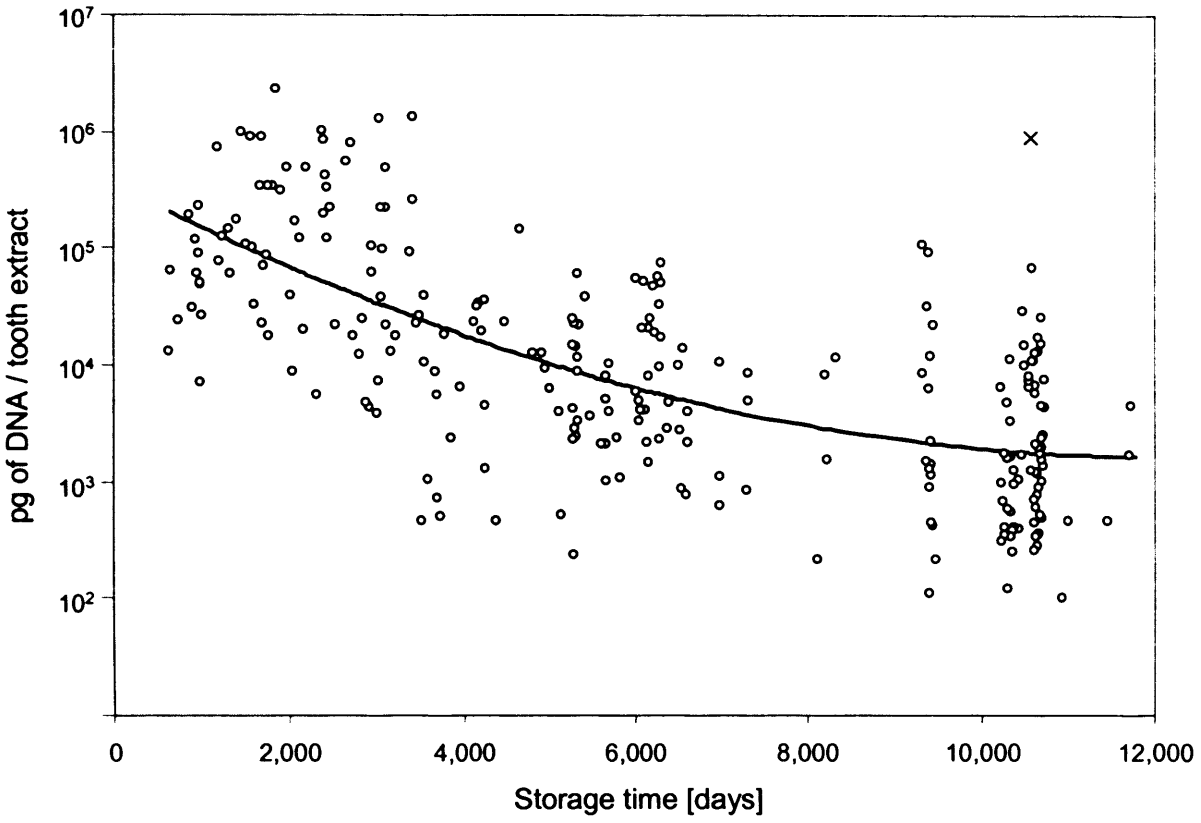

Figure 1 Relationship between the estimated quantity of nuclear DNA (c-myc81 assay) in DNA extractions from teeth versus storage time. Note that values for the estimated quantity of nuclear DNA are shown in a logarithmic scale on the y axis. The cross refers to an outlier, by excluding this sample the equation for the regression is: log(DNA quantity) = 5.550 – 3.862E^{-4} * time + 1.597E^{-8} * time^2 ; r^2 = 0.471).

Across all four loci, the probability of a positive amplification of the two independent PCR reactions declined significantly with storage time (X^2_1 = 151.7; $p < 0.001$, Figure 2). After controlling for storage time, there were also significant differences in the probabilities of amplification across the four microsatellites (X^2_3 = 155.7; $p < 0.001$). The mean observed success-rate in two independent PCR reactions were 0.56 (AHT-130), 0.54 (CXX-466), 0.39 (CXX-374) and 0.27 (CXX-436). Based on their joint confidence intervals (to account for multiple testing) there were significant differences between all pair-wise comparisons across all loci (all $p < 0.0001$), except between loci AHT-130 and CXX-466 (X^2_1 = 0.60; *ns*). Amplification performance among the four canine loci was dependent on fragment-size, as indicated by the dissimilar slopes for positive PCR and as represented by a significant interaction between time and microsatellites (X^2_3 = 33.1; $p < 0.001$, Figure 2). Whilst all four loci showed similar PCR performance in more recently collected tooth samples, the slopes of the

regressions declined at differing rates according to fragment-size (Figure 2), such that the largest microsatellites decayed more rapidly than the shorter ones.

Table 1 GLM of variables determining the estimated total quantity of nuclear DNA extracted from teeth. The estimation of nuclear DNA quantity was based on the c-myc81 assay. Shown are the results for the significant and non-significant coefficients. One outlier (see Figure 1) was excluded from the model. Overall statistic for the GLM was: $F_{5, 252} = 62.94$; $p < 0.001$; $r^2 = 0.555$.

Dependent variable	Log of pgDNA / tooth sample				
Significant coefficients	DF	t	*p*	Estimate	*SE*
(Intercept)				4.7182	0.2312
Storage time [day]	1	-7.193	<0.0001	$-4.198E^{-4}$	$5.836E^{-5}$
Tooth mass [g]	1	5.176	<0.0001	1.2776	0.2468
Storage time $[day]^2$	1	4.165	<0.0001	$1.885E^{-8}$	$4.527E^{-9}$
Human contamination (HLABC-CA2)	1	2.561	<0.02	0.1069	0.0417
Age (Juvenile or adult)	1	2.202	<0.03	0.0953	0.0433
Non-significant coefficients					
Individual age [month]	1	1.899	0.059		
Human contamination (c-myc239)	1	1.221	0.223		
Sex (female)	1	0.235	0.814		
(male)	1	0.931	0.353		

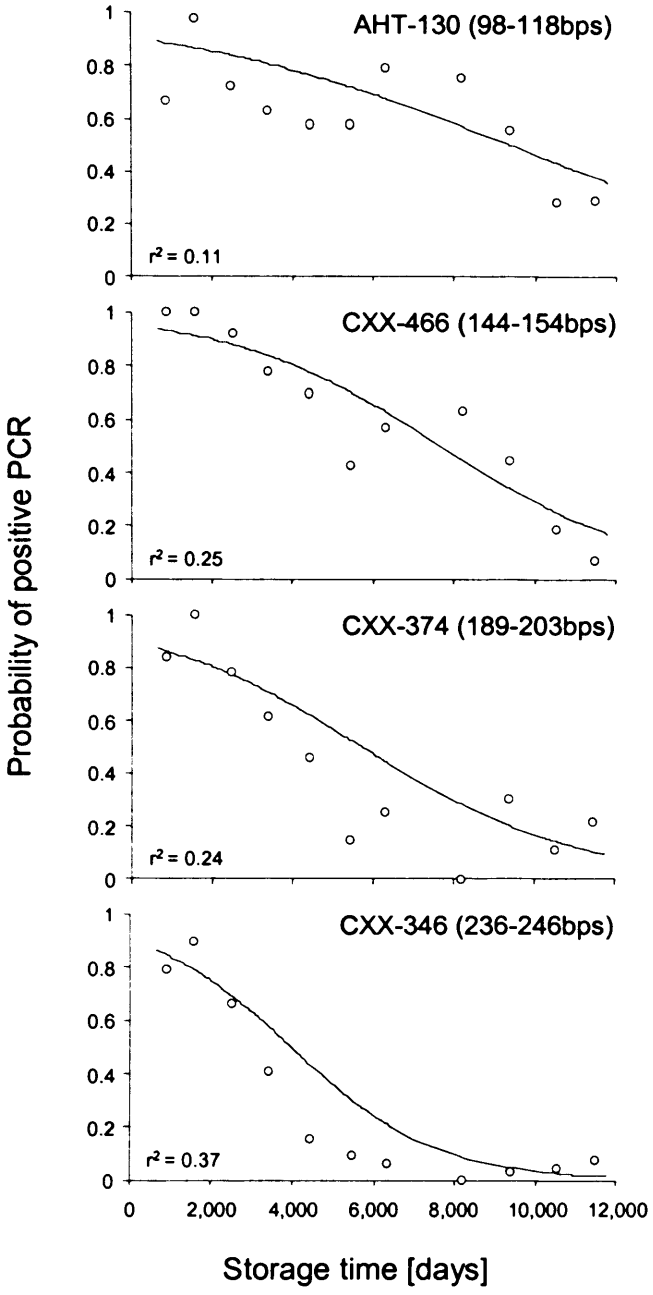

Figure 2 Probability of positive PCR amplification in four microsatellites different in fragment size versus storage time of historic tooth samples. Shown are the predicted models of the logistic regressions for each locus based on two independent PCR amplifications per loci for 257 extracts. Circles indicate categorical means for observed values.

Mean storage time ± *SD* for the two sample sets collected before 1974 and after 1994 were 1,461 ± 472 and 10,640 ± 327 days, respectively. The frequencies of allelic dropout within the subsample '>1994' compared with subsample '<1974' were consistently smaller for the three examined loci (AHT-130: 2.69% vs. 17.91%; CXX-466: 2.50% vs. 19.64% and CXX-374: 8.15% vs. 52.20%). Further the frequency of allelic dropout for both subsamples was considerably higher for the largest examined locus CXX-374 compared with AHT-130 and CXX-466 (Table 2). The frequency of false alleles ranged between 0.0% and 4.00% across the three loci and subsample (Table 2).

Table 2 Frequency of allelic dropout and false alleles of three microsatellite loci in two subsamples of teeth extractions across a total of five independent PCR amplifications with three or more successful amplification. Shown are the total number of tested (n) and successful extracts, mean of successful PCR amplifications per extract, and the percentage (total number) of allelic dropout and false alleles.

	n	Successful extracts		Allelic dropout		False alleles	
AHT-130 (98-118bps)							
< 1974	48	17	3.94	*17.91*	(12)	*2.99*	(2)
> 1994	41	41	4.53	*2.69*	(5)	*1.08*	(2)
CXX-466 (144-154bps)							
< 1974	48	13	4.30	*19.64*	(11)	*1.79*	(1)
> 1994	41	41	4.87	*2.50*	(5)	*1.00*	(2)
CXX-374 (189-203bps)							
< 1974	48	6	4.17	*52.00*	(13)	*4.00*	(2)
> 1994	41	40	4.84	*8.15*	(15)	*0.00*	(0)

Discussion

A unique set of historic tooth samples collected continuously over three decades provided the opportunity to describe and to quantify the pattern of nuclear DNA decay over time. This study indicates that historic teeth can be a good source for extracting DNA even after being autoclaved and stored at room temperature. Similar findings of the usefulness of tooth samples as a reliable source for DNA from museum samples were described *e.g.* by Pichler & Baker (2001) and Pertoldi *et al.* (2001). Nevertheless, nuclear DNA degraded rapidly in a non-linear pattern in the examined teeth and PCR amplification from older samples often failed or did not provide reliable genotyping.

It can be well assumed that the initial treatment of the samples by autoclaving caused a rapid initial decay of DNA whereas the subsequent storage in very dry conditions may have delayed further decay. DNA in dental pulp is thought to be more stable against heating, because the hard tooth tissue mitigates the effect of heating (Murakami *et al.* 2000). The higher amount of tissue within the pulp of a juvenile tooth - which is responsible for the growth of it - determined the greater amount of quantified DNA in juvenile samples. Bones and skulls from vertebrate specimens in museums are often boiled within organic or inorganic solutions to macerate and degrease for preservation (Piechocki 1979). Therefore, similar initial decay as demonstrated in this study might have taken place in other museum collections. On the other hand, even more rapid degradation over storage time may be expected under non-ideal conditions such as the absence of central heating or more fluctuating and higher humidity.

The degradation of DNA in our samples determined also the PCR success-rate over time of the four tested microsatellites differing in fragment size, which is characteristic for the amplification of degraded DNA from ancient material (Hummel *et al.* 1999). As a result of the highly diluted and degraded template DNA in the samples older than 1974, the frequency of allelic dropout and false alleles were consistently higher than in the samples from 1994 onwards. Additionally, the rate of dropout tended to be positively correlated with the fragment size of the examined loci. To address the degraded quality of nuclear DNA and the demonstrated dissimilarity of success-rate in PCR amplification of loci different in size, only short microsatellite markers with small differences in allele sizes should be chosen for studies based on historical material, as recommended by Nielsen *et al.* (1999b).

Human contamination was common in the extracts. Because no precautions were taken when the samples were collected, and when they were moved and archived, human DNA was likely to be transmitted when teeth were handled without adequate precautions (*e.g.* no gloves were used for handling). The results of the two tests for human contamination (c-myc239 and HLABC-CA2) were not identical. Because the human DNA could be expected to be highly diluted, it caused random lack of template DNA for individual PCR amplifications, leading to negative PCR reactions. This effect was more distinct in the microsatellite-based method where less template DNA per

single PCR reaction was used. A second explanation for the dissimilar results of the two tests might lie in the minimum level of human template DNA required for detection in the qPCR assay, which was probably not attained in some of the contemporary samples with a high quantity of red fox DNA. Finally, the 239bp long c-myc239 qPCR could have simply failed because the nuclear DNA was too degraded in older samples. Although the general presence of traces of human DNA does not influence the outcome of non-human species-specific genotyping, the incidence of contamination has to be addressed on an individual level when samples are pre-screened to quantify the amount of nuclear DNA for accurate genotyping (Morin *et al.* 2001).

Comparing the genetic composition of past and recent populations is a convincing approach to gain new and valuable insight in a population's interaction with its environment over time. As demonstrated in this study, nuclear DNA can rapidly decay, leaving only low copy numbers of degraded template DNA for microsatellite amplification. Moreover, the decay may reduce significantly the number of samples suitable for analysis. Since the risk of genotyping error and in particular the frequency of allelic dropout covaries with the available concentration of DNA (Morin *et al.* 2001) and with fragment size (in this study), the genetic polymorphism of older samples can be systematically underestimated. This might be the case when the number of required repetitions for accurate genotyping of homozygotes is defined by the frequencies of allelic dropout averaged over all individuals (Gagneaux *et al.* 1997). Hence, for each individual, independent replications of PCR reactions (Navidi *et al.* 1992, Taberlet *et al.* 1996, but see Valiere *et al.* 2002) are consequently needed for reliable genotyping. This multiple tubes approach (Taberlet *et al.* 1996) requires *a priori*, and without consideration of the likelihood of allelic dropout, as defined by DNA quantity, a substantial number of replicates – including failed PCR amplifications - which will limit the number of analysable loci (Morin *et al.* 2001). Quantification of DNA is extremely useful not only because it identifies those DNA extracts with increased likelihood of dropout, but also because it avoids waste of limited samples when DNA quantity is high (Morin *et al.* 2001).

CHAPTER 2

Short microsatellite DNA markers for the red fox (*Vulpes vulpes*).

Abstract

Seven short microsatellites loci (< 165bps) and species-specific primers were characterized for red foxes with the emphasis to amplify degraded DNA from historic samples. Following PCR amplification using primers developed in the domestic dog, red fox specific primers were designed within the flanking region. The number of detected alleles ranged between six and 15 alleles and the expected heterozygosities ranged between 0.67 and 0.92. No deviations from Hardy-Weinberg equilibrium were detected for any of the markers.

The red fox (*Vulpes vulpes*) is one of the best-studied wild mammals worldwide. A large variety of literature is available on red fox ecology and behaviour, it's introductions and the resulting implications for endangered species and its role as a vector of zoonotic diseases. Several studies have applied dog-specific microsatellite primers to assess the genetic structure between and within red fox populations (Baker *et al.*, 2004; Lade *et al.*, 1996; Robinson, Marks, 2001; Swanson *et al.*, 2005; Wandeler *et al.*, 2003a).

Comparing historic and recent samples allows to assess the temporal dynamics of genetic drift, gene flow and selection. However, DNA degrades over time (Lindahl, 1993) and as a consequence the success of PCR amplification in microsatellites from historic DNA is found to be higher for shorter PCR products (*e.g.* Hummel *et al.*, 1999; Nielsen *et al.*, 1999; Wandeler *et al.*, 2003b). PCR success for historic DNA samples is also reduced by the use of degenerate primers since degenerate primers have an increased likelihood of primer mismatches. Furthermore, primer mismatches can increase the potential of null-alleles. The aim of this study was to design primers that are specific for red foxes and produce short PCR products. New primers were designed in the flanking region of microsatellites amplified using primers characterized in domestic dogs (*Canis familiaris*).

Eight canine microsatellite loci (AHT-142, Holmes *et al. unpublished*; CXX-374, CXX-402, CXX-436, CXX-468, CXX-502, CXX-602, CXX-622; all Ostrander *et al.*, 1995) were selected, based on successful cross-specific amplification of red foxes (Funk, *unpublished*), and screened in three samples representing different Swiss populations. PCR was carried out in a 30 μL reaction volume consisting of 3 μL of template DNA, 0.8 μM of each dNTP, 0.5 U of *taq* polymerase and two different

$MgCl_2$ concentrations (1.5 mM and 3 mM, respectively). PCR amplification was performed in a GeneAmp® PCR System 9700 (ABI) using the following cycling parameters: 4 min of initial denaturation at 95 °C, followed by 30 cycles of 30 s at 94 °C, 30 s at two annealing temperatures (60 °C and 55 °C, respectively) and 30 s extension at 72 °C, and a final extension of 10 min. PCR products were electrophoretically separated on an agarose gel alongside size standards and visually analysed with regard to amplification intensity and size. The most unambiguous PCR products for the three individuals across the two different $MgCl_2$ concentrations and annealing temperatures were pooled for each locus and subsequently purified using a PCR purification kit (QIAquick®; Qiagen). Purified PCR products were cloned using standard TA cloning following the manufacturer's protocol (TOPO TA Cloning® kit or TA Cloning® kit; Invitrogen). Plasmids were tested for the correct insert size by ECO-R1 digestion and plasmid DNA was subsequently purified using the QIAGEN's miniprep kit (QIAprep®). Forward and reverse sequencing was performed using BigDye™ Terminator v3.0 (ABI), Better Buffer (webscientific) chemistry on a ABI Prism® 377 DNA sequencer. Sequences were aligned and edited in BIOEDIT (v.5.0.9.). Between one and six clones were sequenced for each primer pair.

Sequence data of between one and six different clones for each locus revealed microsatellite tandem repeats homologous to the domestic dog. In addition, several point mutations and deletions within the flanking regions were detected (data not shown). Finally, primers specific for red foxes were designed in PRIMER3 (Rozen, Skaletsky, 2000).

Fox-specific primers were tested in 26 foxes from Eastern Switzerland. Genomic DNA was isolated from muscle tissue using a Wizard® SV96 Genomic extraction kit (PROMEGA). Amplification was conducted in a final volume of 6 μL containing 3 μL of PCR master-mix (Qiagen's PCR multiplex kit), 0.2 μM of each primer (one of which was labelled with a fluorescent dye) and 2μL of template DNA. PCR was performed in a GeneAmp® PCR System (ABI) using the following cycling parameters: 15 min of initial denaturation at 95 °C, followed by 30 cycles of 30 s at 94 °C, 120 s at 58 C° and 60 s extension at 72 °C and a final extension of 30 min at 60 °C. Fragment analysis was performed on a ABI Prism® 377 DNA sequencer (ABI).

Fragment analysis for V142, V374, V402, V468, V502, V602 and V622 indicated consistent results across different alleles and individuals. However, allele sizes for V142 and V602 followed a mononucleotide repeat distribution, most likely caused by an inconsistent single nucleotide deletion within the flanking region. Locus V436 showed irregular positive stutter-bands for several of the scored alleles and was therefore excluded from further analyses. The number of alleles per locus, fragment size range and observed and expected heterozygosity are listed in Table 1. PCR success across all individuals and loci was 100%. Using GENEPOP v3.1 (Raymond, Rousset, 1995; probability-test), no significant deviation from Hardy-Weinberg equilibrium was detected. By combining these seven red fox specific genetic markers with eight short canine microsatellite markers (AHT-130, Holmes *et al.*, 1995; CXX-156, CXX-250, CXX-279 Ostrander *et al.*, 1993; CXX-434, CXX-466, CXX-606, CXX-608, Ostrander *et al.*, 1995; all less than 175 bps in size, Wandeler *et al.*, *unpublished*) a set of highly polymorphic genetic markers to study historic samples of red foxes is now available.

Table 1 Characterization of seven red fox (*Vulpes vulpes*) microsatellite loci based on a sample of 26 individuals.

Locus *dog*	*fox*	N_C	Repeat pattern	Primer sequence *5'→3'*	Size range *[bp]*	N_A	H_O	H_E
AHT-142	V142	3	$(TG)_{14,16,18}$	AAGCAGATCCTAGAGCAGCA CCCCACAGTTTAGAAATATCTGC	133 - 148	10	0.85	0.80
CXX-374	V374	6	$(CA)_{8-13}$	GACAGAAAGACAGAAGGCTTAG TACACACAGGAAGTAATGGGG	106 - 118	6	0.88	0.89
CXX-402	V402	3	$(TG)_{9,11,13}$	GGGTAATTCATCCAGTGCCTT TATGCAAACATGCAAACATGC	78 - 90	7	0.69	0.78
CXX-468	V468	4	$(AC)_{16-19}$	TCTCCCACCCAAATCTCTTG GCCTGTAGACTTTTTAGTCCCG	82 - 94	7	0.96	0.92
CXX-502	V502	1	$(AC)_8T(CA)_7$	ACCCAAGTGTCCTCCATAGAT TGGCCAAGTACTCTTCCACT	79 - 91	6	0.62	0.67
CXX-602	V602	5	$(CT)_{13,14,18}(CA)_{15,18,19}$	CAGCCTGGACTACAATTCTCTTT CCCCAAGTCTTTTGTCCAGA	140 - 162	15	0.88	0.77
CXX-622	V622	4	$(TG)_{17-20}$	TTTTTTGAAAAGCACACCC TGCTTTGTGTATCTTTTCTTTC	91 - 115	6	0.73	0.77

N_C, Number of different clone sequences (GenBank accession nos AXXX - AXXX)
N_A, Number of alleles; H_O, observed heterozygosity; H_E expected heterozygosity

CHAPTER 3

Inferring Dispersal in a Continuous Population of Red Foxes Using Genetic Methods.

Abstract

Dispersal is one of the most important factors in shaping the genetic structure of populations. An understanding of dispersal is consequently essential when studying the ecology, evolution and conservation of a species. Yet, gaining direct information on dispersal in natural populations is considered to be difficult. In an attempt to better understand dispersal in red foxes (*Vulpes vulpes*), individual genetic and accurate spatial data of a continuous population in the Swiss Alps (study area of 4189km^2) were combined to obtain indirect estimates of sex-bias, distances and direction of dispersal. A total of 145 tissue samples were sexed using a molecular marker (SRY) and genotyped using 17 microsatellite loci. Isolation-by-distance (*IBD*) was tested by comparing pairwise individual genetic with Euclidian spatial distances. Given the slope of the *IBD* regression and effective population size, the mean effective dispersal distance was inferred and contrasted with a demographic estimation of dispersal distance from mark-recapture studies. Sex-biased dispersal was investigated by comparing sex-specific heterozygote deficits (F_{IS} - values) and *IBD* patterns. Spatial analyses were performed in a geographic information system (*GIS*) based on an elevation model. Pairwise genetic distances between individuals were compared with a sequence of ten spatial distance matrices, which accounted increasingly for the topographic structures of the study area. Significant *IBD* and male-biased dispersal was observed. The effective dispersal distance (3,794m; 95%CI: 2,764-11,134m) inferred from genetic data was considerably smaller compared to the demographic estimate (8,925m) from the literature. The sum of fit (r^2) for the regressions between individual spatial and genetic distances increased when topographic structures were taken into account. Differences between sex-biased dispersal and the estimated genetic and demographic dispersal distance are discussed in respect to the relationship between topography and fine-scale spatial genetic structure.

Introduction

Dispersal and estimating dispersal in the field

Studying dispersal is central to our understanding of the ecology and evolution of species on an individual, population and species level (Clobert *et al.* 2001). *Natal dispersal*, or the permanent movement from an animal's birthplace to that of its first offspring (Greenwood 1980) counteracts local adaptation and genetic drift (*e.g.* Wright 1977). From an ecological viewpoint, dispersal influences the distribution pattern, the dynamics and persistence of populations and therefore affects the abundance of a species and its distribution (Dieckmann *et al.* 1999). In conservation, dispersal can be vital in maintaining gene flow between small populations by reducing the effects of inbreeding (*e.g.* Vila *et al.* 2003) and by allowing the natural re-colonization of areas in which populations have become extinct (Hanski 1998, Sumner *et al.* 2001). Moreover, dispersal and its restoration by management is vital for conservation planning for fragmented populations.

Gaining direct estimates of dispersal distances from natural populations by capture–mark–recapture is difficult (Koenig *et al.* 1996). By applying this method, direct estimates of dispersal can underestimate large-scale dispersal events systematically because the fate of dispersing animals often remains unknown (Koenig *et al.* 1996, Spong & Creel 2001). Although radio-tracking techniques might represent a good alternative approach for studying dispersal pattern (Koenig *et al.* 1996), the logistic and personal effort involved is extensive (Funk 1994, Zimmermann *et al.* unpublished data). Moreover, both methods of assessing direct dispersal distances fail to address the issue of whether successful dispersers reproduce after successful colonization (Koenig *et al.* 1996).

Population genetic methods to infer dispersal

Population genetics has long been recognized to contribute to our understanding of dispersal. Based on Wright's *F*-statistics and neutral genetic markers, indirect estimates for dispersal - by the number of migrants (*Nm*) - can be inferred (*e.g.* Neigel 1997). However, these estimations often estimate historical rather than current degrees of gene flow (Koenig *et al.* 1996, Thompson & Goodman 1996, Rousset 2001; but see Neigel 2002).

An alternative approach is to use 'assignment-tests', which estimate recent migration patterns between known populations by assigning individual genotypes to populations in which their greatest frequency is expected (*e.g.* Paetkau *et al.* 1995, Waser & Strobeck 1998). Because this approach requires a significant level of genetic differentiation among populations (Cornuet *et al.* 1999) it is less suitable when the genetic structure among populations is expected to be small. Assignment-tests rely on *a priori* defined discrete population patterns, which might not reflect population subdivision in reality (Manel *et al.* 2004). Further, these tests are less informative when potential source populations are not sampled. However, such 'cryptic population' can be theoretically detected by using admixture models (*e.g.* STRUCTURE, Prichard *et al.* 2000; Falush *et al.* 2003) and a sufficiently large number of immigrant individuals from the non-sampled population. Finally, it is important to emphasize that all the genetic methods presented above only describe inter-population dispersal patterns and therefore do not infer dispersal patterns within populations.

Population genetics can further help to reveal sex-biased dispersal. While most studies concentrated on addressing sex-biased dispersal relied on sex-specific genetic markers such as mitochondrial DNA (*reviewed in* Prugnolle & Meeus 2002) and more recently Y-linked markers (Petit *et al.* 2002), sex-biased dispersal can also be detected using codominant genetic markers (Goudet *et al.* 2002, Prugnolle & Meeus 2002). Provided that adults are sampled and sampling therefore includes potentially dispersed individuals, theory predicts that the dispersing sex is genetically less structured compared to the more phylopatric sex and should present further a larger heterozygote deficit (Goudet *et al.* 2002).

The non-random spatial distribution of genotypes at a large spatial scale is the result of different processes such as selection, mutation and historic events (*e.g.* post glacial re-colonization; Vekemans & Hardy 2004). Yet at a finer spatial scale, the observed distribution of genotypes is most likely caused by the accumulation of local genetic drift under restricted dispersal (*e.g.* Sumner *et al.* 2001, Vekemans & Hardy 2004). Restricted dispersal will lead to genetic differentiation with increasing spatial distance as predicted by the theory of isolation-by-distance (*IBD*; *e.g.* Wright 1943, Rousset

1997). Consequently, estimating dispersal pattern can be expected to be more accurate on a local population scale (Leblois *et al.* 2003).

Describing the slope of the regression line between genetic and spatial distance amongst individuals can disclose the mean parent-offspring dispersal distances in a continuous population when applied on a small geographical scale alongside data on effective population density (Rousset 2000, Vekemans & Hardy 2004). In this context, the inverse of the slope can be expressed as Wright's (1946) neighbourhood size (*NS*). Nonetheless, spatial data can be expected to explain only a small proportion of the total genetic sampling variance ($r^2 \approx 1\%$) due to the high sampling variance expected when estimating pairwise relatedness or genetic distances on an individual level (Lynch & Ritland 1999, Wang 2002, Coulon *et al.* 2004). Moreover, low explanatory power is a general observation in migration-drift models (Rousset 2000). Whereas most research using an individual based *IBD* approach was done on plant species (*reviewed in* Vekemans & Hardy 2004), studies in animals remain rare with only a few focused on vertebrates to date (Waser & Elliott 1991, Rousset 2000, Leblois *et al.* 2000, Peakall *et al.* 2003, Sumner *et al.* 2001, Caizergues *et al.* 2003, Coulon *et al.* 2004).

Red fox dispersal and social structure

By applying an individual based *IBD* approach; this study combined genetic data based on 17 polymorphic microsatellites with accurate spatial data from a continuous red fox population in a mountainous habitat in Switzerland. To my knowledge, this is one of the first studies investigating dispersal patterns inferred from fine-scale spatial genetic structure in a widely dispersing mammal.

The red fox is a habitat generalist (Macdonald 1980), with an area-wide distribution in Switzerland up to 2500m altitude (Wandeler 1995). For this reason, the red fox represents a good example of a species with a continuous population distribution, necessary for fine-scale *IBD* analyses. To date, the red fox is the main vector of rabies in Western Europe (Steck & Wandeler 1980). Since fox dispersal is considered to be important for the rate of rabies spread (*e.g.* Wandeler *et al.* 1974) dispersal distances and directions in foxes were the subject of several field (*reviewed in* Chautan *et al.* 2000) and simulation studies (*e.g.* Artois *et al.* 1997). Although in general dispersal

distances have been observed to be longer for males (*reviewed in* Trewhella *et al.* 1988), other studies reported differently (Englund 1980; Funk *et al.* 1994). Beeline recovery distances for tagged foxes longer than 300km have been recorded in North America (Rosatte 1992; Allen & Sargeant 1993) while in rural Europe maximum dispersal distances have been reported to be below 100km (*e.g.* Zimen 1984, Trewhella *et al.* 1988, Funk 1994). A negative correlation between population density and dispersal distance has been observed (*reviewed in* Trewhella *et al.* 1988, but see Funk 1994) across different habitat types. In addition, several studies have indicated that dispersal directions in red foxes were altered by environmental factors (*e.g.* topography, habitat type; Zimen 1984) and human built barriers (motorways; Allen & Sargeant 1993, Funk 1994; but see Trewhella & Harris 1990).

Social organization in red fox is variable. They defend territories and live in pairs or in family groups, which can be often explained by the abundance of food and the pattern of fox mortality (Voigt & Macdonald 1984). Fox populations with high densities, such as in urban habitat, are characterized by reduction of reproducing females and the formation of family groups larger than the breeding pair (*review in* Cavallini 1996) Larger groups have been described to include one male and several related females (Voigt & Macdonald 1984). At high density, only a minority of females will rear cubs while barren and socially sub-ordinate females tend to act as helpers (Macdonald 1979, Kolb 1986). In contrast, breading yearling females are common at lower density (Vos 1994). The red fox social organization at high density is reflected by small and vastly overlapping home ranges (Baker *et al.* 1998, Baker *et al.* 2000) and anegative correlation between home range size and population density has been described (White *et al.* 1995).

Objectives

The primary objective of this study was to test the occurrence of *IBD* by analysing a continuous population of red foxes at a local scale. *IBD* could be expected by assuming a predominance of small average dispersal distances in relation to the total spatial expansion of the studied population.

The second objective was to investigate different dispersal patterns of males and females. Based on the observation that dispersal in red foxes is predominantly sex-

biased, differences in sex-specific *IBD* pattern can be hypothesized. Furthermore, males, who are reported to disperse more, could display a higher heterozygote deficit compared to females.

The third objective was to compare an indirect (genetic) estimate of an average dispersal distance in red foxes against a direct (demographic) estimate from published recovery distances of ten mark–recapture studies. Given the difficulty to estimate for long-distance dispersal in field studies, one may assume that indirect estimated dispersal distances inferred in capture–mark–recapture studies should be longer than distances estimated from demographic data.

The final objective was to investigate the effect of topographic structures on the dispersal in red foxes. As reported previously (Zimen 1984, Allen & Sargeant 1993, Funk 1994) dispersal in foxes should follow distinct topographic structures such as river-valleys and mountain ranges. As a result, spatial matrices of individual pairwise distances, which account for topographic structures, can be expected to better explain more of the total genetic sampling variance than pairwise Euclidian distances only.

Methods

Study site and red fox samples

The study area (4189km^2) was located in the eastern part of the Swiss Alps and the Canton Grisons and is surrounded by the watershed of the river Rhine (Figure 1). Local hunters and hunting authorities provided over 380 fox tissue samples between mid November until February of 2001-02 and 2002-03. Because the onset of dispersal in rural areas occurs primarily between September and November in red foxes (*e.g.* Zimen 1984), a high proportion of the sampled foxes could be considered as dispersed or resident individuals. Attention was given to obtaining accurate individual geographic data by evaluating local field names with individual XY-coordinates. Each sampling location was represented by one tissue sample only. Thus, where more than one fox sample was provided from the same sampling location, only one sample was randomly chosen. Finally a sub-sample was selected for a consistent distribution of sampling across the study and to fulfil the required sample size ($n \geq 100$; Leblois *et al.* 2003) for an informative *IBD* analyses based on individual genotypes.

Spatial distances analyses between foxes[5]

Pairwise distances between individual locations were computed in a Geographic Information System (GIS; ArcView®, ESRI) using a cost-friction-analysis based on an elevation model (250x250m grid cell resolution; MONA, GEOSYS). In a cost-friction-analyses a distance / proximity surface (cost-surface) is generated based on a digital map (*e.g.* landscape model, vegetation model, altitude model, or a combination of them) across the area of interest. Based on the digital model used, a value of friction is assigned to each grid cell (*e.g.* the effort of a fox to cross a specific grid cell at a given altitude). All possible paths between two given points are computed. Finally the path with the least sum of friction (also referred to as a least-cost distance or ecological distance) is chosen. However, because red fox specific values of friction for a given altitude were unknown, pairwise distances between individual locations were thus calculated as follows:

A sequence of ten different altitude thresholds (1200m, 1400m, 1600m, 1800m, 2000m, 2200m, 2400m, 2600m, 2800m and 3000m) was arbitrarily defined. For each

[5] GIS analyses were computed by Fridolin Zimmermann, Bern, CH and PW.

given threshold a cost-friction surface was computed across the whole study area. Grid cells were coded as *one* for cells below the given altitude threshold (potential area) and *no data* (impenetrable) for all other cells, respectively. Pairwise distances (least-cost distance) between all individual spatial locations were thus calculated by taking into account only cells below the threshold (see Figure 2 for a hypothetical example). In addition, Euclidian pairwise distances were computed across a cost-friction surface with coded cells as *one* only. Distances calculated by this method do not represent true Euclidian distances (for details see ESRI 1996a-c). However, the method allows them to be directly compared with the pairwise distance calculations for the ten different altitude thresholds.

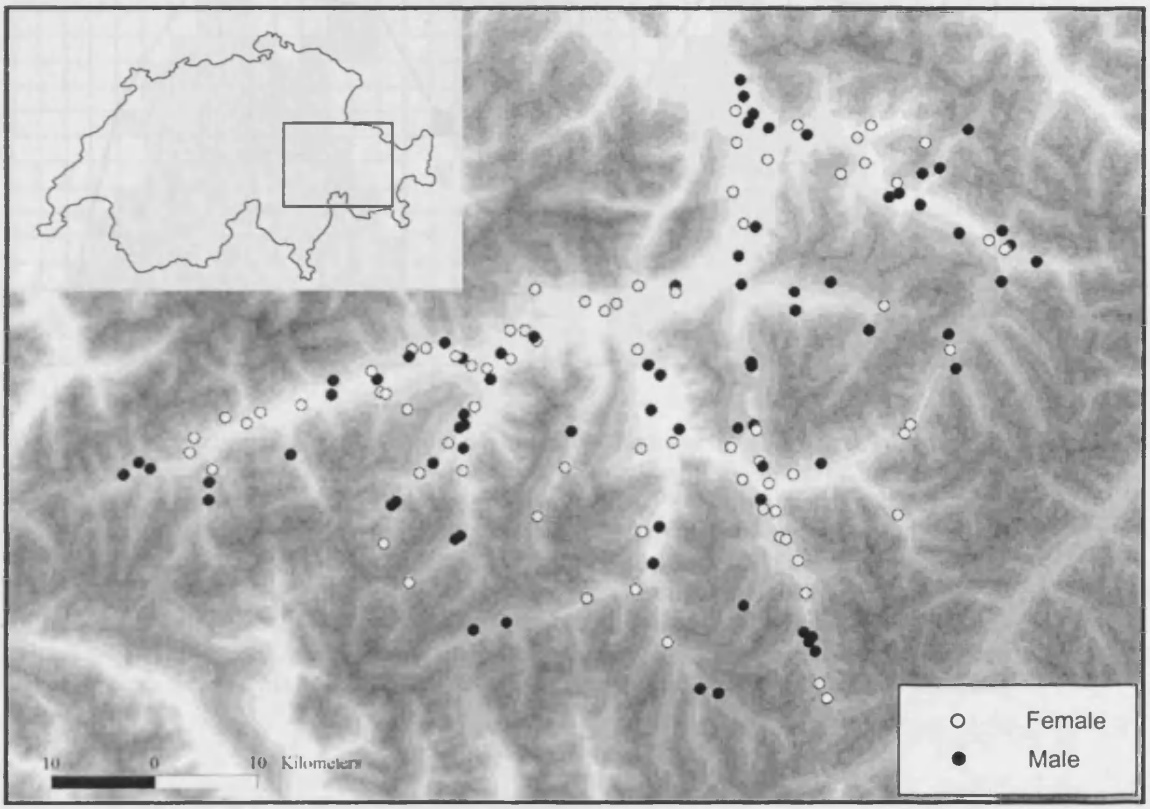

Figure 1 Location of study area in the Swiss Alps (Canton Grisons). Circles indicate individual red fox samples. Grey-scale refers gradually to the elevation (low altitude = white; high altitude = dark-grey).

All pairwise distances for each altitude threshold and all Euclidian distances were combined within a matrix using Rey's (2002) *cost-distance matrix* extension. Analyses were notably eased by the hierarchical topography (watershed) of the study area, which prevented a situation in which individual locations at a given altitude were enclosed by a sequence of grid cells with a higher altitude.

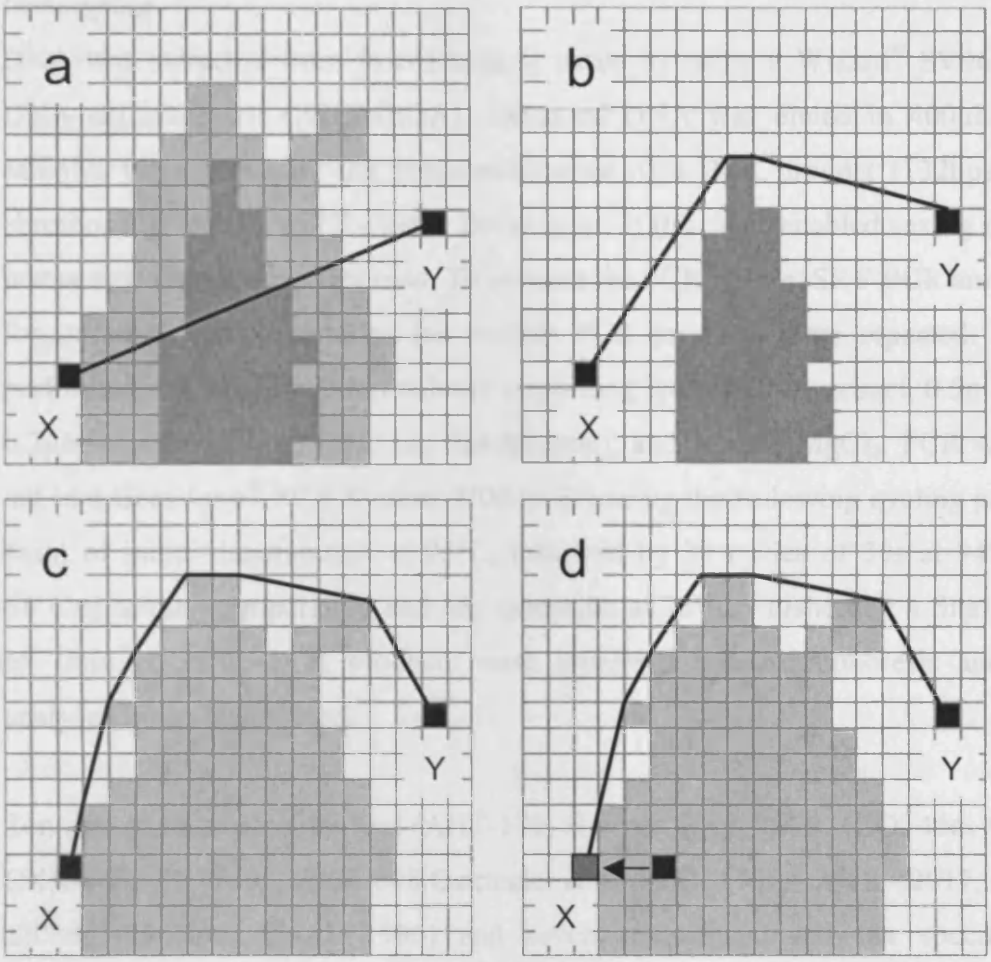

Figure 2 Principal of the calculation of a spatial distance (black lines) between the hypothetical locations of two individuals (*X* and *Y*; filled cell). White, grey and dark-grey represents *low*, *medium* and *high* altitude, respectively. a.) Euclidian distance b.) Distance calculated for a *high* altitude threshold c.) Distance calculated for a *medium* altitude threshold. d.) Hypothetical example of sample *X* collected at the same altitude (*medium*) as the altitude threshold. Sample *X* was at first shifted to the nearest grid cell (fasciated) and an altitude below the threshold. The distance between the new location and sample *Y* was calculated (arrow) and subsequently added to the distance between the new and the original location. Note that the black lines do not exactly reflect the path of how the spatial distances were calculated.

A number of individuals locations were at a higher altitude than the *a priori* set altitude thresholds for some of the spatial matrices. Therefore, these locations were shifted to the nearest grid cell with an elevation below the threshold in question, prior to the cost-friction analyses. Subsequently, the Euclidian distances between the corrected and the original locations were calculated and summarized in an additional correction matrix. Pairwise distances were then calculated by including the corrected locations as described above. Finally, the correction matrix was added to the corresponding distance matrix (Figure 2).

Genotyping

DNA was extracted from frozen muscle tissue by using a Wizard® SV96 Genomic DNA extraction kit (PROMEGA). Extracted DNA was eluted in 400µL H_20. All samples were sexed by the presence/absence of a PCR product (132bps) at a Y-chromosome marker (*SRY* – gene; Breen *et al.* 2001). This enabled sexing of samples whose sex has not been recorded. To account for PCR failure, SRY PCR amplification for possible female samples (no visible PCR product) were repeated. PCR was performed in a 10µL reaction volume containing 2µL of DNA extract, 0.5mM dNTPs, 0.2µM of each primer, 0.3U taq (Invitrogene), and 1.5mM $MgCl_2$. PCR was carried out in a GeneAmp® PCR System 9700 (ABI) using the following cycling parameters: 4min of initial denaturation at 95°C, followed by 30 cycles of 30s at 94°C, 30s at 61°C annealing temperature and 45s extension at 72°C, finished by a final extension of 7min at 72°C. PCR products were separated by electrophoresis and visually analysed on an agarose gel.

Ten canine microsatellite loci (AHT-130, Holmes *et al.* 1995, CXX-156, CXX-279, CXX-466, CXX-606, CXX-608 Ostrander *et al.* 1993, 1995; c2010, c2017, c2054 and c2088; Francisco *et al.* 1996) and seven re-designed red fox specific canine microsatellite loci (V142, V374, V402, V468, V502, V602, V622; Chapter 2) were used in this study. Between three and five loci were amplified within the same PCR reaction using Qiagen's PCR multiplex kit, which co-amplifies numerous primer pairs within the same PCR reaction despite different locus specific PCR conditions. Amplification was carried out in a total volume of 6µL containing 3µL of 2x multiplex master-mix, 0.07 - 0.3µM of each primer and 2µL of template DNA. PCR was performed using a GeneAmp® PCR System 9700 (ABI) and applying the following cycling parameters: 15min of initial denaturation at 95°C, followed by 30 cycles of 30s at 94°C, 120s at 58 - 60°C and 60s extension at 72°C, with a final extension of 30min at 60°C. For all PCR amplifications, a blank sample and three positive controls of known genotypes were used. PCR products were electrophoretically separated on an ABI Prism® 377 DNA sequencer (ABI). Allele sizes were scored against the size standard GS350 Tamra™ (ABI) using GENESCAN™ and GENOTYPER™ software.

General population genetic analyses and testing for sex biased dispersal

To evaluate whether all examined loci could be considered as independent replicates of population structure, genotypic linkage disequilibrium between all pairs of loci (Garnier-Gere & Dillmann 1992) were tested in GENEPOP v3.1 (Raymond & Rousset 1995b). Single locus genetic diversity (H_E; Nei 1987) and probability-tests for deviation from Hardy-Weinberg equilibrium across all samples were computed using the same software package. Critical significance levels were adjusted for multiple tests using Bonferroni corrections (Rice 1989).

To examine current sex-biased dispersal, single locus F_{IS} - values (Weir & Cockerham 1984) were computed across all males and females, respectively, using GENEPOP (Raymond & Rousset 1995b). Pairwise F_{IS} – values for males and females were subsequently compared for statistical significance with a Wilcoxon sign-rank test. The dispersing sex is expected to demonstrate a higher mean F_{IS} compared to the philopatric sex, due to mixture of resident and current immigrant individuals within the tested genepool (Goudet *et al.* 2002). The allele frequency distribution between males and females was compared using a genic differentiation test (Raymond & Rousset 1995a) implemented in GENEPOP.

Analyses of spatial genetic structure

IBD was described using two different individual pairwise genetic estimators (a_r, Rousset 2000 and R_W, Wang 2002; nomenclature based on Van de Casteele *et al.* 2001) and pairwise logarithmic transformed spatial distances. Rousset's (2000) estimator a_r is a genetic distance measure that is analogous to $F_{ST}/(1-F_{ST})$ but is performed between pairs of individuals instead of populations. Moreover, the slope of the regression line between genetic and spatial distances was used to infer effective dispersal distances (Rousset 2000). Unlike other individual genetic estimators, a_r does not depend on a 'reference' population for allele frequency distribution. However, it tends to suffer higher sampling variance and thus has less statistical power (Vekemans & Hardy 2004). Wang's (2002) R_W estimator performed better in a simulation study (Wang 2002) compared to other relatedness estimators (*i.e.* $R_{L\&R}$, Lynch & Ritland 1999; $R_{Q\&G}$, Queller & Goodnight 1989). This was in particular true for uneven allele frequency distributions, which can be expected when using highly polymorphic

markers such as microsatellites. Multilocus estimators were calculated and compared with the logarithmic transformed pairwise Euclidian distances.

The spatial genetic structure was tested for both estimators against the logarithmic (*ln*) transformed Euclidian pairwise spatial distances by assessing the significance of the regression slope using a Mantel test (10,000 permutations of individual spatial location). For computing R_W measures, allele frequency distributions were calculated across all individuals used in this study. Spatial genetic analyses were performed using the software SPAGEDI (Hardy & Vekemans 2002).

Mean gene dispersal distance σ (axial parent-offspring distance; Rousset 2000) per generation$^{1/2}$ was estimated based on the regression slope between a_r against the *ln* transformed spatial distance. The inverse of the slope (*blog*) equals $4\pi D\sigma^2$ in a two-dimensional space per generation (Rousset 2000) and can be further referred as *neighbourhood* (Wright 1946) or *neighbourhood-size* (*NS*, e.g. Sumner *et al.* 2001). *NS* can be interpreted as the number of individuals defining the strength of local genetic drift (Wright 1946). The parameter D is the effective population density, which is the effective population size (N_e) divided by the area (km^2) of the study site (Rousset 1997).

N_e was calculated for populations with overlapping generations based on demographic data (Johnson 1977). Assuming a constant population size, sex ratio and age distribution, N_e can be estimated in terms of two matrices specifying the passage of genes between different age groups (and sexes) and the number of individuals in each age group (equation 10 in Johnson 1977). An estimate of the effective population density D was calculated based on the average number of killed (hunting and roadkill) red foxes for 2001 and 2002 in the study area. However, because no detailed demographic data were available for this population the N_e estimations were based on the following demographic data sets: a global estimate of juvenile - adult ratio in Switzerland (Rabies data set; n = 4122) and a life table of 160 adult foxes from the Canton Aargau from 1995 to 2000 (Appendix; Chapter 4). Because a significant proportion of adult foxes in their second year may not reproduce (Harris & Smith 1987, Vos 1994), a second estimation of the effective density (D_{mod}) was computed by applying a 50% reduced reproduction for this age class.

The effective dispersal distance σ was calculated for the two effective densities D and D_{mod} across all pairwise spatial distances (global regression). Approximate 95% confidence intervals were computed as ± 2*SE*, where *SE* is the standard error of *blog* estimated by jackknifing over loci (Fenster *et al.* 2003). The linear relationship between genetic and spatial distance can be expected to hold best only within the distance range σ - 20σ (for details see Rousset 1997, 2000). Therefore, an iterative approach (Heuertz *et al.* 2003) was applied to estimate σ for both densities D and D_{mod}. At first, $\hat{\sigma}$ was extracted from the global regressions covering all pairwise distance comparisons for each of the two densities and subsequently new estimates of $D\sigma^2$ were calculated based on a restricted regression considering distances only between $\hat{\sigma}$ and $20\hat{\sigma}$. These procedures were repeated until $\hat{\sigma}$ estimations stabilized and converted (Vekemans & Hardy 2004). Approximate confidence intervals of 95% for the σ - values were computed.

The two indirect genetic σ estimations for both densities D and D_{mod} were compared with a demographic estimation of σ. The parameter σ was estimated using a linear regression between the mean inverse beeline recovery distances (km) for tagged males and females against fox density (family groups * km^{-2}) across ten red fox populations of different habitat types (Trewhella *et al.* 1988). The density of family groups (*FD*) across the whole study area was calculated as follows: it was assumed that the population density was constant and that the number of dead foxes reported (based on the annual hunting and road-kill statistic from the Canton Grisons) within the study area equalled the number of the annual generation of cubs (Wandeler *et al.* 1974). Then,

$$FD = \text{number of fox family groups km}^{-2} = \frac{\text{number of dead foxes}}{\text{study area km}^{-2} * \text{mean litter size}}$$

where mean litter size was assumed to be 4.7 (Wandeler *et al.* 1974; Harris & Trewhella 1988). Subsequently, the mean recovery distance for males and females was derived using equations 5 and 7 from Trewhella *et al.*'s (1988) publication. To allow for direct comparison of genetic and demographic σ estimation, the mean recovery distance was averaged across males and females. Finally, to account for the

non-axial estimation of individual movements of the recovery distance the demographic σ estimation was divided by two (for details see Sumner *et al.* 2001).

All ten spatial matrices computed in GIS were *ln* transformed and regressed against two pairwise genetic (a_r and R_W) matrices in SPAGEDI (Hardy & Vekemans 2002). For each individual regression the measure of fit (r^2 – value) was recorded.

To compare sex specific dispersal patterns, fine-scale spatial genetic structure was assessed independently for males and females. Average (± *SE* jackknifed over loci) relatedness (R_W; Wang 2002) for seven *a priori* defined and by the natural logarithm (*ln*) transformed distance categories (<8,106m, 8,107m – 12,182m, 12,183m – 18,174m, 18,175m – 27,113m, 27,114m – 40,447m, 40,448m – 60,340m and >60,341m) were computed in SPAGEDI (Hardy & Vekemans 2002). Spatial data were based on the altitude threshold matrix with the best measure of fit (highest r^2 - value) of genetic against spatial distances (see paragraph above). Allele frequency distributions were calculated across all individuals used in this study.

Results

Sampling and spatial GIS analyses

A total of 145 individual samples from red foxes (73 males and 72 females) were used in this study. Mean altitude for all individual locations was 1169m (min 505m; max 1944m, for spatial distribution see Figure 1). The potential surface (the surface below a given altitude threshold) for computing pairwise distances decreased markedly for each lower altitude threshold to less than 15% for the *1200m* threshold (Table 1). In contrast, the average distance and standard deviation across all individuals increased for each lower threshold from 34,951m ± 6,953m for the *3000m* - to 45,236m ± 10,046m for the *1200m* altitude threshold (Table 1). The total number of corrected individual locations increased from 4 (*2.8%*) to 76 (*52.4%*; Table 1) individuals for the four lowest altitude thresholds.

Table 1 Spatial distances between red fox samples are summarized in an Euclidian (*E*) and a sequence of ten altitude matrices. Shown are the potential surface, the mean ± *SD* of pairwise individual spatial distances and the absolute and relative number of corrected individual locations and pairwise distances.

Altitude threshold matrix	Potential area (Surface below a given threshold)		Pairwise spatial distance		Corrected individual locations	
	Area [km²]	*%*	*Mean [m]*	*SD [m]*	*#*	*%*
E	4189	*100.0*	34950	6935		
3000	4166	*99.9*	34951	6935		
2800	4068	*97.1*	34956	6937		
2600	3787	*90.4*	35080	7011		
2400	3296	*78.7*	36117	7513		
2200	2741	*65.4*	37407	7883		
2000	2198	*52.5*	38431	8222		
1800	1698	*40.5*	39600	8528	4	*2.8*
1600	1262	*30.1*	41819	9536	17	*11.7*
1400	884	*21.1*	44042	9861	41	*28.3*
1200	594	*14.2*	45236	10046	76	*52.4*

Microsatellite genotyping and sex biased dispersal

Total genotyping success across all samples and the 17 loci was *99.9%*. No significant linkage disequilibrium was found among all pairs of loci after adjusting for multiple comparisons (data not shown; k=136; all tests $p > 0.05/k$ with Bonferroni correction of $\alpha = 0.05$). Single locus genetic diversity (H_E) across all samples was high ranging from 0.599 (V502) to 0.914 (V602) with a multilocus mean ± *SD* of 0.808 ± 0.077. The total number of alleles per locus ranged from four (c2010) to 20 (c2054; mean ± *SD* = 10.24 ± 3.78; Table 2). Deviation from Hardy-Weinberg was significant for loci V622 (p = 0.021) and c2017 (p = 0.030), whilst no significant deviation was observed after correcting for multiple testing. In contrast, the overall deviation across all loci was significant ($X^2 = 49.4$; $df = 34$; $p < 0.05$; Fisher's method, Table 2).

Observed F_{IS} – values across loci were significantly higher in males (mean ± *SD* = 0.027 ± 0.056) than in females (mean ± *SD* = -0.008 ± 0.055; n = 17, $z = 2.3432$, $p<0.02$; Wilcoxon sign-rank test; Table 2). A total of twelve (6.9%) and five (2.9%) sex-specific alleles were recorded in males and females respectively. Global test for allele frequency distribution (Genic test) across all loci revealed no difference in allele frequency distribution between sexes ($X^2 = 32.9$; $df = 34$; $p = 0.523$; Fisher's method).

Table 2 Measures of genetic diversity and inbreeding coefficients in red foxes for all individuals, and for females (f; N= 72) and males (m; N=73) only. Shown are the number of detected alleles (*A*), expected heterozygosity (H_E ; Nei 1987), F_{IS} values (Weir & Cockerham 1984) and *p* – value for the probability of Hardy–Weinberg deviation for each locus and multilocus means ± *SD*.

	N	*A*			H_E			F_{IS}			*HW*
Locus	*all*	*all*	*f*	*m*	*all*	*f*	*m*	*all*	*f*	*m*	*p-value* [a]
AHT-130	145	10	10	9	0.815	0.802	0.822	-0.050	-0.074	-0.033	0.528
V142	145	13	11	13	0.881	0.889	0.874	-0.002	0.000	-0.003	0.490
CXX-156	145	9	9	9	0.841	0.840	0.844	0.008	-0.075	0.091	0.605
CXX-279	145	10	9	10	0.842	0.839	0.845	0.033	0.040	0.028	0.110
V374	145	6	6	6	0.797	0.795	0.796	-0.074	-0.084	-0.068	0.295
V402	145	7	7	7	0.821	0.815	0.828	0.017	0.012	0.024	0.394
CXX-466	145	8	8	7	0.747	0.735	0.749	0.031	0.037	0.012	0.063
V468	145	10	9	9	0.834	0.839	0.834	-0.017	-0.060	0.031	0.273
V502	145	8	7	8	0.599	0.578	0.620	0.045	0.014	0.073	0.757
V602	145	17	16	17	0.914	0.915	0.915	0.050	0.029	0.072	0.221
CXX-606	145	10	7	10	0.794	0.784	0.807	-0.033	-0.028	-0.036	0.613
CXX-608	145	10	8	10	0.806	0.797	0.818	-0.044	-0.081	-0.005	0.446
V622	144	10	9	10	0.820	0.825	0.817	0.103	0.041	0.168	0.030
c2010	145	4	4	4	0.674	0.679	0.670	0.099	0.121	0.080	0.243
c2017	145	11	11	11	0.839	0.818	0.851	0.006	-0.001	0.003	0.021
c2054	145	20	20	18	0.901	0.903	0.900	-0.010	-0.031	0.011	0.164
c2088	144	11	11	11	0.811	0.805	0.820	0.007	0.000	0.018	0.461
mean		**10.2**	**9.5**	**9.9**	**0.808**	**0.803**	**0.812**	**0.010**	**-0.008**	**0.027**	**0.043** [b]
SD		3.78	3.75	3.54	0.077	0.081	0.074	0.048	0.055	0.056	

[a]Probability test (Raymond & Rousset 1995b), [b]combined p-value after Fisher's methods

Isolation by distance

Both matrices of pairwise a_r and R_W estimators showed a significant correlation with the logarithmic transformed Euclidian spatial distances (a_r: *blog* = 0.00740 $p <$ 0.0005, r^2 = 0.0054; R_W: *blog* = - 0.00981, $p < 0.0001$, r^2 = 0.0038; Mantel test; for details see Table 3). This strongly indicates *IBD*. Two loci (V602 and c2054) exceeded the recommended level of genetic diversity (> 0.85) for unbiased estimation of σ (Leblois *et al.* 2003). However, comparing single locus *blog* - values and single locus H_E didn't reveal a correlation (n = 17; a_r: r = -0.108; R_W: r = 0.145).

The regression slope between the genetic, a_r, and the logarithmic transformed spatial distances corresponded to a *NS* of 135.1 individuals (95% confidence interval = 78.5 - 484.6 individuals). Based on the estimated annual number of 2,412 dead foxes in the study area between 2001 and 2002 and from the used live-table for red foxes, the computed N_e and generation interval L were 3907 individuals and 2.75 years respectively. Assuming that only 50% of one year old foxes reproduce, N_e estimation

decreased to 3,646 individuals (L = 3.24 years) resulting in a N_e/N ratio (N = adult population size per generation) of 0.44 and 0.35, respectively (see Appendix A1 for details). Effective population densities based on D and D_{mod} were 0.933 and 0.870 respectively. These corresponded to mean axial dispersal distances σ across all pairwise spatial distances (global regressions) of 3,395m (2,588 – 6,429m, 95% confidence interval) for D and 3,516m (2,680 – 6,658m) for D_{mod}, respectively (Table 5).

Table 3 Results of the global regressions between individual pairwise genetic distances (a_r) and Euclidian spatial distances, and between relatedness (R_W) and Euclidian spatial distances in red foxes. For each locus, the microsatellite repeat structure (2 for di-nucleotides, 4 for tetra-nucleotides) and the *blog* – values (slope) for a_r and R_W, respectively, are shown. The summary statistics show multilocus means and *SE (*Jackknifed over loci*)*.

Microsatellite	*Microsatellite repeat pattern*	*blog - values*	
		a_r	R_W
AHT-130	2	0.0067	-0.0113
V142	2	0.0030	-0.0128
CXX-156	2	0.0107	-0.0060
CXX-279	2	0.0002	0.0029
V374	2	-0.0058	0.0104
V402	2	0.0285	-0.0296
CXX-466	2	0.0195	-0.0279
V468	2	0.0123	-0.0309
V502	2	0.0212	-0.0239
V602	2	0.0195	-0.0145
CXX-606	2	0.0152	-0.0215
CXX-608	2	0.0046	-0.0032
V622	2	0.0164	0.0031
c2010	4	-0.0094	0.0049
c2017	4	-0.0045	0.0039
c2054	4	-0.0045	-0.0016
c2088	4	-0.0043	0.0002
mean		**0.0074**	**-0.0098**
SE		0.0027	0.0031

NS calculated from the inverse slope of the restricted regressions for D (162.3) and D_{mod} (157.4) were larger compared to the *NS* derived from the global regression (*NS* = 135.1; Table 4). The restricted regressions result in estimated mean axial dispersal distances σ for D and D_{mod} of 3,720m (2691 – 12,534 m, 95% confidence interval)

and 3,794m (2764 – 11134m) respectively. Both slopes deviated significantly from zero (*D*: $p < 0.005$, $r^2 = 0.0027$; D_{mod}: $p < 0.005$, $r^2 = 0.0028$; Mantel tests).

Estimated fox density *FD* (total number of fox families*km^{-2}) was 0.123, resulting in a demographic σ - value of 8,925m. Compared with the mean values of the genetic estimation for the effective dispersal distance, the demographic σ estimation was considerable larger, but was within the 95% confidence interval of restricted regression (Table 4).

Table 4 Indirect estimation of the average dispersal distance in red foxes for the effective population densities *D* and D_{mod}. Shown are the genetic estimates for the global and restricted regressions for 'neighbourhood size' (*NS*), effective dispersal distance σ per generation$^{1/2}$, 95% confidence interval for σ, absolute and relative number of individual pairwise comparisons (see text for details).

Effective density [Individuals * generation/km^2]	*NS* [Individuals]	$\sigma_{Genetic}$ [m/generation$^{1/2}$]	*95% CI* [m/generation$^{1/2}$]	*N* [dyads]	*%* [dyads]
Global regression					
D = 0.933	135.1	3395	2588 - 6429	10440	*100*
D_{mod} = 0.870	135.1	3516	2680 - 6658	10440	*100*
Restricted regression					
D = 0.933	162.3	3720	2691 - 12534	9973	*95.5*
D_{mod} = 0.870	157.4	**3794**	2764 - 11134	9999	*95.8*

Table 5 Estimation of σ from demographic data based on Trewhella's (1988) function between red fox density and the recovery distances of tagged individuals. Shown are the demographic estimates of the recovery distance for males, females and across both sexes and the effective dispersal distance σ.

Fox density [Family groups/km^2]	*Expected recovery distance* [m]			$\sigma_{Demographic}$ [m]
	Males	*Female*	*Average*	
FD = 0.123	24,828	10,873	17,850	**8,925**

Measures of fit (r^2) for the regressions of the two genetic estimators a_r and R_W against the Euclidian and the ten altitude matrices are shown in Figure 3. For both genetic estimators the highest r^2 – values were computed with the *1400m*-altitude matrix (a_r: 0.0082; R_W: 0.0042). The *1400m*-altitude matrix explained 53.2% and 9.6% more of

the genetic variance compared with the Euclidian matrix for the a_r and R_W estimators, respectively (Figure 3). Overall, the variance explained by using the a_r estimator was higher compared with the R_W relatedness estimator.

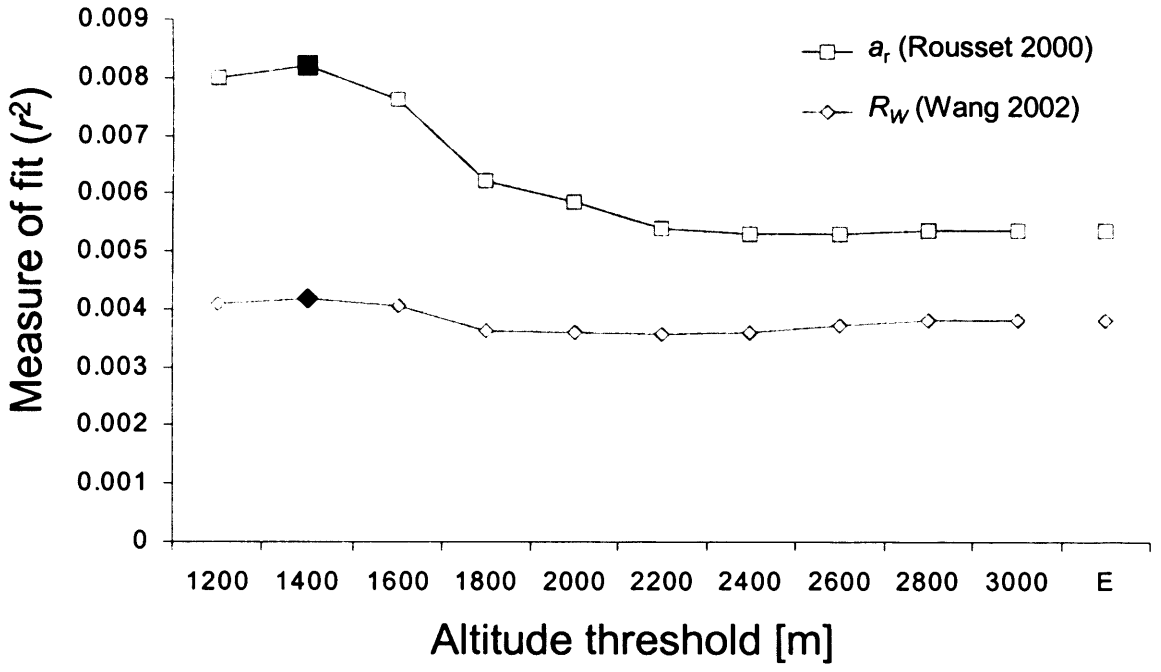

Figure 3 Results of the isolation-by-distance analyses between pairwise individual genetic and *ln* transformed spatial distances in a continuous red fox population. Shown are measures of fit (r^2 – values) for global regressions using two genetic estimates (a_r Rousset 2000; R_W Wang 2002) against a spatial Euclidian matrix (E) and a sequence of ten different spatial matrices. Each of theses spatial matrices accounted gradually for the topographic structure of the landscape by restricting pairwise spatial distance calculations to pre-defined altitude thresholds (see text for details). Filled symbols refer to the highest observed r^2 – value.

Sex specific *IBD* patterns for seven distance categories are shown in Figure 4. A general pattern of *IBD* for males and females was observed. Females were more closely related to each other than males were across all distance categories, with the exception of the second distance category (8,107 – 12,182m), where the highest average relatedness across males was found. Across all samples and pairwise spatial distances, relatedness amongst females was greater than relatedness amongst males ($z = -2.864$; $n_{Loci} = 17$; $p < 0.005$; Wilcoxon signed-rank test).

Discussion

Given the central importance of studying dispersal in order to understand the ecology and evolution of a species, it is essential that reliable and precise information on dispersal pattern is obtained. In this study we found evidence of male biased dispersal and topographic effects on dispersal direction, and we obtained an estimate for average dispersal distance in red foxes by applying population genetic methods in combination with geographic and demographic data. This study is the first to reveal sex-biased and directed dispersal pattern in red foxes using genetic methods, demonstrating the potential usefulness of individual based *IBD* methods, especially for widely dispersing species.

Isolation by distance

A strong *IBD* pattern was found between pairwise individual genetic and spatial distances. This demonstrated a non-random distribution of genotypes, indicating that red foxes in close proximity to each other are genetically more alike than individuals separated over longer distances. As predicted, dispersal was restricted and thus could not counteract local genetic drift. This result is in agreement with Trewhella *et al.'s* (1988) review on several red fox studies, where the recovery distance of tagged foxes was generally short with only a few long distance movements. In contrast, beeline recovery distances of over 300km in tagged red foxes (Rosatte 1992, Allen & Sargeant 1993) were recorded, being more than twice as long as the total width of the study area. This comparison illustrates that dispersal distances in red foxes are flexible and differ between populations and at different population densities. The observed *IBD* pattern also questions the assumption that the development of fine-scale spatial genetic structure is unlikely to occur in widely dispersing taxa (Peakall *et al.* 2003). Moreover, these results leave little doubt that *IBD* can be tested in a wide number of different animal taxa, provided that sufficient genetic markers are used in combination with a thorough sampling regime.

Sex-biased dispersal

Based on the comparison between the observed sex-specific F_{IS}-values, dispersal was male biased, indicating an existing mixed male population of resident and immigrant individuals (Goudet *et al.* 2002). In addition, the trend of the observed higher number of sex-specific private alleles detected in male foxes emphasized that males were the sex that dispersed the most. The observed differences between the sex specific F_{IS} - values indicated that the recent dispersal rate was sufficient to be detected yet not widespread enough to erase the signature of genetic differentiation between the study and the adjacent populations.

Breeding groups are an important component of population structure, yet they are ignored in most population genetic models (Sugg *et al.* 1996) as well as in the methods (*F*-statistics, *IBD*) applied in this study. As social organization in red foxes is complex (Cavallini 1996) the general deficit of heterozygosity observed might reflect some unaccounted social subdivision in the examined population. In fact, the observed significant *IBD* pattern specifies per se non-random mating. However, unclear were the potential effects of the social system on the differences observed in the sex-specific F_{IS} – values. It should be noted, that the difference in F_{IS} – values revealed current dispersal within an interval of one generation rather than a historic dispersal pattern (Goudet *et al.* 2002). Nonetheless, by incorporating only one sample from the same sampling site (Figure 1) sampling of closely related females occupying the same territory could be eliminated.

Inferring a sex-biased dispersal pattern from sex-specific *IBD* pattern (Figure 4) proved to be more difficult. Females, showed consistently higher relatedness amongst themselves compared with males for the seven spatial distance categories. Yet, despite the expected lower population structure in the more dispersive sex (Goudet *et al.* 2002) males showed a distinct *IBD* pattern (Figure 4). Sex-biased dispersal was further revealed by the observed higher mean relatedness among male foxes in the second distance category (8,107-12,182m) in relation to the first spatial distance category (Figure 4), which could indicate that a significant proportion of male foxes examined did in fact move away from their place of birth. Examining *IBD* patterns on a sex-specific level reduced the number of pairwise comparisons (dyads) per distance category to one quarter. For that reason, the number of seven arbitrary defined

distance categories was a trade-off between the level of variance per category expected and the spatial resolution of the analyses.

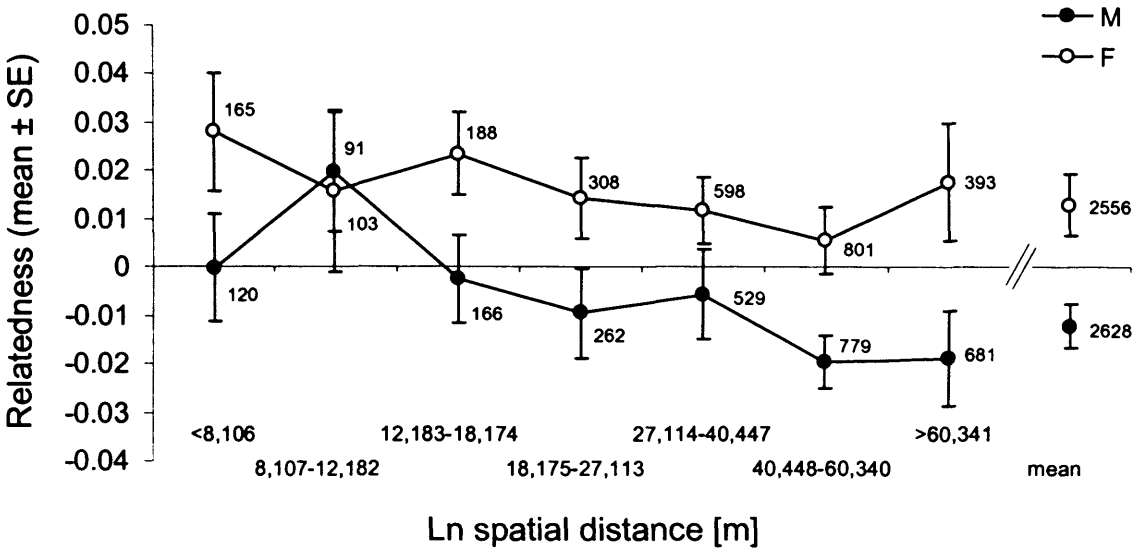

Figure 4 Sex-specific isolation-by-distance in a continuous red fox population. Shown are the average (± *SE;* jackknifing over loci) relatedness (R_W Wang 2002) for males and females for seven *log* transformed and *a priori* defined distance categories. Spatial data were based on the *1400m* threshold altitude matrix (see text for details). Figures represent the total number of dyads for each distance category.

The interpretation of sex-biased dispersal by applying autosomal genetic markers revealed to be pretty complex. Although both methods suggested male-biased dispersal, alternative explanations could not be entirely excluded. Furthermore the results of the *IBD* analyses disclosed the need for future simulation studies to investigate the conditions under which sex-biased dispersal pattern can be expected using individually based analyses. Finally, sex-biased dispersal could also be assessed using an assignment test implemented in GENECLASS2 (Piry *et al.* 2004). Although this study consists only of one population, GENECLASS2 computes a probability - value for each individual genotype belonging to the focal population. By comparing the sex – ratio of individual genotypes with a low probability value (*e.g.* < 0.01) it should be possible to identify differences in sex biased dispersal.

The observed pattern of male biased dispersal confirmed previous results of studies addressing sex-specific dispersal pattern in red foxes and reflects the general rule according to which males represent the more dispersive sex among most carnivores and mammals (Waser 1996). These data were consistent with results from mark-recapture studies, where mean recovery distances for males foxes were significantly compared with females (*reviewed in* Trewhella *et al.* 1988, Allen & Sargeant 1993).
It is important to note that although the two methods applied highlighted male-biased dispersal, they did not reveal any successful reproduction by individuals who moved to a new location through *natal dispersal.* In fact, the observed mortality of dispersing foxes was described to be significantly higher (*reviewed in* Chautan *et al.* 2000, Harris and Trewhella 1988; Woollard & Harris 1990) compared with philopatric individuals. Therefore, a significant proportion of dispersed males could be expected to have died before reproducing successfully. Actual gene flow between the studied population and its surroundings might therefore be lower than assumed by the apparent number of detected current immigrants.

Dispersal distances

The average dispersal distance σ for the effective population densities D and the more realistic density D_{mod} were smaller than the demographic σ values for the extrapolated and corresponding fox density *FD.* Furthermore, simulations indicated that a twofold difference in accuracy between the demographic and genetic estimates can be expected (Rousset 2000). The deviation between the two estimates may be explained by the lack of precision in one or both of the estimates. Therefore some potential causes of imprecision and / or biases are specified and discussed below:

The model assumptions for the genetic estimation of σ might not reflect reality (Rousset 2000; Sumner *et al.* 2001). The effective fox density was likely to be uneven across the study area because fox abundance is higher at lower altitude (Wandeler 1995), resulting in a lower level of precision of the genetic estimation. As determined by the estimated σ value, the study site somewhat exceeded the recommended area of $10\sigma * 10\sigma$ for an unbiased estimation of $D\sigma^2$ (Rousset 2000; Leblois *et al.* 2003). Due to the expected mutation process and the high mutation rate of microsatellites, sampling at large distances can lead to an underestimation of the regression slope and

therefore to an overestimation of $D\sigma^2$ (Leblois *et al.* 2003). This bias might to some degree be reflected by the estimated average multilocus relatedness for males and females examined for the largest pairwise distance category (> 60,340m), which did not follow the general trend of *IBD* (Figure 4). In contrast, the restricted regression analyses for the two given effective densities resulted in less steep slopes (smaller *blog* – values) and thus longer estimates of dispersal distance.

The examined red fox population was subject to a two - to threefold density increase following a severe rabies epidemic in the early 1980s along a long-term trend of a growing caring-capacity for foxes in Switzerland (Breitenmoser unpublished; Chapter 4). It can therefore be speculated that the population might not yet be in a drift-migration equilibrium and so the $D\sigma^2$ estimation reflects past rather than recent demographic parameters (Leblois *et al.* 2004).

Trewhella *et al.'s* (1988) general regression model for the average beeline recovery distance in relation to the observed density was inferred from studies across different habitat types. Thus, deviations between this model and the specific study area could be expected, especially since the study site is in an Alpine habitat, which was not included in Trewhella *et al.*'s (1988) analysis. In addition, the genetic estimation of σ refers to a time period of one generation. In contrast, no temporal information was available for the demographic σ estimation derived from the literature. Moreover, although foxes are thought to disperse predominantly as juveniles, dispersal of adult individuals was reported in other studies (Harris & Trewhella 1988; Zimen 1984). Hence, given that the time period over which capture-mark-recapture studies were conducted, the demographic estimation of σ might be therefore underestimated.

The recorded difference between indirect and direct dispersal distance estimation contradicted the prediction that, because of the difficulty to detect long dispersal distances, the genetic estimation should be longer (*but see* Rousset 2001). In fact, the estimated genetic distance was substantially smaller than the dispersal distance inferred from demographic data. As previously discussed, it is important to distinguish between an individual that moved to a new location and an individual which moved and subsequently reproduced successfully. The genetic estimation of dispersal distances addressed the actual genetic input that dispersed foxes had in the examined

population. In contrast, the demographic estimate of beeline recovery distances represents spatial movement of individuals only. Despite the methodological constraints imposed by the limited demographic data available, it can be assumed that actual gene flow appears more spatially restricted when inferred from demographic data only. So far, only a few studies (Rousset *et al.* 2000, Sumner *et al.* 2001) have compared direct and indirect dispersal distances in animals. Therefore a general discussion of observed differences between genetic and demographic dispersal distances is inappropriate. However, it is well accepted that the cost of dispersal is higher than that for phylopatric behaviour (*e.g.* Rousset & Gandon 2002) and thus mortality for dispersing individuals is high. As a result, effective dispersal distances that are small in relation to demographic estimates can be expected across a wider range of species.

Dispersal and topographic structures

Despite the calculated differences of the two pairwise genetic estimators a_r and R_W, the results across the ten spatial matrices were similar with both estimators, achieving the highest r^2- values with the *1400m*-altitude matrix. Although expected, the overall genetic variance explained by the set of different spatial matrices was small (< 1%). Consequently it would be useful to validate the observed r^2 - values with simulated values for both pairwise genetic estimators under ideal conditions. In fact, an informative simulation study across the whole range of individual relatedness and distance estimators (*for a summary see* Vekemans & Hardy 2004) would help to choose the most appropriate genetic estimator for future individual based *IBD* analyses. Furthermore, a primary objective was to keep the spatial analyses in *GIS* as simple and thus transparent as possible. Therefore it is reasonable, that a more complex cost-friction analysis (*e.g.* energetic model, habitat model) based on additional assumptions, could have helped to explain more of the genetic sampling variation compared with the results from the ten altitude threshold matrices.

Despite an expected continuum of fox abundance up to 2500m elevation, the best fit between genetic and spatial distances in the individual based *IBD* analyses was observed for the second lowest (*1400m*) altitude threshold matrix. The most parsimonious explanation for this result is that red foxes disperse along valleys rather

than across them and thus supports the assumption that dispersal direction in red foxes can be altered by topography. Moreover, it emphasizes that habitat requirements during dispersal might be different to general habitat requirements in red foxes. The topographic effect on red fox dispersal direction was indirectly reflected by the spread of the last rabies epidemic (1967–96) in Switzerland (Kappeler 1991). The rabies epidemic was observed to be repeatedly channelled and delayed by various natural and artificial structures, such as lakes and large rivers, mountain chains over 2000m altitude, agglomerations and fenced-off motorways (Kappeler 1991). To the best of my knowledge this is the first genetic study showing that red foxes prefer to disperse along topographic features. Furthermore the present study confirms the findings of ecological data (Zimen 1984, Funk 1994).

White *at al.* (1995) demonstrated a negative relationship between red fox density and home range size. As previously discussed, red fox density is likely to be higher at lower altitude than at higher altitude. Assuming that red fox dispersal distances are reflected by the number of territories crossed rather than by an absolute distance in meters (Macdonald & Bacon 1982, Trewhella *et al.* 1988), the expected average dispersal distance at lower altitude is likely to be shorter. Under these conditions and by neglecting any topographic effects on dispersal direction, the best fit for an *IBD* analysis between genetic and spatial distances should be demonstrated with an Euclidian distance matrix. Consequently, the actual effect of topographic structures on dispersal direction might be even more pronounced than observed.

Conclusions

This study demonstrates a strong relationship between the topography of a landscape and the fine-scale spatial genetic structure of red foxes. This study demonstrated that spatial data computed using *GIS* methods, based on accurate individual sampling and combined with genetic data based on a set polymorphic loci, can help to analyse the landscape context of dispersal (Coulon *et al.* 2004, Sacks *et al.* 2004). While this study incorporated elevation data for the spatial analyses only, future studies might benefit from a growing set of geographic reference data (*e.g.* high resolution height models, landscape models including a set of thematic layers such as habitat, human use, etc.). This study further pointed out the possibility to gain indirect estimates of

dispersal distances and sex-biased dispersal. In general, it follows the emerging field of moving from population genetic research based on allele frequencies and arbitrary defined populations to research centred on analysing individual multilocus genotypes in a continuous population (Vrana & Wheeler 1992, Manel *et al.* 2003, Coulon *et al.* 2004). Given the potential to obtain diverse information on dispersal, combining individual spatial and genetic data from continuous populations might soon be the method of choice to infer data of dispersal pattern in ecology and evolution.

CHAPTER 4

Temporal Demography and Genetic Diversity of a Red Fox Population Following a Rabies Epizootic.

Abstract

Infectious diseases can pose a serious threat to natural population viability. In this study, the demography and genetic variation of a local red fox (*Vulpes vulpes*) population (411km^2, Switzerland) before, during and after a rabies epizootic from 1966 onwards were analysed. Post mortem data on rabies tests (n=2658), juvenile - adult ratio (n=1628), accurate adult age (n=561) and sex (n=1612) were complemented by small-scale roadkill (roadkill index) and hunting records (hunting index). A total of 16 polymorphic microsatellite loci were successfully amplified in historic tooth and tissue samples (n=184). In particular, care was taken to account for genotyping reliability. In 1975, the red fox population declined by 79% based on the roadkill index as a result of the first rabies infection. Following this decline, the population increased continuously by over 600% (roadkill index) until it reached a plateau in the mid-1990s, which likely corresponded with the carrying capacity. Throughout these 35 years, the age distribution altered significantly. Whilst the juvenile proportion decreased from 56% to 40% during the phase of population growth (1976-94), the average adult age increased from 1.78 to 2.86 years. In contrast, no long-term trends in heterozyosity (H_O and H_E), allelic diversity and inbreeding coefficient (F_{IS}) could be identified although for all three estimators considerable variation was found both short-term and longer-term. Alterations in the demographic structure were explained by a general lower mortality subsequent to the population decline and by variance in female reproduction over time. The interpretation of the absence of a genetic bottleneck needs to take into account immigration and the relation between remnant local and regional effective population size following the first rabies infection.

Introduction

Infectious diseases are considered to play a central role in natural systems, ranging from influencing species compositions in ecological communities to the genetic diversity of hosts (Altizer *et al.* 2003). Because of their potential to trigger sudden and unexpected epidemics (Altizer *et al.* 2003), infectious diseases can pose a serious threat to endangered species and small populations (*e.g.* Smith 1982, May 1988). They can negatively influence population viability by direct deterministic extinction or by suppressing the size or growth rate and thus making small populations vulnerable to stochastic factors (Woodroffe 1999). The biggest threat usually comes from virulent pathogens, which can 'spill over' from other and more numerous host species (Woodroffe 1999, see also Daszak *et al.* 2000). Carnivores in particular are vulnerable to infectious disease and several dramatic declines in populations of different species have occurred since the beginning of the 1990s (*reviewed in* Funk *et al.* 2001). However, the effect of infectious disease and its dynamics in wild populations is complex and our understanding of mechanics, dynamics and persistence of disease is still poor (Funk *et al.* 2001).

Infectious diseases can have serious consequences to the genetic diversity of populations by causing drastic reductions in population size (O'Brien & Evermann 1988). In general, demographic bottlenecks can limit the adaptive potential of a population and increase the probability of extinction due to a higher rate of inbreeding, fixation of deleterious alleles and loss of genetic variation (*e.g.* Lande 1988). Furthermore, the potential genetic consequences caused by a demographic bottleneck such as a strong selection for resistance against an infectious disease, might further reduce genetic diversity (O'Brien & Evermann 1988). Despite the importance of infectious diseases in conservation, little is known about the genetic consequences caused by diseases in natural populations. This applies to small and large populations. An apparent explanation for this deficit may be the absence of pre-bottleneck sampling, which is essential for assessing the temporal genetic diversity of populations.

The dynamics of gene flow and selection in natural populations on a spatial and temporal scale is fundamental in ecological and evolutionary processes. While a large number of studies exist on genetic differentiation on a spatial scale, relatively little effort has been directed towards studies on temporal dynamics of genetic diversity, drift and gene flow in natural populations (Nielsen *et al.* 1999a). Nonetheless, it is widely accepted that observed genetic patterns are stable over time and that other factors, which may cause temporal genetic differences, are negligible (Tessier & Bernatchez 1999).

In conservation, knowledge of the demographic history of populations is important when making decisions about population management (Bruford & Beaumont 1999). Consequently, current low levels of genetic variability based on neutral genetic markers have been used to infer past population bottlenecks (*e.g.* O'Brien *et al.* 1983, Ellegren *et al.* 1996). Data on allele frequencies could further help to identify recent bottlenecked populations by testing for heterozygosity excess (Luikart & Cornuet 1998). However, analysing DNA from historical samples collected before bottlenecks or from extinct populations could give more informative insight into the past demographic history of populations and species (Bouzat *et al.* 1998). Furthermore, by combining historical with recent samples, levels of genetic diversity could be compared across different time periods, while the rate in which diversity has changed can be estimated (Pichler & Baker 2000).

Since DNA gradually degrades over time (*reviewed in* Lindahl 1993), the extracted DNA from historic samples can be expected to be highly degraded and diluted. Development of molecular methods in general, and short polymorphic genetic markers amplified by PCR, for example microsatellites, have nonetheless allowed even genetic data to be gained from traces of nuclear DNA (*e.g.* Bouzat *et al.* 1998, Nielsen *et al.* 1999b, Chapter 1). However, along with the necessity to verify sample authenticity (Höss 2000), genotyping errors due to highly diluted historic samples can be expected (*e.g.* Navidi *et al.* 1992, Taberlet *et al.* 1996, Chapter 1).

It is obvious that the main problem of using historic samples for population genetic studies - apart from dealing with low copy and quality DNA - is related to sampling. Investigations based on historic samples rely almost explicitly on museum collections, and obviously, these collections have not been created to conduct population genetic

studies in the first place. Therefore, sample sizes have often been inadequate to estimate allele frequencies for a given population (Nielsen *et al.* 1999a). In addition, information on individual samples (*e.g.* age, sex, sampling site) is often limited. Exceptions are long-term collections of scale samples for age surveillance of fish populations (*e.g.* Nielsen *et al.* 1999a, Heath *et al.* 2002, Meldgaard *et al.* 2003).

Most studies using historic samples have focussed on reconstructing phylogenies based on mitochondrial DNA sequence variability (*e.g.* Leonard *et al.* 2000, Hammond *et al.* 2001, Shapiro *et al.* 2002). In contrast, relatively few studies have addressed temporal population genetic structure by comparing the genetic diversity inferred from autosomal inherited genetic markers (*e.g.* microsatellites) between historic and contemporary samples (Bouzat *et al.* 1998, Nielsen *et al.* 1999a, Groombridge *et al.* 2000, Pertoldi *et al.* 2001, Walker *et al.* 2001, Larson *et al.* 2002, Miller & Waits 2003).

The present study assessed the dynamics of a red fox population in Switzerland following a rabies epizootic and investigates its effects on the demography and the genetic diversity of the population. Rabies is a viral infection in mammalian species of the central nervous system (Blancou *et al.* 1991). The principal hosts and vectors for the classical rabies are the domestic dog (urban rabies) and the red fox (silvatic rabies, Macdonald 1980). Red foxes are very susceptible to rabies infection (Macdonald & Voigt 1985) and dependent on the initial population density, their populations can be severely reduced by it (Anderson *et al.* 1981, Macdonald & Voigt 1985). Despite the high selective pressure imposed by the high rabies-induced mortality, red foxes seem however, not to have developed resistance to rabies (Macdonald & Voigt 1985). In this context, silvatic rabies differs from a general host-parasite evolution model, where the host's immune competence is thought to counteract parasite virulence (*e.g.* Wakelin & Apanius 1997). Consequently, the epidemic of rabies is tightly associated with the social structure, population dynamics and ecology of the red fox, the only vector species in Western Europe (*e.g.* Steck & Wandeler 1980, Macdonald 1980, Anderson *et al.* 1981). Based on the findings of numerous studies on fox density and social organisation, models of fox contact rate and its implication for rabies control have been developed (*e.g.* Trewhella & Harris 1988, White *et al.* 1995). In general, the dynamics of rabies is a function of fox density, dispersal and the carrying capacity of the habitat type (Steck & Wandeler 1980, Macdonald 1980, Funk 1994). The mass immunisation of the principal

wild host with live attenuated, and later recombinant vaccines, led to the successful establishment of oral immunisation of red foxes (Wandeler 2000).

The current silvatic rabies epizootic in Europe started in Poland in 1939 and subsequently spread westwards (Macdonald 1980). In Western Europe, the disease reached its maximum extension around the early 1980s, before oral vaccination campaigns led to a significant decrease in the number of rabies cases (Stöhr & Meslin 1996). At present, red fox rabies is no longer present in most initially infected Western European countries, while in Eastern Europe the epizootic has remained prevalent (www.who-rabies-bulletin.org).

The rabies epizootic reached Northern Switzerland in 1967 and subsequently swept through the country. In the 1980s, the cumulative area infected reached 55% of the total area of Switzerland, but following the successful initiation of oral wildlife vaccination, the disease was soon eliminated from most parts of Switzerland (Kappeler 1991). Since September 1996, no more rabid foxes have been recorded and in 1999, Switzerland was declared rabies-free according to WHO guidelines (Breitenmoser *et al.* 2000).

Since 1967, the European rabies epizootic has been thoroughly monitored by sampling red foxes throughout Switzerland. In addition, local hunting authorities recorded long-term roadkill and hunting data. By combining these post-mortem data with a comprehensive collection of historic tooth samples of foxes accumulated during the epizootic, this study aimed to assess the demography and genetic structure in a local red fox population before, during and after a rabies infection.
The study had three main objectives: i) To assess the population dynamics of red foxes over the last 35 years in relation to the observed number of recorded rabies cases. ii) To investigate the effect of the induced mortality on age structure and sex ratio. iii) To assess temporal genetic changes in genetic structure following the rabies epizootic by using polymorphic microsatellites markers.

Materials and Methods

Historic samples and study area

Between 1967 and 2000, hunters and game wardens provided more than 50,000 fox carcasses for the surveillance of the epizootic to the Swiss Rabies Centre at the University of Bern. Individual data for each fox was systematically recorded including date of delivery, sex, sampling site and results from the rabies virus test. For monitoring the oral wildlife vaccination, fox samples were additionally tested for the successful uptake of the vaccine bait. To discriminate between juveniles and adults the relative width of the pulp cavity of a canine tooth was measured using X-ray (Kappeler 1985). In order to extract the caninus tooth, the lower jaw of the fox carcass was removed and subsequently autoclaved with the objective to eradicate any potential rabies virus and to facilitate the removal of the tooth. Therefore, one tooth per fox sample was systematically collected and stored. Throughout the rabies epizootic, a total of over 28,000 individual tooth samples were systematically collected.

Figure 1 Location of the study area (411km^2; grey area) in the Canton Aargau, Switzerland. The dark and light lines represent rivers and approximate hunting ground boundaries, respectively.

Despite the large number of teeth available, samples were not randomly distributed in time or space. In general, sampling efforts were biased towards rabies-infected areas and vaccination zones. Since the objective of this study was to investigate a continuously sampled population over time, a confined study area was selected in Northern Switzerland (Canton Aargau). This 411km^2 area is encompassed by the two main rivers Rhine and Aare (Figure 1), which prevented the spread of the first rabies wave in 1967. However, in 1975 the epizootic swept across the whole region. Nevertheless, foxes were collected from 1967 onwards, thus providing pre- samples before the rabies infection hit the study area. Following some single positive rabies records in the late 1980s and the 1990s, a continuous surveillance of the disease and vaccination programme was necessary. To supplement the historic tooth collection, recent tissue samples were provided by the local hunting authorities in 2001-02.

Rabies epidemic and demographic data

Based on the available data records from the study area, the annual numbers of observed positive rabies cases per km^2 (rabies index), and the annual and three-year sliding means for female and juvenile proportions of the red fox population studied were computed. Additionally, a number of historic and recently collected teeth from adult foxes were accurately aged; the root-tip was removed and subsequently aged by counting annual cementum lines following a modified protocol by Kappeler (1985) based on Grue & Jensen's (1973) method[6]. Annual mean and three-year sliding means for adult age were computed. Furthermore, the age distribution based on accurate individual age data from adult foxes collected in 1971-73, 1983-85 and 1996-98 was tested in a contingency table. Hence an unbiased estimate of the p - value of the probability test (Fisher's exact test) was performed by a Markov chain method using the sub-program STRUCT implemented in GENEPOP (Raymond & Rousset 1995b).

To assess the red fox population dynamics, an additional and independent data set of the annual number of foxes killed by traffic (roads and rails) and hunting was provided by the hunting authorities of the Canton Aargau for the study area between 1970 and 1967, respectively. These data records were based on individual or joint local hunting grounds on a borough level (Figure 1). To account for missing data and the size of individual hunting grounds, roadkill and hunting data were recorded as the number of foxes killed

[6] All tooth samples were aged by Matthias Ulrich, Bern, CH.

per km^2 (roadkill index and hunting index) for each hunting ground. Annual means, three-year sliding means and standard errors (*SE*) across grounds were computed. Finally, the annual growth rate of the fox populations was calculated as: $r_i = ln\ (N_{[roadkill\text{-}index]\ i} / N_{[roadkill\text{-}index]\ i\text{-}1})$ (McCallum 2000). All data records and analyses were based on biological years by assuming that all foxes were born on the 1st April.

Laboratory work

Only individual samples with a complete record, i.e. accurate age, date of delivery, sex, sampling site, rabies test results and an undamaged tooth sample, were selected for genetic analyses. DNA was extracted from the tooth using a silica-based spin column (QIAquick® – PCR purification kits, Qiagen). In brief, the whole canine tooth or the remaining tooth crown (≈ 0.7g) for juveniles and accurately aged adults, respectively, were ground to powder using a steel mortar. After decalcification (EDTA, pH8.0, 0.5M, 72h), samples were digested (proteinase K) twice overnight. DNA was bound to the silica membrane by vacuuming the supernatant through the QIAquick column, purified following the manufacturers protocol (for details see Chapter 1) and finally eluted in 200μL of H_20. DNA from recent tissue samples was extracted using a DNeasy® tissue kit (Qiagen).

Based on the results of successful PCR amplification in historic tooth extracts in relation to different microsatellite loci in size (Chapter 1), only loci were used with less than 170 bps of maximum fragment size. Nine canine microsatellite loci (AHT-130, Holmes *et al.* 1995; CXX-156, CXX-250, CXX-279, CXX-434, CXX-466, CXX-606, CXX-608 Ostrander *et al.* 1993, 1995; and c2088; Francisco *et al.* 1996) and seven re-designed red fox-specific canine microsatellite (V142, V374, V402, V468, V502, V602, V622; Chapter 2) were used in this study. Single PCR reactions for loci AHT-130, CXX-156, CXX-250, CXX-434, CXX-466, CXX-608 and c2088 were performed in a total volume of 6μL containing 2μL of template DNA, following a hotstart PCR protocol (for details see Chapter 1). For all other loci, PCR efficiency and success was significantly improved by using Qiagen's PCR multiplex kit. Between two and three loci were co-amplified. PCR was carried out in a total volume of 8μL containing 4μL of multiplex PCR master-mix, 1.2μg BSA, 0.08-0.4μM of each primer and 3μL of template DNA. PCR amplifications were performed in a GeneAmp® PCR System 9700 (ABI) using the following cycling parameters: 12mins of initial denaturation at 95°C, followed by 40

cycles of 30s at 94°C, 120s at 58°C and 60s extension at 72°C, with a final extension of 30mins at 60°C. All PCR products were electrophoretically separated using an ABI Prism® 377 DNA sequencer (ABI). Allele sizes were scored against the size standard GS350 Tamra™ (ABI) using GENESCAN™ Analysis and GENOTYPE™ software.

To account for allelic drop-out and false alleles by PCR amplification of microsatellite loci from highly diluted DNA (*e.g.* Navidi *et al.* 1992, Gagneaux *et al.* 1997, Morin *et al.* 2001, Chapter 1), the nuclear DNA concentration for all individual tooth samples was initially estimated by a quantitative PCR (5' exonuclease assay), which targets a 81 bps portion of the highly conserved *c-myc proto-oncogene* (Morin *et al.* 2001, for details see Chapter 1). Only samples with an estimated DNA concentration of 5 pg/μL or more were considered for subsequent microsatellite genotyping. Heterozygote genotypes were independently and successfully amplified at least twice, whereas homozygote genotypes were repeated according to the estimated DNA concentration (Morin *et al.* 2001). Hence, extracts with an estimated concentration of more than 200pg for a single PCR reaction were amplified twice, samples between 100 – 200pg, four times and extracts with less than 100pg at least five times. DNA extraction of all tooth samples and PCR mix preparations were performed within a spatially isolated laboratory dedicated for working with low-copy DNA samples. Special care was taken to avoid cross-contamination and contamination with contemporary DNA. Quantitative PCR assays were carried out at the Laboratories for Conservation Genetics in Leipzig, Germany.

Population genetic analyses

Global estimates of single locus genetic diversity (H_E; Nei 1987) and observed heterozygosity (H_O) across all samples and years were computed in GENEPOP (Raymond & Rousset 1995b). Genotypic linkage disequilibrium between all pairs of loci (Garnier-Gere & Dillmann 1992) was tested in GENEPOP. Using the same software, single and multilocus deviation from Hardy-Weinberg equilibrium was tested (probability test). Annual estimates for H_E, H_O and the inbreeding coefficient F_{IS} (Weir & Cockerham 1984) were calculated using the same software package. Further, to estimate the allelic diversity (A_3), the mean number and *SE* of detected alleles across all loci were permuted (1000 iterations) for a minimum number of three individuals for each year using POPASSIGN (Funk, *unpublished*). To account for missing genotypes, permutations were computed for each locus independently. A genic differentiation test

across all annual samples was applied to test for the global allelic distribution using GENEPOP (Raymond & Rousset 1995b). For each locus a contingency table was computed and an unbiased estimate of the p - value of the probability test was performed (Raymond & Rousset 1995a). Subsequently, single locus probability values were combined according to Fisher's method (Sokal & Rolf 1995). Because alleles are expected to be lost faster than heterozygosity following a demographic bottleneck (Luikart & Cornuet 1998), annual A_3 and H_E measures were correlated to identify a potential recent bottleneck. For all population genetic analyses on an annual basis, individual samples were allocated to their year of birth, with the exception of nine temporally isolated individuals, which were assigned to either the previous or the following year.

To establish a smoother function of the observed genetic estimates over time, annual multilocus means were also computed for H_E, H_O, F_{IS} and A_3 by including all individual samples born within a time period of three years. In contrast to the single annual values, an individual sample could thus be represented in up to three annual genetic estimates. Finally, global genic differentiation and F_{ST} - values were computed across all individual samples from 1971-73, 1983-85 and 1996-98.

Results

Population dynamics and demography

Annual roadkill and hunting data were available for up to 40 local hunting grounds and combined, represented 95.6% (mean: 9.8km^2; min – max: 2.5 – 30.5km^2) of the total size of the study area (Table 1). From 1967 to 2000 a total of 2658 fox carcasses from the study area were posted to the Rabies Centre. 742 foxes were tested rabies positive, peaking in 1975 with 558 recorded cases (rabies index = 1.36). The whole region remained rabies-infected until 1984 and was re-infected in the first half of the 1990s (Table 1; Figure 2). Between 1984-86 and 1989-98, the red fox population studied was subjected to oral rabies vaccination. Post-mortem data on sex and age (juvenile and adults) were recorded for 1612 and 1628 individuals, respectively. The absence of data recording was prominent for the first three years of rabies surveillance and during the

first rabies wave between 1974 and 1976, while from 1978 onwards, records were complete. A total of 561 adult individuals were accurately aged (Table 1).

A positive correlation between the roadkill and hunting index was observed and subsequently improved when an outlier (1975) was excluded (roadkill index = 0.013 + 3.54*hunting index; r = 0.93, n = 30). After the first rabies infection in 1975, the roadkill index in 1976 dropped from 0.445 to 0.0175 by 79.2%, indicating a severe decline in population size. However, following the rabies-induced population crash, the roadkill index increased by over 600%, therefore exceeding pre-rabies population size from the mid-1980s onwards. The dynamics of this population can be divided into three periods: 'pre-rabies' (≤ 1976), 'recovery and growth' (1977-94) and 'carrying capacity' (≥ 1995; Figure 2). Finally, the average annual population growth rate between 1970 and 2000 was 0.031.

Mean ± *SD* of female and juvenile proportion across all years was 0.45 ± 0.08 and 0.47 ± 0.13, respectively (Table 1). During the period of population recovery the estimated proportion of juveniles declined from 56% to 40% (juvenile proportion = 20.5 - 0.0101*year; n = 17; r = -0.51; Figure 2). Although there was no apparent trend for the sex ratio observed, the proportion of recorded females in relation to males was low between 1981 and 1988 (0.35 – 0.44). The ratio between rabies-infected and non-infected foxes was not affected by sex or age (adults versus juveniles), although the observed proportion of infected males compared to females tended to be higher (sex: $X^2_{1;1612}$ = 3.008; p = 0.08; age: $X^2_{1;1628}$ = 0.73; p>0.39; Chi–square test). Following the first rabies infection, average adult individual observations increased from 1.78 (1984) to 2.86 years (1994) during the population growth period (mean adult age = -211.1 + 0.107*year; n = 10; r = 0.85; Figure 2). The observed distribution of adult age classes for 1971-73, 1983-85 and 1996-98 differed significantly ($p < 0.009$, Table 2). Finally, no adult individual collected and accurately aged between 1983 and 1985 (n = 63) was older than five years (Table 2).

Table 1 Summary of the demographic and epidemic data for a red fox population (Canton Aargau, Switzerland) following a rabies epizootic from 1966-2001. Shown are the annual (biological year) data / estimates for sample size of provided foxes and recovered individual tooth samples, absolute number of recorded rabies cases and rabies index (recorded positive cases per km^2), oral vaccination (yes / no), female and juvenile population ratios, average adult age, average (± *SE*) roadkill and hunting index and growth rate (McCallum 2000).

Year	Sample size		Rabies & Vaccination			Sex ratio & Age structure						Roadkill & Growth rate				Hunting		
	Foxes	Teeth	Rabies cases		Vacc.	Female prop.		Juvenile prop.		Adult age		Index (cases/km^2)			Growth	Index (cases/km^2)		
	N	*N*	*N*	*index*	*yes/no*	*Mean*	*N*	*Mean*	*N*	*Mean*	*N*	*Mean*	*SE*	*N*	*r*	*Mean*	*SE*	*N*
1966	-	-	-	-	-	-	-	-	-	-	-	-	-	-	-	1.89	1.37	38
1967	38	0	0	0.000	0	-	-	-	-	-	-	-	-	-	-	2.32	1.06	38
1968	32	0	0	0.000	0	0.38	13	0.69	13	-	-	-	-	-	-	1.32	0.81	32
1969	13	4	0	0.000	0	0.60	10	0.40	10	3.00	3	-	-	-	-	0.86	0.68	32
1970	7	4	0	0.000	0	0.50	6	0.29	7	1.00	3	0.18	0.17	35	-	0.74	0.61	38
1971	89	10	0	0.000	0	0.47	87	0.80	87	2.00	14	0.26	0.30	39	0.56	0.87	0.53	38
1972	177	70	0	0.000	0	0.47	177	0.51	176	2.35	62	0.34	0.35	40	0.17	1.36	0.71	38
1973	133	45	0	0.000	0	0.52	111	0.47	111	2.07	44	0.27	0.25	40	-0.34	1.27	0.88	38
1974	115	0	3	0.007	0	-	-	-	-	-	-	0.44	0.33	38	0.29	2.02	1.05	38
1975	854	25	558	1.358	0	0.33	39	0.46	37	3.10	10	0.43	0.44	33	0.29	4.98	2.71	37
1976	6	0	2	0.005	0	-	-	-	-	-	-	0.09	0.17	40	-0.94	0.32	0.31	38
1977	4	0	0	0.000	0	-	-	-	-	-	-	0.14	0.21	40	0.17	0.35	0.32	38
1978	10	3	5	0.012	0	0.56	9	0.60	10	-	-	0.15	0.21	40	0.00	0.48	0.42	38
1979	56	4	45	0.109	0	0.40	55	0.60	55	1.67	3	0.17	0.24	39	0.14	1.12	0.78	37
1980	10	0	9	0.022	0	0.56	9	0.44	9	-	-	0.11	0.16	40	-0.42	0.29	0.36	38
1981	23	0	16	0.039	0	0.35	23	0.70	23	-	-	0.14	0.23	40	0.37	0.27	0.32	38
1982	10	1	7	0.017	0	0.44	9	0.40	10	-	-	0.12	0.17	40	-0.26	0.30	0.29	38
1983	25	1	15	0.036	0	0.42	24	0.54	24	-	-	0.21	0.24	40	0.32	0.34	0.29	38
1984	70	71	24	0.058	1	0.35	66	0.39	70	1.53	43	0.21	0.23	40	-0.03	0.40	0.41	38
1985	67	62	0	0.000	1	0.35	65	0.63	67	1.75	20	0.26	0.30	39	0.25	0.70	0.49	38
1986	82	78	0	0.000	1	0.41	79	0.52	82	2.14	36	0.24	0.21	39	-0.37	0.97	0.53	38
1987	45	23	0	0.000	0	0.43	44	0.53	45	-	1	0.41	0.43	39	0.74	1.42	0.86	38
1988	25	23	0	0.000	0	0.36	25	0.36	25	2.42	12	0.50	0.40	39	-0.07	1.51	0.88	38
1989	50	49	1	0.002	1	0.50	48	0.37	49	1.92	26	0.50	0.42	39	0.04	2.48	1.93	37
1990	34	33	1	0.002	1	0.53	34	0.53	34	2.25	8	0.51	0.34	39	-0.20	2.54	1.72	38
1991	136	130	1	0.002	1	0.46	136	0.42	136	2.43	60	0.58	0.40	40	0.15	2.35	1.35	38
1992	91	88	5	0.012	1	0.36	91	0.41	91	2.57	44	0.61	0.50	38	0.22	1.61	0.99	38
1993	116	109	19	0.046	1	0.45	114	0.43	116	3.00	47	0.60	0.38	40	-0.26	2.18	1.23	38
1994	135	117	29	0.071	1	0.45	133	0.45	135	2.50	26	0.73	0.44	40	0.15	2.11	1.17	38
1995	65	53	2	0.005	1	0.49	65	0.28	65	3.09	33	0.61	0.44	40	-0.01	2.22	1.03	38
1996	50	47	0	0.000	1	0.43	49	0.44	50	2.92	24	0.69	0.45	40	0.02	2.29	1.28	38
1997	25	24	0	0.000	1	0.44	25	0.20	25	2.27	15	0.62	0.38	40	-0.17	2.16	1.00	38
1998	35	33	-	-	1	0.49	35	0.37	35	3.00	14	0.58	0.39	40	0.05	2.23	1.36	38
1999	12	5	-	-	0	0.58	12	0.50	12	3.50	2	0.71	0.46	40	0.16	2.48	1.45	38
2000	2	2	-	-	0	-	-	-	-	-	2	0.78	0.42	40	-0.07	2.58	1.79	38
2001	16	16	-	-	0	0.3125	16	0.44	16	2	9	-	-	-	-	-	-	-
Mean	75.9	32.3	-	-	-	0.447	-	0.472	-	2.369	-	0.394	0.324	-	0.031	1.524	0.941	-
SD	-	-	-	-	-	0.077	-	0.130	-	0.602	-	0.218	0.106	-	-	1.005	0.549	-
Total	2658	1130	742	-	13	-	1609	-	1625	-	561	-	-	-	-	-	-	-

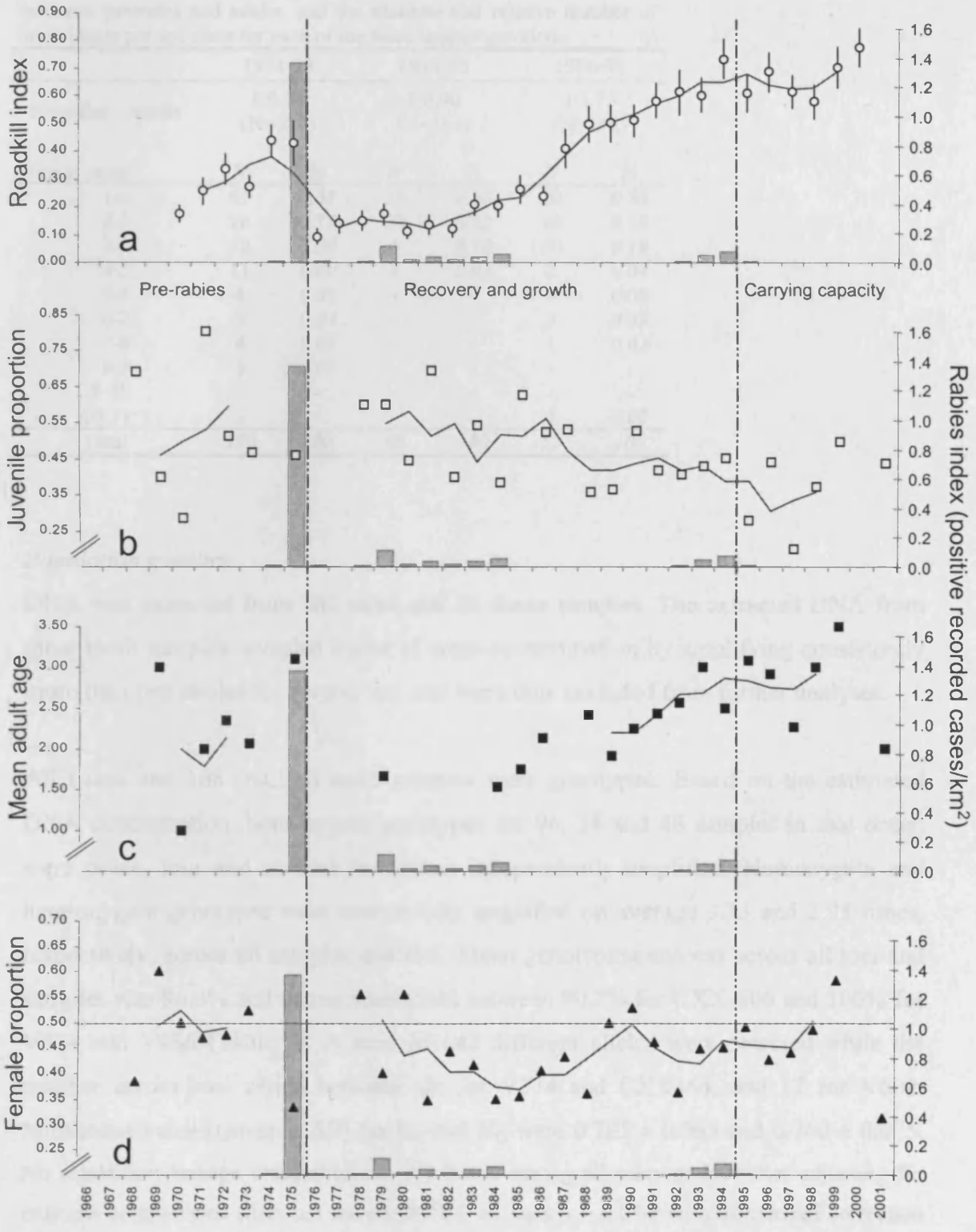

Figure 2 The dynamics of population size (mean ± SE, roadkill index; a), juvenile proportion (b), average adult age (c) and sex ratio (female proportion; d) of a red fox population (Aargau, Switzerland) in relation to a rabies epizootic (rabies index, grey bars) from 1966-2001. Shown are annual means (symbols) and three-year sliding means. (For details see Table 1).

Table 2 Age distribution of a red fox population (Aargau, Switzerland) for three time periods following a rabies epizootic. Shown are the ratios between juveniles and adults, and the absolute and relative number of individuals per age class for each of the three sampling periods.

	1971-73		1983-85		1996-98	
Juveniles : Adults	1:0.76 (N=374)		1:0.96 (N=161)		1:1.75 (N=110)	
Age in years	*N*	*%*	*N*	*%*	*N*	*%*
1-2	65	*0.54*	35	*0.56*	20	*0.38*
2-3	20	*0.17*	20	*0.32*	10	*0.19*
3-4	10	*0.08*	6	*0.10*	10	*0.19*
4-5	11	*0.09*	2	*0.03*	2	*0.04*
5-6	4	*0.03*	-	-	4	*0.08*
6-7	5	*0.04*	-	-	5	*0.09*
7-8	4	*0.03*	-	-	1	*0.02*
8-9	1	*0.01*	-	-	-	-
9-10	-	-	-	-	-	-
10-11	-	-	-	-	1	*0.02*
Total	120	*100*	63	*100*	53	*100*

Population genetics

DNA was extracted from 262 tooth and 16 tissue samples. The extracted DNA from three tooth samples revealed traces of cross-contamination by amplifying consistently more than two alleles for several loci and were thus excluded from further analyses.

All tissue and 168 (64.1%) tooth samples were genotyped. Based on the estimated DNA concentration, homozygote genotypes for 96, 24 and 48 samples in that order, were twice, four and at least five times independently amplified. Homozygote and heterozygote genotypes were successfully amplified on average 3.33 and 2.95 times, respectively, across all samples and loci. Mean genotyping success across all loci and samples was 96.3% and varied across loci between 90.2% for CXX-606 and 100% for V374 and V486 (Table 3). A total of 142 different alleles were detected while the number across loci varied between six for V374 and CXX466, and 17 for V602. Multilocus values (mean ± *SD*) for H_E and H_O were 0.785 ± 0.065 and 0.760 ± 0.075. No significant linkage disequilibrium was found among all pairs of loci after adjusting for multiple comparisons (data not shown; k=136; all tests $p > 0.05/k$ with Bonferroni correction of $\alpha = 0.05$). None of the loci departed from Hardy-Weinberg equilibrium after Bonferroni correction for multiple testing ($\alpha = 0.05$; k =16), but the global multilocus value deviated significantly (Fisher's method: $p < 0.0002$). A slightly positive F_{IS} - value (mean ± *SD*) of 0.032 ± 060 across loci was observed (Table 3).

Table 3 Summary of the observed genetic diversity, PCR success and the number of independent PCR repetitions for accurate microsatellite genotyping across all historic (n= 168) and recent (n = 16) red fox samples collected continuously over 35 years. Shown are single-locus values for the absolute and relative number of successful genotyping, average number of independent and successful PCR repetitions for homozygote (*Hom*) and heterozygote (*Het*) genotypes, range of microsatellite fragment size, number of detected alleles (*A*), expected (H_E; Nei 1987) and observed heterozygosity (H_O), inbreeding coefficient (F_{IS}; Weir & Cockerham 1984) and *p* - values for Hardy-Weinberg deviation.

	PCR success & PCR repetitions						Genetic diversity & Test for HW-deviation				
	Success*		Repetitions[a]		Fragment-size [bps]						HW-test[b]
Locus	N	%	*Hom*	*Het*	*Min*	*Max*	*A*	H_E	H_O	F_{IS}	*p**
AHT-130	167	99.5	4.36	3.51	98	120	8	0.741	0.743	-0.003	0.047
V142	159	95.1	2.58	2.62	133	147	10	0.875	0.840	0.040	0.589
CXX-156	161	96.2	3.15	2.95	131	131	9	0.797	0.746	0.064	0.023
CXX-250	161	96.2	3.44	2.63	124	140	9	0.805	0.802	0.003	0.091
CXX-279	161	96.2	2.79	2.65	114	142	9	0.788	0.825	-0.047	0.315
V374	168	100.0	3.78	3.92	106	118	6	0.813	0.766	0.057	0.086
V402	167	99.5	2.91	2.39	78	90	7	0.784	0.798	-0.018	0.234
CXX-434	158	94.6	4.15	3.37	102	110	7	0.709	0.655	0.076	0.385
CXX-466	162	96.7	3.74	3.98	144	154	6	0.735	0.787	-0.071	0.179
V486	168	100.0	3.11	2.98	82	98	9	0.835	0.793	0.049	0.728
V502	166	98.9	2.87	2.17	79	95	9	0.656	0.560	0.146	0.071
V602	164	97.8	3.52	3.00	140	172	17	0.904	0.878	0.029	0.076
CXX-606	150	90.2	2.66	2.43	152	166	8	0.709	0.735	-0.037	0.565
CXX-608	158	94.6	2.82	2.75	129	147	8	0.778	0.770	0.010	0.056
V622	153	91.8	2.95	2.59	91	119	9	0.835	0.763	0.086	0.020
c2088	156	93.5	4.09	3.01	116	156	11	0.802	0.703	0.124	0.015
Mean	**161.2**	**96.3**	**3.33**	**2.95**	**113.7**	**131.6**	**8.88**	**0.785**	**0.760**	**0.032**	**0.0002**
SD	5.4	-	0.57	0.53	23.8	25.4	2.55	0.064	0.075	0.060	-

[a] Based on historic samples only.
[b] *p* - value (probability test; Raymond & Rousset 1995a) before Bonferroni correction for multiple testing.

The temporal allelic distribution across loci and the 27 annual samples did not differ significantly (Fisher's method, $X^2 = 45.39$; $df = 32$; $p > 0.059$), although the computed p – value was just outside the significance level of 0.05. The dynamics of the annual and the combined three year multilocus means for H_E, H_O, A_3 and F_{IS} are shown in Table 4 and Figure 3. None of the temporal trends of H_E, H_O and A_3 indicated a reduction of genetic diversity following the rabies-induced population crash in 1975. Indeed, H_E and A_3 demonstrated a slightly higher genetic diversity after the epidemic (Figure 3).

Table 4 Summary of the population genetic estimates for a red fox population (Aargau, Switzerland) following a rabies epizootic from 1966-2001. Shown are the sample size for extracted historic tooth samples (N_{EX}), successful genotyped samples (N_{GT}), samples sorted by year of birth (N_B), samples used to calculate annual estimates for one year only (N_1) and for three years pooled (N_3). Annual multilocus means and *SE* (across loci) for the inbreeding coefficient (F_{IS}; Nei 1987), expected (H_E; Nei 1987) and observed heterozygosity (H_O), and allelic richness (randomised across three individuals) are calculated for one year and three years pooled.

Year	Sample size					Annual population genetics (one year)								Annual population genetics (three years pooled)							
	N_{EX}	N_{GT}	N_B	N_1	N_3	F_{IS}		H_E		H_O		A_3		F_{IS}		H_E		H_O		A_3	
						mean	*SE*	mean	*SE*	mean	*SE*	mean	*SE*	mean	*SE*	mean	*SE*	mean	*SE*	mean	*SE*
1966	-	-	4	5	-	0.101	0.067	0.735	0.039	0.669	0.060	3.455	0.210	-	-	-	-	-	-	-	-
1967	-	-	1		10	-	-	-	-	-	-	-	-	0.065	0.043	0.755	0.026	0.717	0.047	3.526	0.167
1968	-	-	5	5	8	-0.047	0.053	0.748	0.041	0.778	0.059	3.533	0.246	-0.030	0.054	0.753	0.027	0.772	0.046	3.511	0.177
1969	4	2	2	-	10	-	-	-	-	-	-	-	-	-0.055	0.060	0.753	0.029	0.784	0.044	3.542	0.198
1970	4	0	3	5	12	-0.064	0.092	0.765	0.029	0.797	0.062	3.525	0.233	0.007	0.035	0.787	0.020	0.778	0.029	3.724	0.150
1971	5	0	7	7	17	0.042	0.050	0.805	0.022	0.776	0.046	3.819	0.179	0.045	0.035	0.784	0.019	0.750	0.033	3.707	0.140
1972	44	20	7	8	15	0.074	0.055	0.770	0.023	0.720	0.048	3.623	0.161	0.049	0.040	0.784	0.020	0.748	0.039	3.705	0.150
1973	29	5	1	-	9	-	-	-	-	-	-	-	-	0.074	0.050	0.766	0.022	0.716	0.045	3.582	0.150
1974	0	0	1	-	8	-	-	-	-	-	-	-	-	0.084	0.065	0.761	0.031	0.698	0.055	3.519	0.157
1975	18	10	6	7		0.060	0.060	0.746	0.039	0.704	0.058	3.493	0.184	-	-	-	-	-	-	-	-
1976	0	0	-	-	-	-	-	-	-	-	-	-	-	-	-	-	-	-	-	-	-
1977	0	0	-	-	-	-	-	-	-	-	-	-	-	-	-	-	-	-	-	-	-
1978	3	2	3	5	-	0.095	0.041	0.810	0.022	0.738	0.035	3.828	0.169	-	-	-	-	-	-	-	-
1979	4	1	2	-	6	-	-	-	-	-	-	-	-	0.084	0.035	0.799	0.022	0.738	0.034	3.785	0.158
1980	0	0	1	-	6	-	-	-	-	-	-	-	-	0.037	0.046	0.772	0.024	0.748	0.043	3.656	0.157
1981	0	0	3	4	11	0.041	0.082	0.789	0.031	0.766	0.070	3.737	0.171	0.025	0.044	0.766	0.022	0.747	0.039	3.583	0.136
1982	1	0	7	7	18	0.031	0.060	0.766	0.025	0.738	0.044	3.537	0.170	0.002	0.032	0.771	0.017	0.769	0.028	3.618	0.115
1983	0	0	8	8	22	-0.036	0.051	0.773	0.020	0.796	0.040	3.666	0.117	0.002	0.030	0.771	0.017	0.771	0.030	3.631	0.118
1984	22	19	7	7	20	-0.002	0.069	0.777	0.026	0.774	0.055	3.655	0.183	-0.021	0.030	0.777	0.017	0.792	0.026	3.687	0.114
1985	10	4	5	5	20	-0.008	0.044	0.808	0.016	0.814	0.037	3.808	0.141	0.030	0.028	0.797	0.014	0.775	0.029	3.736	0.130
1986	16	13	8	8	19	0.089	0.057	0.812	0.017	0.746	0.050	3.791	0.154	0.017	0.029	0.796	0.015	0.780	0.024	3.735	0.120
1987	3	2	6	6	20	-0.026	0.057	0.785	0.021	0.794	0.036	3.735	0.162	0.037	0.029	0.803	0.016	0.771	0.023	3.762	0.125
1988	4	4	6	6	19	-0.017	0.061	0.778	0.021	0.781	0.039	3.633	0.121	-0.021	0.029	0.781	0.020	0.793	0.022	3.696	0.136
1989	8	6	7	7	19	-0.034	0.066	0.764	0.030	0.793	0.058	3.652	0.222	-0.019	0.029	0.775	0.021	0.786	0.024	3.650	0.152
1990	3	3	6	6	20	-0.024	0.052	0.770	0.025	0.777	0.034	3.577	0.180	-0.033	0.035	0.785	0.021	0.809	0.030	3.735	0.153
1991	13	8	7	7	21	-0.033	0.033	0.823	0.018	0.847	0.031	3.986	0.166	0.000	0.031	0.776	0.019	0.775	0.028	3.647	0.152
1992	10	10	8	8	22	0.070	0.052	0.763	0.024	0.711	0.042	3.559	0.175	0.055	0.026	0.786	0.018	0.744	0.026	3.684	0.136
1993	10	8	7	7	23	0.137	0.067	0.783	0.024	0.677	0.056	3.573	0.175	0.075	0.035	0.787	0.018	0.729	0.031	3.669	0.139
1994	9	9	8	8	23	0.035	0.060	0.814	0.020	0.789	0.051	3.901	0.154	0.051	0.034	0.795	0.017	0.757	0.031	3.740	0.133
1995	9	9	8	8	24	-0.012	0.045	0.784	0.018	0.789	0.032	3.702	0.134	0.040	0.038	0.794	0.016	0.763	0.033	3.729	0.111
1996	12	12	8	8	25	0.093	0.057	0.785	0.020	0.711	0.042	3.605	0.123	0.015	0.026	0.787	0.016	0.775	0.024	3.692	0.118
1997	8	8	9	9	23	-0.031	0.042	0.797	0.017	0.819	0.036	3.807	0.149	0.033	0.026	0.780	0.016	0.753	0.021	3.633	0.115
1998	10	10	6	6	22	0.085	0.042	0.772	0.021	0.708	0.032	3.559	0.162	0.007	0.030	0.778	0.018	0.772	0.028	3.677	0.136
1999	3	3	7	8	14	0.012	0.052	0.780	0.027	0.765	0.039	3.696	0.177	0.039	0.040	0.774	0.022	0.740	0.029	3.645	0.152
2000	0	0	1	-	17	-	-	-	-	-	-	-	-	0.063	0.030	0.790	0.021	0.742	0.029	3.723	0.149
2001	*16	*16	9	9	-	0.085	0.035	0.787	0.023	0.722	0.032	3.713	0.142	-	-	-	-	-	-	-	-
Mea	-	-	-	-	-	0.027	0.056	0.781	0.024	0.759	0.045	3.673	0.169	0.025	0.036	0.779	0.020	0.760	0.032	3.664	0.141
Total	278	184	184	184	-	-	-	-	-	-	-	-	-	-	-	-	-	-	-	-	-

* Tissue sample

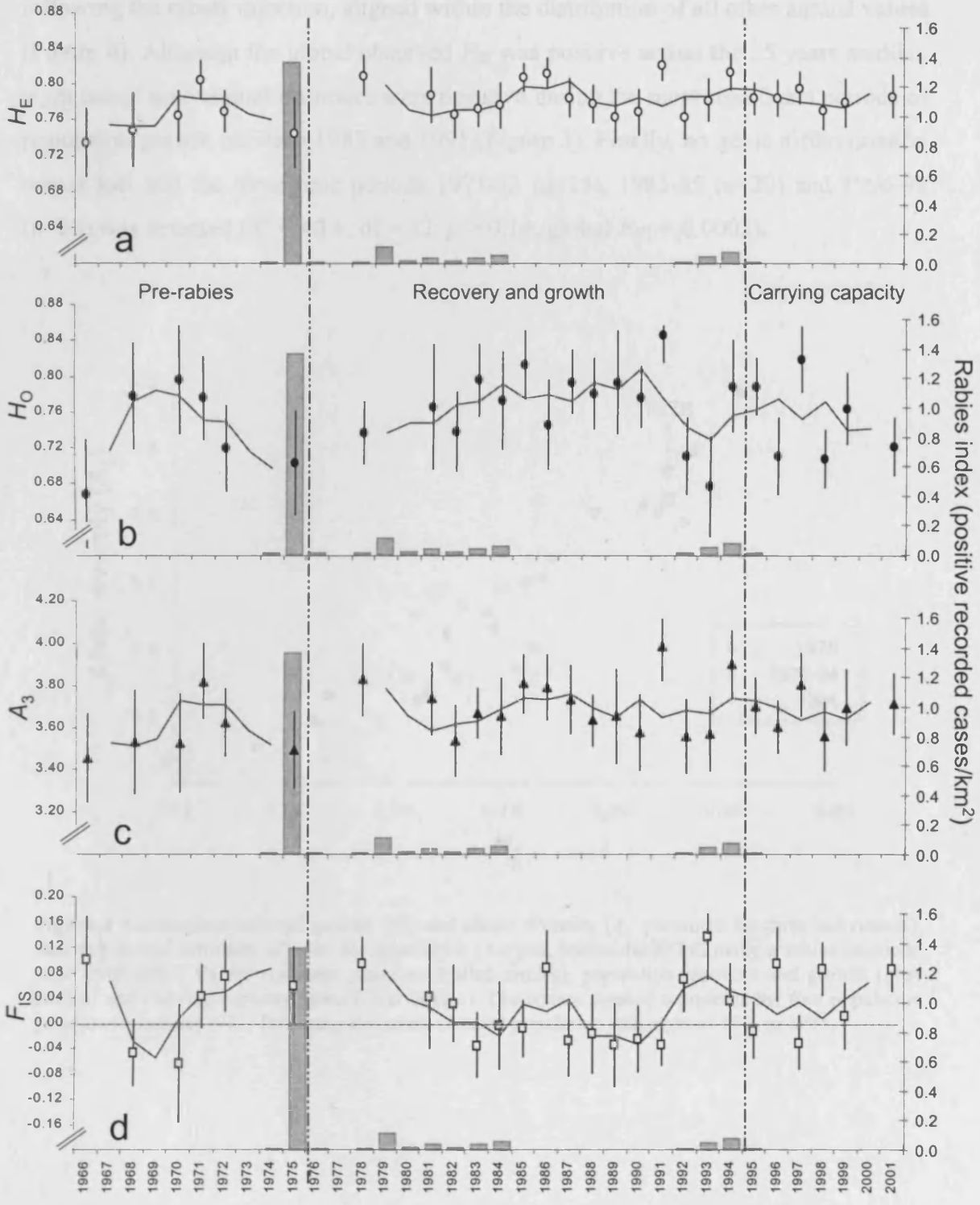

Figure 3 Temporal population genetics of a red fox population (Aargau, Switzerland) following a rabies epizootic from 1966-2001. Shown are the annual means (symbols) ± *SE* (calculated across loci) and three-year means (lines) for expected (a; H_E) and observed heterozygosity (b; H_O), allelic richness (c; A_3, permuted for three individuals) and inbreeding coefficient (d; F_{IS}). Grey bars represent the annual number of recorded rabies cases in red foxes (rabies index). For details see Table 1 and 4.

The first annual estimate obtained for H_E and A_3 (1978), after the population reduction following the rabies infection, aligned within the distribution of all other annual values (Figure 4). Although the global observed F_{IS} was positive across the 35 years studied, eight out of nine annual estimates were negative during the most significant periods of population growth between 1983 and 1991 (Figure 3). Finally, no genic differentiation across loci and the three time periods 1971-73 (n=15), 1983-85 (n=20) and 1996-98 (n=23) was detected ($X^2 = 40.6$; df = 32; $p > 0.14$; global $F_{ST} = 0.0002$).

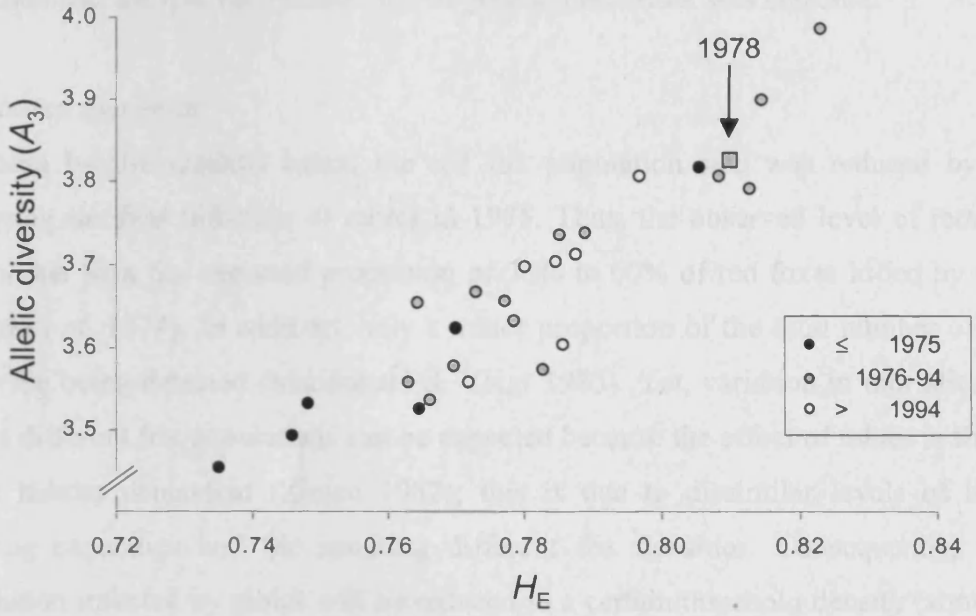

Figure 4 Relationship between genetic (H_E) and allelic diversity (A_3; permuted for three individuals), showing annual estimates of a red fox population (Aargau, Switzerland) following a rabies epizootic from 1966-2001. Values represent pre-rabies (filled circles), population recovery and growth (grey circles) and carrying capacity phase (clear circles). The square symbol represents the first population genetic estimation (1978) following the rabies-induced population reduction of 79% in 1975.

Discussion

A combination of detailed and long-term epidemiological, demographic and population genetic data enabled questions on the effects of a rabies epizootic on the population dynamics, age structure and genetic diversity in a local red fox population to be addressed. The main findings were as follows: i) Following the rabies outbreak, the red fox population was estimated to be reduced by 79%. Subsequent to this reduction the population size increased by over 600% until it most likely reached its carrying capacity. ii) The age distribution altered over time following the population reduction and the recovery phase. iii) No genetic bottleneck was detected.

Population dynamics

Indicated by the roadkill index, the red fox population size was reduced by 79% following the first infection of rabies in 1975. Thus, the observed level of reduction was higher than the expected proportion of 50% to 60% of red foxes killed by rabies (Bögel *et al.* 1974). In addition, only a minor proportion of the total number of rabid foxes are being detected (Macdonald & Voigt 1985). Yet, variation in mortality rates across different fox populations can be expected because the effect of rabies is thought to be habitat dependent (Zimen 1982); this is due to dissimilar levels of habitat carrying capacities and the resulting different fox densities. Consequently, a fox population infected by rabies will be reduced to a certain threshold density (about one fox per km^2), where the epizootic cannot be transmitted further independently from its preliminary density (*see also* Anderson *et al.* 1981). Similar levels of mortality (70%) were recorded in Scandinavian red fox populations, which were infested by sarcoptic mange (Lindström *et al.* 1994). Furthermore, Young (1994) reported levels of die-offs between 50-85% for different diseases and carnivore species. However, it is important to emphasise that rabies-induced mortality might be much higher, when the disease is transmitted via a sympatric reservoir host. For example, severe population declines were reported in the Ethiopian wolf *Canis simiensis* (*see* Sillerio-Zubiri *et al.* 1996) and the African wild dog *Lycaon pictus* (*see* Alexander *et al.* 1993) after transmission of rabies through domestic dogs.

Human intervention such as disproportionately high hunting pressure during the peak of the rabies epizootic in 1975 is likely to have affected the observed population

reduction. In fact, more than 2000 foxes were culled in the study area during the first year of the rabies epizootic. In contrast, it can be speculated that most of these foxes would have been killed by rabies nonetheless. It can be assumed, that the fox density dropped substantially below the expected threshold of one fox per km^2. The low number or absence of recorded rabies cases in the following three years (1976-78) further supports this assumption. Hence, the population size for the study area ($411km^2$) following the first rabies infection could have significantly dropped below 400 individuals.

In 1988, the population reached the same density as before the rabies outbreak. The red fox population continued to grow until it reached a population plateau in the mid-1990s. Furthermore, fox abundance subsequently experienced a two-fold increase following the progressive elimination of rabies. Indeed, this observation is consistent with the general trend of a current high abundance of red foxes in Switzerland (Breitenmoser, *unpublished data*) and Europe (*reviewed in* Chautan *et al.* 2000). Moreover, this highlights the mounting potential of re-infection of rabies or infection of other zoonoses (Chautan *et al.* 2000).

Finally, it is important to emphasise, that although the study area was unaffected by the first rabies wave between 1968-70, the red fox population studied was nonetheless subject to population control measures such as gassing of dens (until 1972) and high hunting pressure. Therefore, the population dynamic and the pre-rabies data on population demography and genetic might have been altered by human interventions and do not precisely reflect an altogether rabies unbiased population structure.

Demography and age structure

The observed age distribution changed significantly over time. The high rabies-induced mortality alongside human intervention in 1975, lead to a significant reduction in adult average age and an increase in the proportion of juveniles in the subsequent decade. Moreover, the age distribution continued to change after reaching pre-rabies density. Given the age distribution before the rabies infection, only a small number of adult animals older than three years would have survived the epizootic. Indeed, no individual older than five years was found between 1976 and 1985.

Following the observed reduction of population size, an increased reproduction could have compensated for the observed losses and could have consequently advanced the long-term population growth. The reproduction of fox populations depends on litter size and the proportion of adult females reproducing, while female productivity can differ between areas and, where food availability cycles, between years (Macdonald & Voigt 1985). Nonetheless, whether litter size increases in a reduced fox population is controversial. No difference in the mean number of litter sizes, by counting placental scars between rabies-endemic and rabies-free areas, has been found (Wandeler *et al.* 1974, Vos 1994). In contrast, Funk (1994) revealed a significant increase in litter size, defined as counted cubs at the den, following a rabies outbreak.

The proportion of barren females and, in particular, the postponement of reproduction by subordinate and younger females (Macdonald 1979, *reviewed in* Cavallini 1996), is thought to be density-dependent (Englund 1980, Macdonald 1980). The red fox social structure varies from monogamous pairs to small to medium-sized groups, while groups consist of a dominant breeding pair and one or more subdominant females (Cavallini 1996, but see Baker *et al.* 1998). Furthermore, Baker *et al.* (2000) revealed a decline in group size following a mange epizootic in an urban fox population. It can thus be assumed that following the first rabies infection most animals, which survived the epizootic, could have indeed reproduced in the following years. In contrast, a significant portion of subordinate and younger females are likely not to have reproduced before 1975 and, in particular, subsequent to the population growth since the mid-1980s (Vos 1995). Despite the broad range of data available for female productivity, in relation to population density, ecological factors and social status, little is known about male reproductive success.

Combining the results of the observed age distribution and the variance of female reproduction in relation to population density and to the rabies epidemic, the average generation time was not constant over time. Therefore, a considerable shorter generation time subsequent to the rabies infection could be expected.

Alongside the observed and expected temporal changes in mortality and reproduction, the rabies epizootic may also have affected dispersal patterns. In this context, an area with a transiently disease-induced high mortality could act as a 'sink', whereas the

'source' is an area with no or little mortality (Artois *et al.* 1990, Zimen 1984). Thus, the rabies-affected population studied should consist of a mixture of resident survivors and predominantly juvenile immigrants (Harris 1977). Furthermore, the overall expected sex ratio should be male-biased based on the assumption that males in red foxes are in general the more dispersive sex (*reviewed in* Trewhella *et al.* 1988, Chapter 3). Although the observed juvenile ratio was high subsequent to the rabies-induced population reduction, the data collected do not allow us to distinguish between immigration and, as previously discussed, changes in mortality rates and reproduction. Nonetheless, the higher proportion of males observed in the mid-1980s might indicate some immigration into the study area.

Population genetics

The DNA extracted from the historic tooth samples was poor in terms of quality (DNA degeneration) and quantity, which further decreased with storage time (Chapter 1). Consequently, one third of all extracts, with a bias towards older samples, was not suitable for microsatellite genotyping due to the estimated insufficient DNA concentration (<5pg/μl, Morin *et al.* 2001; Chapter 1). Furthermore, because of the highly degenerated DNA observed, only loci with a maximum of 170 bps in fragment - size could be amplified by PCR. Thus, the operational range of the ABI Prism® 377 sequencer was limited to less than 100 bps (78–172 bps). Therefore, only between two and three loci could simultaneously be electrophoretically separated and analysed.

Knowledge of the accurate age of each genotyped individual allowed us to assign each sample to its year of birth. This approach was preferred to sorting the samples into years of delivery, because by doing so, changes in genetic diversity could be immediately detected. In contrast, each individual was represented in one annual sample only. Thus, differences in reproductive success across individuals, which can be expected to correlate with sample age, were not considered. Sorting individual samples by age of birth, improved the sample distribution significantly over time, yet resulted in small annual sample sizes.

In contrast to the temporal age distribution, no evidence was found for the alteration of the genetic population structure during the rabies-induced demographic bottleneck and the subsequent population growth. The following three interpretations might help to explain the observed results.

Firstly, because the transmission of rabies in a red fox population is density-dependent, the disease is unable to persist at a given density threshold within a population (Anderson *et al.* 1981). Therefore, a certain number of foxes should have survived rabies. Although the red fox population size in the study area was considerably reduced as revealed by the roadkill records, the effective local population size (N_e), based upon the non-infected individuals by rabies, remained sufficiently large to maintain the pre-rabies genetic diversity. Subsequent to the demographic bottleneck, the high reproductive potential of red foxes and the resulting population recovery prevented further genetic drift over time. Similar results were observed in a natural rabbit population reduced by the rabbit viral haemorraghic disease (Queney *et al.* 2000). Despite the estimated high mortality of 88-99% no loss of genetic diversity was detected following the bottleneck by comparing the genetic diversity over time; this was due to the sufficiently large remnant population size and a fast population recovery (Queney *et al.* 2000).

Secondly, immigration could have prevented the lasting effects of a genetic bottleneck. As previously discussed, the high rabies-induced mortality might have acted as a demographic 'sink'. Thus, dispersing and predominantly juvenile foxes could have moved into the rabies-affected study area following the infection. The importance of immigration for rescue of a small and inbred wolf population *Canis lupus* was reported by Vila *et al.* (2003). Further, the ephemerality of a natural demographic bottleneck, which was caused by a severe winter storm in an insular population of song sparrows *Melospiza melodia,* was demonstrated by Keller *et al.* (2001). While the genetic diversity had declined after the demographic bottleneck, the genetic diversity regained pre-bottleneck levels within three years ($\approx$ one generation) of the crash due to migration (Keller *et al.* 2001). In the present study, historic samples were only available for one year (1978) out of five years subsequent to the rabies-induced population decline. Therefore a potential short-term genetic bottleneck might not have been noticed. However, this is dependent upon the assumption that the rabies epizootic caused a temporal heterogeneous distribution of mortality across the whole region to create demographic 'sinks' and 'sources'. Successful immigration might also be reflected by the observed negative F_{IS} - values during the most significant period of population growth in the mid-1980s.

Thirdly, the red fox is a habitat generalist (Macdonald 1980), with an area-wide distribution in Switzerland up to 2500m altitude (Wandeler 1995). Despite being partially enclosed by two rivers, the examined red fox population might represent only a portion of the regional population rather than an isolated part. Hence, although the rabies epizootic swept throughout the whole region and reduced the red fox density substantially, the regional N_e can be expected to have remained sufficiently large enough to have maintained all the genetic diversity existing before the rabies epizootic. Assuming a continuous red fox population and a spatial genetic structure following an isolation-by-distance pattern (Chapter 3, Chapter 5), dispersal should have obscured local deficits in genetic diversity within a few generations. In fact, the spatial genetic structure of red foxes in Switzerland can be expected to be only moderately differentiated (Chapter 5, but see Wandeler *et al.* 2003a).

Although no clear long-term trends in genetic diversity were detected, variation in annual estimations of H_O, H_E, F_{IS} was found both short-term and longer-term. In particular, annual F_{IS} - estimates varied considerably. Moreover this variation could be observed, when annual estimations were calculated based on samples pooled over three years. This result contradicts therefore studies which inferred general levels of genetic diversity and population inbreeding from temporal point-estimates.

Detecting losses of genetic diversity following a demographic bottleneck by using historic samples proves in general to be difficult. For example, Nielsen *et al.* (1999a) described the temporal population genetics in Atlantic salmon *Salmo salar*, but found the genetic diversity to be unaffected over time. Similar results were found for the European otter *Luttra luttra* (*see* Pertoldi *et al.* 2001) and Scandinavian wolverine *Gulo gulo* (*see* Walker *et al.* 2001). In both studies the historic samples did not show higher levels of genetic variability compared to contemporary samples, despite a significant reduction of population size in both species over the last century. In contrast, declines in genetic variation in the Greater Prairie chicken *Tympanuchus cupido* (*see* Bouzat *et al.* 1998), Mauritius kestrel *Falco punctatus* (*see* Groombridge *et al.* 2000) and sea otter *Enhydra lutris* (*see* Larson *et al.* 2002) were revealed by comparing pre- and post-bottleneck genetic diversity.

The overall European red fox population and the studied population are thought to have experienced long-term population growth due to an increased carrying capacity independent from the recent rabies epizootic (*reviewed in* Chautan *et al.* 2000). Although the rabies-induced effects on the population dynamics and demography are evident in the earlier years following the first infection in 1975, the effects might have been much less evident in the long-term. Although no apparent temporal genetic effect could be revealed in relation to the rabies-induced demographic bottleneck, all four population genetic estimates and in particular the F_{IS} - values showed considerable variation over time (Figure 3). However, red fox social structure is very variable, ranging from a monogamous pair at lower population size to complex family groups at higher densities (Cavallini 1996). Therefore, this variation observed might be caused by the six-fold increase in population size and its effect on the red fox social structure, rather than by the initially expected consequences of the rabies-induced demographic bottleneck.

CHAPTER 5

Density-Dependent Dispersal in a Continuous Red Fox Population with Changing Density.

Abstract

Dispersal and effective population size (N_e) are fundamental parameters of ecological and evolutionary processes. Whilst a growing number of studies have addressed the effects of demographic heterogeneities over time on N_e (*e.g.* bottlenecks), much less is known about such effects on dispersal and the resulting genetic structure within and between populations. In this study, the spatio-temporal genetic structure was assessed for a red fox (*Vulpes vulpes*) population in Switzerland during an estimated two to threefold density increase following a rabies epizootic. Under isolation-by-distance (*IBD*), the balance between gene dispersal and effective population density defines the level of local genetic drift in a continuous population and therefore its spatial genetic structure. Moreover, theoretical and empirical studies predict a negative correlation between dispersal and population density in red foxes. To assess the effects of an increasing density on the spatial genetic structure in a natural population, microsatellite data (nine loci) for three distinct time periods (1971-73; 1982-84, and 2001-03) representing ten to fourteen generations, were collected in a 4189km^2 Alpine area using historic tooth (n = 214) and recent tissue samples (n = 118). Individual samples were collected in topographically distinct sampling sites within the study area. Although allele frequencies between time periods (1971-73 *vs.* 1982-84 and 1982-84 *vs.* 2001-03 were significantly different, the observed level of temporal genetic differentiation was small (F_{ST}: 0.009 ± 0.013 and 0.005 ± 0.007, respectively). Significant *IBD* was revealed when pairwise relatedness and spatial distances between individual samples were compared for the time periods 1982-84 and 2001-03 whilst a lower level of genetic structure was observed for the period 1971-73. Similarly, temporal discrepancies were reflected by global F_{ST} – values calculated across sampling sites for each time period (1971-73: 0.002 ± 0.013; 1982-84: 0.008 ± 0.010; 2001-03: 0.012 ± 0.009). Furthermore, inferring gene dispersal distances for the three sampling periods confirmed the predictions of negative density-dependent dispersal.

Introduction

Effective population size (N_e) and dispersal are important parameters in evolutionary processes (*e.g.* Leblois *et al.* 2003). N_e determines rates of loss or maintenance of genetic variation, selection efficiency, inbreeding and inbreeding depression, while dispersal and the resulting gene flow counteracts local adaptation and genetic drift (*e.g.* Wright 1977, Hartl & Clark 1977). However, both demographic parameters are subject to spatial and in particular temporal heterogeneities and, therefore, are often not constant over space and time. In conservation, demographic bottlenecks are expected to reduce levels of genetic variation (Nei *et al.* 1975) and, if N_e is maintained at a small size over a long period, higher levels of inbreeding may result, which in turn might result in inbreeding depression leading to a reduction in fitness (Keller & Waller 2002). In contrast, dispersal between small populations can increase meta-population size and reduce the effects of inbreeding and loss of genetic variability (*e.g.* Keller *et al.* 2001; Vila *et al.* 2003).

Several population genetic methods allow the estimation of the variance N_e based on neutral genetic markers (*reviewed in* Schwarz *et al.* 1998, Beaumont 2003). One method of inferring demographic history employs population genetic theory that relates the structure of allelic genealogies observed in recent samples to historical changes in N_e (Beaumont 1999, Storz & Beaumont 2002). In addition, N_e of a population can be inferred based on temporal changes of neutral allele frequencies between samples of populations collected at different time intervals (*e.g.* Berthier *et al.* 2002, Wang 2001, Wang & Whitlock 2003, Tallmon *et al.* 2004). In this context, historic samples from museums can serve as a valuable source of reference (Bouzat *et al.* 1998).

It has been noted that the usefulness and practicality of historic samples for population genetic studies are often restricted by inadequate sampling and DNA quality (Nielsen 1999a, Chapter 1). Historic collections were often not conducted for the purpose of a population genetic study and, therefore, often lack adequate individual sampling information (*e.g.* age, sex, accurate data on sampling site) and sample size (Nielsen 1999a, Chapter 1). In addition, DNA degrades over time (*reviewed in* Lindahl 1993, Chapter 1). As a consequence, extracted DNA is not only highly degraded but also

highly diluted and can be contaminated (Chapter 1). Therefore, reliable genotyping from historic samples is particularly difficult (Taberlet *et al.* 1996, Höss 2000, Chapter 1). Despite these issues, the use of archival DNA samples in population genetic studies has increased recently using mitochondrial DNA markers (*e.g.* Pichler & Baker 2000, Matocq & Villablanca 2001) and nuclear DNA markers (Bouzat *et al.* 1998, Nielsen *et al* 1999a, Groombridge *et al.* 2000, Pertoldi *et al.* 2001, Walker *et al.* 2001, Larson *et al.* 2002, Miller & Waits 2003).

Environmental conditions such as habitat quality, social and demographic structures and population density, can induce dispersal of species (*reviewed in* Ims & Hjermann 2001). In particular, several empirical studies suggest that for many species dispersal rate depends on local population density and can be positively or negatively-density dependent (for references see Travis *et al.* 1999). Negative density-dependent effects on dispersal, in which a smaller fraction of individuals disperse at higher density, can be expected in territorial animals (reviewed in Wolff 1997). According to theoretical model territoriality can suppress migration by increasing costs of emigration due to the social fence of aggressive and territorial individuals. In this context, dispersal distances should experience the least resistance and lowest cost and thus should be smaller at higher density (from Wolff 1997).

Several studies have estimated dispersal rates in natural populations based on direct demographic methods (*e.g.* capture-mark-recapture and radio–telemetry; *reviewed in* Bennetts *et al.* 2001) and indirect population genetic methods (*e.g.* Rousset 2001, Chapter 2). However, discrepancies between indirect and direct estimations have often been attributed to the general inadequacy of the assumptions of genetic models such as the Wright-Fisher population model and the violation of the assumption of demographic stability in time and space (Leblois *et al.* 2003, 2004).

Restricted dispersal in space, together with local genetic drift, leads to genetic differentiation with increasing spatial distance as described by the theory of isolation-by-distance (*IBD*; *e.g.* Wright 1943, Rousset 1997). A substantial number of studies assessed *IBD* by comparing the genetic and spatial distance between populations (*e.g.* Slatkin 1993, Rueness *et al.* 2003). More recently, restricted dispersal has also been demonstrated for a number of species in a continuous population using individual

based genetic and geographic data (for animals see: *e.g.* Rousset 2000, Spong & Creel 2001, Sumner *et al.* 2001; Chapter 2; for a review of plants see: Vekemans & Hardy 2004).

Following Wright (1943), models of *IBD* consider 'neighbourhood size' (*NS*) as the basic unit of population structure. Although the biological significance of *NS* is often difficult to assess and even misleading (e.g. Rousset 1997), *NS* is a convenient way to express the balance between genetic drift and gene dispersal (Vekemans & Hardy 2004). In a continuous population *NS* can be calculated as the inverse of the regression slope (*blog*) between genetic and spatial distances (Rousset 1997, 2000). *NS* equals the product of $4\pi D\sigma^2$, where D is the effective population density and σ^2 a measure for gene dispersal, the average squared parent-offspring distance (for details see Chapter 2, Sumner *et al.* 2001). In an growing population (increasing D) but with constant gene dispersal σ, *NS* will increase representing a lower level of spatial genetic differentiation (flatter regression slope). In contrast, *NS* will remain unchanged if a shorter average dispersal distance can keep the product of $D\sigma^2$ constant. Investigating the population genetic structure at a local scale has the additional advantage that mutation processes and the potential non-neutrality of the genetic markers applied have little or no effect on the estimation of the product $D\sigma^2$ (Rousset 2000, Leblois *et al.* 2003). Although some empirical studies have described spatial genetic differentiation across natural populations for different time periods (*e.g.* Nielsen *et al* 1999a, Tessier & Bernatchez 1999, Pertoldi *et al.* 2001), so far and to the best of my knowledge, no study investigated temporal changes in spatial genetic structure within populations.

Here I present the first empirical study which describes the spatial genetic structure of a continuous natural population for different time periods. The study investigated the genetic structure of an increasing red fox population in the Swiss Alps, following the recovery of a rabies epizootic.

With an area-wide distribution of up to 2500m altitude in Switzerland, the red fox is a habitat generalist (Wandeler 1995, Macdonald 1980). For that reason, the red fox represents a good example of a territorial species with a continuous population distribution. By comparing pairwise genetic and spatial distances of individual fox

dyads, *IBD* pattern was found in a red fox population in the Swiss Alps (Chapter 2). Moreover, dispersal was male biased and dispersal was shown being affected by topography (Chapter 2). A review of capture-mark-recapture studies in different habitats demonstrated that red fox dispersal distances is density-dependent, based on a negative correlation found between the recovery distance of tagged foxes and estimated population density (Trewhella *et al.* 1988). However, exceptions from this general rule have also been reported (Funk 1994).

The current silvatic rabies epizootic in Europe started in Poland in 1939, spread westwards and reached Switzerland in 1967 (Macdonald 1980). The red fox is the main vector of this epizootic (Steck & Wandeler 1980). After 1967, rabies swept throughout Switzerland before the disease was successfully eliminated by oral wildlife vaccination in 1999 (Kappeler 1991, Breitenmoser *et al.* 2000, Chapter 3). After the cessation of rabies as a substantial mortality factor, the population density increased. This increase in population density appears to follow a long-term increase of red fox carrying capacity (Breitenmoser *unpublished*, Chautan *et al.* 2000). Throughout the rabies epizootic, the disease was monitored by sampling fox carcasses across Switzerland. Consequently, a large set of post-mortem and epidemiological data along an extensive collection of individual tooth samples were compiled over the last three decades (for details see Chapter 2, Chapter 3). Depending on their initial population density, red fox populations can be severely reduced by rabies (Anderson *et al.* 1981, Bögel *et al.* 1974, Chapter 3). Whilst this reduction of population size and density can change the age structure of a population, the genetic variation might remain unaffected (Chapter 3). Dispersal in foxes affects the rate of the spread of rabies (Wandeler *et al.* 1974). Consequently, research on red fox dispersal has been the subject of several field (reviewed in Chautan *et al.* 2000) and simulation studies (Artois *et al.* 1997, Tischendorf *et al.* 1998).

The objective of this study was to assess the spatial and temporal genetic structure of a Alpine red fox population in Switzerland over three decades following significant changes in population density, induced by the arrival and the eradication of rabies. The genetic structure of a continuous population for three distinct time periods (1971-73, 1982-84 and 2001-03) was assessed based on microsatellite data from historic tooth and recent tissue samples.

Material and Methods

Study area and sampling

The study area was situated in the Eastern Alps of Switzerland (Canton Grisons), identical with the study area from Chapter 2. Unlike in Chapter 2, sampling was restricted to five distinct sites (160 – 693km^2) representing 50.4% of the total study area (GR_{1-4} and GR_6; Figure 1).

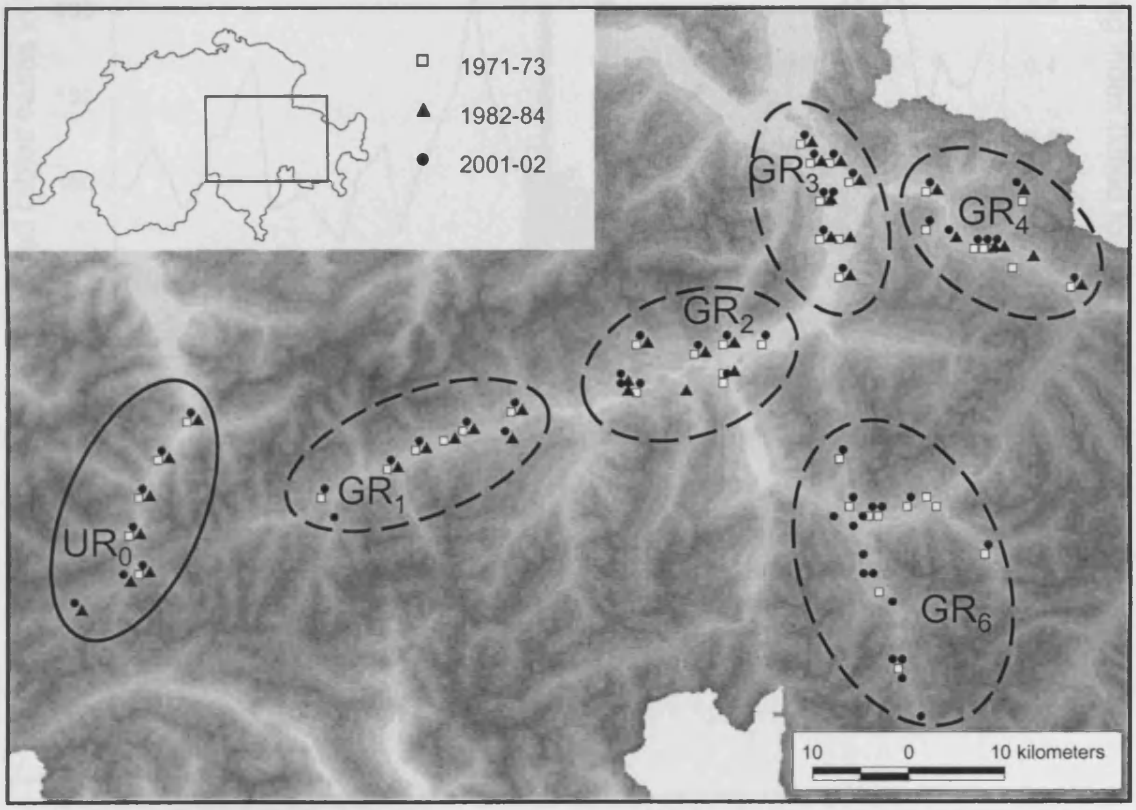

Figure 1 Red fox sampling sites in the study (dash line; Canton Grisons) and control area (solid line; Canton Uri) in Switzerland. Shown are individual sampling locations (boroughs) for three time periods. Grey scale refers gradually to the elevation (low altitude = white; high altitude = dark-grey). Note that one symbol might represent several individuals from the same period and sampling location.

Fox samples were chosen for three short time periods: early rabies (1971-73) late rabies (1982-84) and post rabies (2001-03; Figure 2). Fox samples from 1971-73 and 1982-84 derived from a large collection of historic teeth samples collected throughout Switzerland following the last rabies epizootic (for details see Chapter 1, Chapter 3). No historic samples were available for sampling site GR_6 and time period 1982-84. For

time period 2001-03, local hunting authorities provided tissue samples (Chapter 2). In addition, historic and recent samples for the same time periods were included from an adjacent control area (UR_0; Canton Uri) that was not affected by rabies. Data on sex, individual sampling location (local borough name) and results from rabies virus tests were available for all collected foxes.

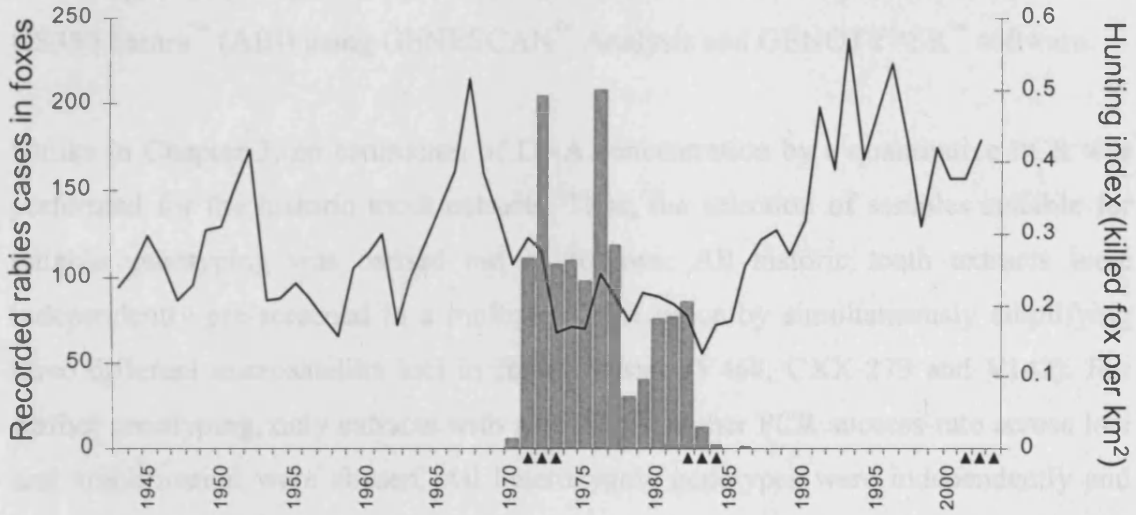

Figure 2 Dynamic of an Alpine red fox population (Canton Grisons; Switzerland) in relation to rabies over the last sixty years. Shown are the annual numbers km^{-2} of foxes killed by hunting (black line) and the total number of recorded rabid foxes (grey bars). Triangles represent years of sampling (time periods). Note that due to the rabies epizootic the hunting pressure was likely higher between the years 1966 and ca. 1980.

Laboratory work

DNA was extracted from historic tooth samples using silica-based spin columns (QIAquick® – PCR purification kits, Qiagen; Yang *et al.* 1998). The whole canine tooth or the tooth crown only was pulverized in a steel mortar. After decalcification (EDTA, 0.5M, pH 8.0) and digestion (proteinase K), DNA was bound to the silica membrane by vacuuming the supernatant through a QIAquick column. Subsequently, the extracted DNA was purified and eluted in 150µL H_20 (for details see Chapter 1). DNA from recent samples (2001-03) was extracted from muscle tissue by using a Wizard® SV96 Genomic DNA extraction kit (PROMEGA) following the manufacturer's protocol and subsequently eluted in 400µL H_20.

Based on previous results of the PCR amplification success-rate of microsatellite loci in historic extracts (Chapter 1 and Chapter 3), four canine (AHT-130, Holmes *et al.* 1995; CXX-156, CXX-279, Ostrander *et al.* 1993; CXX-466, Ostrander *et al.* 1995) and five re-designed red fox specific microsatellites (V142, V374, V402, V468, V502, Chapter 1) were used. Up to three loci were co-amplified using the Qiagen PCR multiplex kit. PCR conditions were identical with the conditions described in Chapter 3. Amplified products were electrophoretically separated using an ABI Prism® 377 DNA sequencer (ABI). Subsequently, allele sizes were scored against the size standard GS350 Tamra™ (ABI) using GENESCAN™ Analysis and GENOTYPER™ software.

Unlike in Chapter 3, no estimation of DNA concentration by a quantitative PCR was performed for the historic tooth extracts. Thus, the selection of samples suitable for reliable genotyping was carried out as follows: All historic tooth extracts were independently pre-screened in a multiplex PCR twice by simultaneously amplifying three different microsatellite loci in fragment size (V468, CXX-279 and V142). For further genotyping, only extracts with a 66% or a higher PCR success-rate across loci and amplification were chosen. All heterozygote genotypes were independently and successfully amplified at least twice. Potential homozygote genotypes for the historic samples from 1971-73 and 1982-84 were successfully amplified for at least four and three times, respectively based on previous experiences (Chapter 1, Chapter 3). Special care was taken to avoid cross-contamination and contamination with contemporary DNA. Consequently, historic DNA extraction and PCR preparation were performed within a spatially isolated laboratory dedicated for working with low-copy DNA.

Population genetic analyses

Single and multi-locus genetic diversity (H_E, Nei 1987; mean ± *SD*, jackknifed over loci) for all sampling sites (GR_{1-4}, GR_6 and UR_0) and for all three time periods (1971-73, 1982-84 and 2001-03) were calculated in GENEPOP, v3.1 (Raymond & Rousset 1995b). Using the same software package, global H_E, observed heterozygosity (H_O), and inbreeding coefficient (F_{IS}; Weir & Cockerham 1984) across all samples (mean ± *SD*, jackknifed across loci) for each of the three time periods were computed. Additionally, single-locus deviation from Hardy-Weinberg equilibrium was tested for the three time periods separately (probability-test in GENEPOP). Subsequently, single-

locus probability-values were combined according Fisher's method (Sokal & Rolf 1995).

The distribution of allele frequencies for each time period across sampling sites (GR_{1-4} and GR_6) was assessed using the genic differentiation test (Raymond & Rousset 1995a) implemented in GENEPOP (Raymond & Rousset 1995b). To estimate the spatial genetic differentiation for each period, global single-locus F_{ST}–values were calculated across sampling sites and subsequently averaged across loci (mean ± *SD*, jackknifed over loci). No historic samples were available for sampling site GR_6 in 1982-84, and therefore analyses were repeated for the time periods 1971-73 and 2001-03 by excluding site GR_6. Finally, single-locus F_{ST}–values for each time period (1971-73 vs. 1982-84; 1971-73 vs. 2001-03; 1982-84 vs. 2001-03) were compared using a Wilcoxon sign-rank test.

The temporal genetic differentiation (F_{ST}) between 1971-73 and 1982-84 and 1982-84 and 2001-03, respectively, was estimated for the whole study area. Pairwise single-locus F_{ST}- values for each of the four sampling sites GR_{1-4} were calculated and subsequently averaged (mean ± *SD*, jackknifed over loci) across sampling sites and loci. In addition, the allelic distribution between 1971-73 and 1982-84 and 1982-84 and 2001-03, respectively, was assessed for each sampling site (GR_{1-4}; genic differentiation test; Raymond & Rousset 1995a). Finally, for each of the two temporal comparisons the probability-values across sampling sites were combined according to Fisher's method (Sokal & Rolf 1995)

Global multi-locus values for H_E, H_O and F_{IS} (mean ± SD, jackknifed over loci) across the three time periods were calculated for the control area (UR) using GENEPOP (Raymond & Rousset 1995b). In addition, allelic distributions (genic differentiation test) and global F_{ST}- values across loci and the three time periods were calculated.

No temporal difference in allelic distribution (genic differentiation test) was revealed for the control area (UR) across sampling periods (see results section). Consequently, all samples from the control area were pooled irrespective of sampling period for subsequent analyses. Pairwise genetic differentiation and allelic distribution (genic differentiation test) was assessed between each sampling site of the study area and the

control area. For each of the three time periods, computed F_{ST} – values were averaged across sampling sites and loci (mean ± *SD*, jackknifed over loci). Single-locus probability-values for the genic differentiation test were combined across sites and loci (Fisher's method). Analyses were repeated for the two periods 1971-73 and 1982-84 by excluding site GR_6.

Finally, critical significance levels were adjusted for multiple testing by Bonferroni corrections (Rice 1989).

Individual based IBD analyses

For the study area (GR_{1-4} and GR_6) and each time period, pairwise spatial distances between individual locations were computed in a Geographic Information System (GIS; ArcView; ESRI 1996a-c)[7]. Because precise data for individual geographic sampling locations for the time period 1971-73 were not available, spatial analyses for all time periods were computed based on administrative community (borough) data. Therefore, the geographic location of an individual sample was approximated by the location (XY-coordinates) of the borough's church tower. Previous results demonstrated that the topographic structure of a landscape could alter the fine-scale spatial genetic structure of red foxes (Chapter 2). Therefore, two different spatial distance matrixes for each of the three time periods were computed. The first matrix represented pairwise Euclidian distances between individuals. The second matrix was computed in a cost-friction analysis. A cost-surface was generated based on an elevation model (MONA, GEOSYS) across the study area and a geographic distance (least cost distance) between individual locations was calculated restricted to areas below an altitude of 1400m. By doing so, pairwise spatial distances between individuals were calculated around rather than across mountain ridges (for details see Chapter 2).

Pairwise relatedness was estimated using Wang's (2002) R_W - estimator. For computing R_W - values, the expected allele frequencies were calculated across all individuals (study area) for each of the three time periods. To account for imprecision in the geographic origin of the samples, pairwise genetic and spatial data for individuals representing the same borough were excluded from further analyses. For

[7] GIS analyses were computed by Fridolin Zimmermann, Bern, CH and PW.

each sampling period, the slope (*blog* - values; inverse of *NS*) was computed. *IBD* was tested by assessing the significance of the regression slope between the genetic matrix and each of the two logarithmic transformed spatial matrixes for each of the three time periods in a Mantel test (10,000 permutations of spatial location). Mean relatedness for five *a priori* defined and by the natural logarithm transformed distance categories (<8956m, 8956m - 16317m, 16318m – 29733m, 29734m – 54176m and >54176m, 1400m-altitude threshold matrix) were computed for each time period. *SE* were calculated by jackknifing over loci. All spatial genetic analyses were performed using the software SPAGEDI (Hardy & Vekemans 2002). Finally, average parent-offspring distances (σ) were assessed for each of the three time periods based on an initial effective population density (*D*) of 0.87 individual*km^{-2} for the sampling period 2001-03 (for details see Chapter 2). To account for lower historic population density, two independent σ estimations were performed for the sampling periods 1971-73 and 1982-84 based on densities of 0.435 and 0.290 individual*km^{-2} representing an assumed population increase of two and three times, respectively.

Results

Microsatellite genotyping

The genomic DNA of 262 and 125 historic tooth samples from the time periods 1971-73 and 1982-84, respectively, was extracted. After pre-screening, 107 (40.8%; 1971-73) and 97 (77.6%; 1982-84) extracts were selected for further genotyping (Table 1). Independent PCR amplifications for hetero- and homozygote genotypes were (± *SD*, jackknifed over loci) 3.88 ± 0.50 and 4.64 ± 0.37 times (1971-73) and 3.04 ± 0.17 and 3.66 ± 0.45 times (1982-84), respectively. Total success-rate of genotyping across loci and all historic samples was 87.3% and varied across loci between 72.5% for CXX-466 and 99.5% for V486 and V502 (Table 2, Table 3). A strong correlation between genotyping success-rate and maximal microsatellite fragment-size was found ($r = -0.98$, $n = 9$). Finally, a total of 118 tissue samples were extracted and subsequently genotyped, of which 90 (76.3%) samples were also used in Chapter 2.

Table 1 Summary of red fox samples from the control area (Canton Uri; Switzerland) and study area (Canton Grisons, Switzerland). The number of extracted historic tooth and tissue samples (N_{EX}) and successfully genotyped samples (N) are shown for all sampling sites and for three time periods.

Sampling site	1971-73 Tooth			1982-84 Tooth			2001-03 Tissue	**Total**
	N_{EX}	N	%	N_{EX}	N	%	N	**N**
Control area								
UR_0	26	16	*61.5*	23	20	*87.0*	19	**55**
Study area								
GR_1	40	15	*37.5*	28	18	*64.3*	20	**53**
GR_2	44	15	*34.1*	25	19	*76.0*	19	**53**
GR_3	52	23	*44.2*	24	21	*87.5*	20	**64**
GR_4	43	18	*41.9*	25	19	*76.0*	20	**57**
GR_6	57	20	*35.1*	-	-	-	20	**40**
Total	**262**	**107**	***40.8***	**125**	**97**	***77.6***	**118**	**322**

Population genetic analyses based on sampling areas

Total number of detected alleles per locus and across all individual samples (study and control area) ranged from seven alleles (V374, V402, CXX-466) to thirteen alleles (V142; mean ± *SD* = 9.22 ± 1.99). Genetic diversity (H_E; mean ± *SD*, jackknifed over loci) across study sites varied between 0.761 ± 0.145 (GR_3, 2001-02) and 0.805 ± 0.080 (GR_1, 1971-73; Table 2) for the study area and between 0.791 ± 0.058 (UR_0, 1982-84) and 0.809 ± 0.050 (UR_0, 2001-2003; Table 3) for the control area.

Overall observed (H_O) and expected heterozygosity (H_E) for the three time periods and the study area were 0.808 ± 0.141 and 0.795 ± 0.092 (1971-73), 0.807 ± 0.169 and 0.800 ± 0.096 (1982-84) and 0.795 ± 0.107 and 0.793 ± 0.098 (2001-03), respectively. Multi-locus F_{IS} – values for the three periods were -0.011 ± 0.079, -0.001 ± 0.115 and –0.002 ± 0.048, respectively (Table 2). No significant deviation from Hardy-Weinberg equilibrium was observed after correcting for multiple testing across loci (Bonferroni correction; $\alpha = 0.05$; k = 9, Sokal & Rolf 1995, Table 2).

Table 2 Measures of genetic diversity for nine microsatellite in red foxes (study area, Canton Grisons; Switzerland) across five sampling sites (GR1 - GR4, GR6) and three time periods. For each of the three periods and sites single-locus estimates of the number of individual genotypes (N_{GT}), genetic diversity (H_E; Nei 1987) are shown. In addition, for each period N_{GT}, H_E, observed heterozygosity (H_O), allelic diversity (A), inbreeding coefficients (F_{IS}; Weir and Cockerham 1984) and p-value for the probability of Hardy-Weinberg deviation across all samples are summarized. The summary statistics shows multi-locus means and *SD* jackknifed over loci.

Microsatellie	GR_1		GR_2		GR_3		GR_4		GR_6		All individual samples						
	N_{GT}	H_E	N_{GT}	H_E	N_{GT}	H_E	N_{GT}	H_E	N_{GT}	H_E	N_{GT}	%	A	H_O	H_E	F_{IS}	P^a
1971-73	n=15		n=15		n=23		n=18		n=20		n=91						
AHT-130	11	0.844	14	0.762	19	0.829	11	0.874	17	0.811	72	*79.1*	9	0.861	0.815	-0.057	0.309
V142	8	0.875	11	0.874	20	0.891	13	0.889	14	0.907	66	*72.5*	13	0.939	0.893	-0.053	0.018
CXX-156	8	0.842	11	0.836	21	0.812	13	0.742	15	0.844	68	*74.7*	10	0.824	0.819	-0.006	0.801
CXX-279	11	0.810	11	0.857	22	0.818	13	0.834	14	0.780	71	*78.0*	10	0.831	0.828	-0.004	0.392
V374	11	0.853	13	0.843	22	0.802	15	0.811	18	0.783	79	*86.8*	6	0.810	0.821	0.014	0.192
V402	14	0.762	15	0.832	23	0.794	18	0.816	20	0.826	90	*98.9*	7	0.811	0.818	0.008	0.276
CXX-466	9	0.745	12	0.743	18	0.773	10	0.747	12	0.685	61	*67.0*	6	0.770	0.734	-0.050	0.209
V486	14	0.868	15	0.814	23	0.788	18	0.822	20	0.829	90	*98.9*	9	0.911	0.828	-0.101	0.389
V502	14	0.646	15	0.639	23	0.572	18	0.592	20	0.603	90	*98.9*	9	0.511	0.603	0.153	0.169
mean	11.1	**0.805**	13.0	**0.800**	21.2	**0.787**	14.3	**0.792**	16.7	**0.785**	76.3	***83.9***	**8.78**	**0.808**	**0.795**	**-0.011**	**0.077**[b]
SD		0.080		0.079		0.102		0.097		0.096			2.31	0.141	0.092	0.079	
1982-84	n=18		n=19		n=21		n=19				n=77						
AHT-130	17	0.783	18	0.835	21	0.829	19	0.791			75	*97.4*	10	0.893	0.820	-0.090	0.186
V142	13	0.868	16	0.897	20	0.868	17	0.875			66	*85.7*	11	0.879	0.882	0.004	0.711
CXX-156	13	0.840	14	0.847	19	0.845	16	0.831			62	*80.5*	11	0.871	0.839	-0.038	0.504
CXX-279	16	0.887	15	0.814	19	0.787	19	0.846			69	*89.6*	10	0.899	0.840	-0.070	0.151
V374	16	0.710	19	0.794	20	0.836	18	0.800			73	*94.8*	7	0.795	0.792	-0.003	0.067
V402	18	0.816	19	0.825	21	0.846	19	0.852			77	*100.0*	7	0.844	0.839	-0.007	0.076
CXX-466	14	0.802	14	0.791	17	0.783	16	0.794			61	*79.2*	7	0.820	0.788	-0.041	0.171
V486	18	0.803	19	0.727	21	0.765	19	0.822			77	*100.0*	9	0.805	0.799	-0.007	0.240
V502	18	0.673	19	0.639	21	0.617	19	0.437			77	*100.0*	7	0.455	0.597	0.240	0.007
mean	15.9	**0.798**	17.0	**0.796**	19.9	**0.797**	18.0	**0.783**			70.8	***91.9***	**8.78**	**0.807**	**0.800**	**-0.001**	**0.007**[b]
SD		0.072		0.080		0.086		0.170					1.80	0.169	0.096	0.115	
2001-2003	n=20		n=19		n=20		n=20		n=20		n=99						
AHT-130	20	0.850	19	0.789	20	0.764	20	0.846	20	0.781	99	*100*	10	0.869	0.810	-0.073	0.514
V142	20	0.872	19	0.896	20	0.876	20	0.873	20	0.878	99	*100*	12	0.919	0.885	-0.039	0.657
CXX-156	20	0.851	19	0.832	20	0.801	20	0.831	20	0.821	99	*100*	9	0.778	0.827	0.060	0.373
CXX-279	20	0.835	19	0.782	20	0.753	20	0.803	20	0.887	99	*100*	9	0.788	0.824	0.044	0.079
V374	20	0.753	19	0.794	20	0.785	20	0.812	20	0.799	99	*100*	6	0.818	0.785	-0.043	0.242
V402	20	0.812	19	0.782	20	0.778	20	0.846	20	0.835	99	*100*	7	0.778	0.819	0.051	0.208
CXX-466	20	0.749	19	0.694	20	0.764	20	0.801	20	0.719	99	*100*	8	0.758	0.755	-0.004	0.399
V486	20	0.799	19	0.851	20	0.874	20	0.779	20	0.856	99	*100*	9	0.869	0.844	-0.030	0.453
V502	20	0.705	19	0.617	20	0.455	20	0.546	20	0.556	99	*100*	8	0.576	0.587	0.019	0.777
mean	20.0	**0.803**	19.0	**0.782**	20.0	**0.761**	20.0	**0.793**	20.0	**0.792**	99.0	***100***	**8.67**	**0.795**	**0.793**	**-0.002**	**0.383**[b]
SD		0.058		0.087		0.145		0.118		0.113			1.81	0.107	0.098	0.048	

[a] p- value (probability –test; Raymond & Rousset 1995b); [b] combined p-value after Fisher's methods

Global deviation (Fisher's method) from Hardy-Weinberg equilibrium was significant for the second time period (X^2 = 36.0, df = 18, p < 0.007; Bonferroni correction: α = 0.05; k = 3; 1982-84), while non-significant deviations were observed for the time period 1971-73 (X^2 = 27.1, df = 18, p = 0.077) and 2001-03 (X^2 = 19.1, df = 18, p = 0.383; Table 2).

Table 3 Measures of genetic diversity of red foxes for the control area (Canton Uri; Switzerland) for three time periods. Shown are single-locus values for nine microsatellite loci of the number of individual genotypes (N_{GT}) and genetic diversity (H_E) for each time period and N_{GT}, H_E, observed heterozygosity (H_O), allelic diversity (A), inbreeding coefficients (F_{IS}) across all samples. The summary statistics shows multi-locus means and *SD* jackknifed over loci.

Microsatellite	1971-73		1982-84		2001-03		All individual samples					
	N_{GT}	H_E	N_{GT}	H_E	N_{GT}	H_E	N_{GT}	%	A	H_O	H_E	F_{IS}
	n=16		n=20		n=19		n=55					
AHT-130	16	0.756	15	0.708	19	0.817	50	*90.9*	8	0.780	0.765	-0.020
V142	14	0.881	11	0.840	19	0.853	44	*80.0*	12	0.886	0.848	-0.045
CXX-156	15	0.828	13	0.871	19	0.842	47	*85.5*	8	0.872	0.850	-0.026
CXX-279	13	0.843	14	0.751	19	0.828	46	*83.6*	9	0.804	0.814	0.012
V374	16	0.802	19	0.808	19	0.795	54	*98.2*	6	0.815	0.802	-0.016
V402	16	0.847	19	0.825	19	0.788	54	*98.2*	7	0.833	0.810	-0.029
CXX-466	12	0.859	14	0.802	19	0.785	45	*81.8*	7	0.822	0.807	-0.019
V486	16	0.774	20	0.803	19	0.862	55	*100.0*	8	0.745	0.819	0.090
V502	16	0.669	20	0.710	19	0.710	55	*100.0*	7	0.691	0.693	0.003
mean	14.9	**0.807**	16.1	**0.791**	19.0	**0.809**	50.0	***90.1***	**8.00**	**0.806**	**0.801**	**-0.006**
SD		0.069		0.058		0.050			1.92	0.063	0.052	0.045

Global test for the spatial genic differentiation across sampling sites revealed a difference in the distribution of allele frequency for the time period 1971 –73 (X^2 = 33.9, df = 18, p = 0.013) across all sampling sites (GR_{1-4} and GR_6); but no genic differentiation was revealed when calculated across four sampling sites (GR_{1-4}) (X^2 = 29.2, df = 18, p = 0.046; Bonferroni correction: α = 0.05; k = 3). The genic differentiation test for the two later time periods was significant across all sampling sites (2001-03: X^2 = 54.9, df = 18, p < 0.0001; GR_{1-4} and GR_6) and across the four selected sites (1982-84: X^2 = 50.3, df = 18, p < 0.0001; 2001-03: X^2 = 52.5, df = 18, p < 0.0001; GR_{1-4}). Global F_{ST} values for the three time periods and across the four sampling sites GR_{1-4} were 0.002 ± 0.013 in 1971-73, 0.008 ± 0.010 in 1982-84 and 0.012 ± 0.009 in 2001-2003, respectively. Across all sampling sites (GR_{1-4} and GR_6), global F_{ST}–values for the time period 1971-73 and 2001-03 were 0.003 ± 0.009 and 0.009 ± 0.008, respectively (Figure 3).

No pairwise differences in the spatial genetic differentiation based on single-locus F_{ST} - values between the three time periods were detected (1971-73 vs. 1982-84: z = -1.186, $p < 0.24$; 1971-73 vs. 2001-03: z = -1.244, $p < 0.21$; 1982-84 vs. 2001-03: z = -0.770, $p < 0.44$; for all test: n = 9; Wilcoxon signed-rank test; Figure 3).

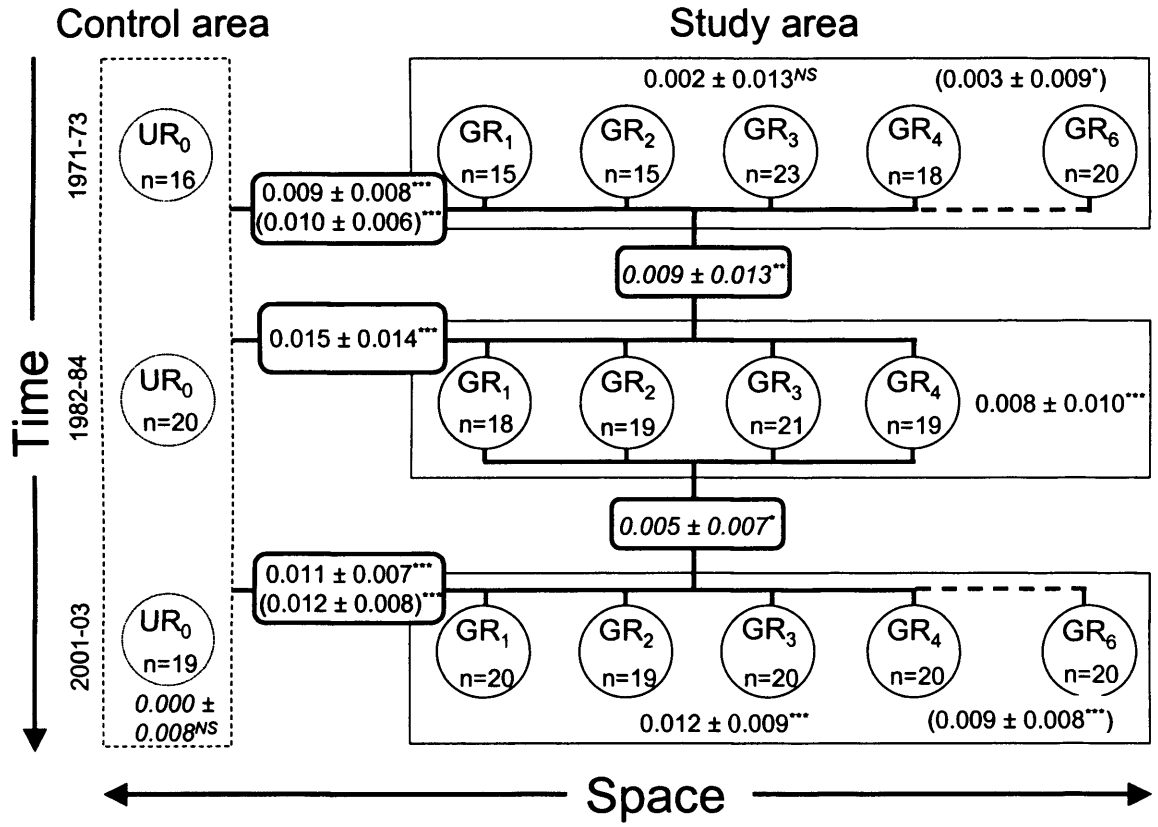

Figure 3 Spatio - temporal population genetic differentiation in red foxes (Canton Uri and Grisons; Switzerland) following a rabies epizootic. Circles represent individual sampling sites. Rounded boxes show temporal and spatial pairwise F_{ST} – values (mean ± *SD*, jackknifed over loci). Numbers within the large square boxes represent global F_{ST} - values. Values in brackets were calculated based on all (incl. GR_6) sampling sites. Differences in allele frequencies were assessed using a genic differentiation test (Raymond & Rousset 1995a; * = $p < 0.05$; ** = $p < 0.01$; *** = $p < 0.001$; ^{NS} = not significant). Thick dashed and solid lines represent the path how genetic differentiation (F_{ST} and genetic differentiation test) were calculated for all sites (dashed) and for all sites exclusive GR_6.

Temporal genetic differentiation, as calculated by pairwise F_{ST}, for the study area (GR_{1-4}) of 1971-73 *vs.* 1982-84 and of 1982-84 *vs.* 2001-03 was 0.008 ± 0.013 and 0.005 ± 0.007, respectively. For both comparisons, the genic differentiation test was significant (1971-73 vs. 1982-84: $X^2 = 38.7$, $df = 18$, $p < 0.003$; 1982-84 vs. 2001-03: $X^2 = 33.4$, $df = 18$, $p < 0.015$; Bonferroni correction: $\alpha < 0.05$, $k = 2$; Figure 3).

For the control area UR, overall H_O, H_E and F_{IS} averaged across loci and across all fox samples were 0.806 ± 0.063, 0.801 ± 0.052 and –0.006 ± 0.045, respectively (Table 3). No genic differentiation over time was detected across the three time periods (X^2 = 17.3, df = 18, $p < 0.503$; F_{ST} = 0.000 ± 0.008).

Finally, the spatial genetic differentiation (F_{ST}) between control area (UR) and the study area (GR_{1-4}) for the three time periods were 0.009 ± 0.008 (1971-73), 0.015 ± 0.014 (1982-84) and 0.011 ± 0.007 (2001-03), respectively. Based on all sampling sites (GR_{1-4} and GR_6), overall F_{ST} for the time period 1971-73 and 2001-03 were 0.010 ± 0.006 and 0.012 ± 0.008. The test for allelic differentiation between the control and the study area for all three time periods was significant based on four sampling sites (GR_{1-4}: 1971-73: X^2 = 84.9; 1982-84: X^2 = 117.2; 2001-03: X^2 = 88.4; all df = 18, $p <$ 0.0001) and based on all sampling sites (GR_{1-4}: and GR_6: 1971-73: X^2 = 103.0; 2001-03: X^2 = 102.6; all df = 18, $p < 0.0001$; Figure 3).

IBD analyses of pairs of individuals

Three historic samples (G196, G197, G335; all 1971-73) with less than four successfully genotyped loci were excluded from subsequent *IBD* analysis. Average Euclidian distances (mean ± *SD*) between individual samples for the three time periods 1971-73, 1982-83 and 2001-03 were 32,043m ± 8,448m, 30,465m ± 6,849m and 35,732m ± 7,094m, respectively. Averaged geographic distances (mean ± *SD*) between individuals computed in GIS and restricted below a 1400m-altitude threshold were 38,755m ± 9,806m (1971-73), 32,410m ± 7,342m (1982-84) and 41,089m ± 9,008m (2001-03).

A total of 119 dyads (3.11%) in 1971-73, 109 dyads (3.73%) in 1982-83 and 103 dyads (2.12%) in 2001-03 were excluded for the Mantel tests, because they were individuals from the same borough (Table 4). No significant correlation between the logarithmic transformed Euclidian distances and the genetic relatedness (R_W) was detected for the time period 1971-73 (*blog* = -0.0012, r^2 = 0.002, p = 0.0747, n = 88; Mantel test). In contrast, significant *IBD* patterns were revealed for the time periods 1982-84 (*blog* = -0.026, r^2 = 0.012, $p < 0.0001$, n = 77) and 2001-03 (*blog* = -0.021, r^2 = 0.010, $p < 0.0001$, n = 99; Mantel test, Table 4, Figure 4a).

Based on the spatial distances computed below a 1400m-altitude threshold, no significant *IBD* was observed for the time period 1971-73 (*blog* = -0.009, r^2 = 0.001, p = 0.1061), while the correlation was significant for 1982-84 (*blog* = -0.026, r^2 = 0.011, $p < 0.0001$) and 2001-03 (*blog* = -0.019, r^2 = 0.009, $p < 0.0001$; Table 4, Figure 4).

Table 4 Results of the isolation-by-distance (*IBD*) analyses in a continuous red fox population for three time periods. Shown are the number of used and excluded dyads, the slope, slope *SE*, intercept and measure of fit (r^2) for the regression computations between spatial distance (*log* transformed) and relatedness (R_W; Wang 2002). Results are shown for two spatial distance matrices: Euclidian distances and spatial distances, which accounted for the topography of the study area given an *a priori* defined altitude threshold of 1400m altitude (see text for details). The significance of the slopes was assessed in a Mantel test.

	1971-73 n=88	1982-84 n=77	2001-03 n=99
Dyads			
all	3828	2926	4851
excluded (same borough)	119	109	103
used	3709	2817	4748
Euclidian			
Slope	-0.0117	-0.0255	-0.0209
SE Slope	0.0497	0.0393	0.0225
Intercept	0.1245	0.2523	0.2175
r^2	0.0018	0.0115	0.0095
p	0.0747	< 0.0001	< 0.0001
1400m altitude threshold			
Slope (*blog*)	-0.0090	-0.0249	-0.0189
SE Slope	0.0476	0.0380	0.0202
Intercept	0.0984	0.2476	0.1989
r^2	0.0013	0.0114	0.0088
p	0.1061	< 0.0001	< 0.0001

The fine-scale spatial genetic structures for five *a priori* defined spatial categories and for the three time periods are shown in Figure 4b. In general, all three sampling periods demonstrated a decrease of average relatedness with each longer spatial category (Table 5). However, a noticeable deviation from *IBD* pattern was revealed for the period 1971-73 in the second spatial category (8956m - 16317m; Figure 4).

Table 5 Summary of the isolation-by-distance (*IBD*) analyses in red foxes for five *a priori* defined spatial distance classes and three time periods. The number of dyads, the percentages that each individual is represented in a given distance class (%partic), the average and *SE* of relatedness (R_W, Wang 2002) are presented for each distance class and time period. Spatial distances were corrected for the topography of the study area. (1400m altitude threshold, see text for details).

	1971-73 n=88		1982-84 n=77		2001-03 n=99	
Spatial distances						
Spatial classes	Dyads	*%partic*	Dyads	*%partic*	Dyads	*%partic*
< 8956m	475	*100*	432	*100*	513	*99*
8956 - 16317m	390	*97.7*	391	*97.4*	430	*100*
16318 - 29733m	683	*100*	702	*100*	765	*100*
29734 - 54176m	1055	*100*	829	*100*	1578	*100*
> 54176m	1225	*86.4*	572	*83.1*	1565	*94.9*
Total	3828		2926		4851	
Relatedness (R_W, Wang 2002)						
Spatial classes	Mean	*SE*	Mean	*SE*	Mean	*SE*
< 8956m	0.022	0.064	0.019	0.091	0.037	0.021
8956 - 16317m	-0.007	0.072	0.021	0.075	0.014	0.049
16318 - 29733m	0.022	0.047	0.021	0.097	0.019	0.033
29734 - 54176m	-0.001	0.059	-0.023	0.087	0.003	0.025
> 54176m	-0.002	0.078	-0.039	0.076	-0.018	0.024
Total	0.005	0.057	-0.004	0.079	0.003	0.012

Based on the computed *blog* - values for each of the three time periods and an assumed two and three-times population increase, the estimated σ - values were 4508m and 5522m for the sampling period 1971 – 73 and 2711m and 3320m for the period 1982-84 (Table 6).

Table 6 Estimates for gene dispersal (σ) and effective population density (D) for three time periods in an increasing red fox population. Shown are values for D, σ, estimated slope between genetic and spatial distance (*blog*) and 'neighbourhood size' (*NS*) for two levels (2 x and 3 x) of assumed population increase in relation to the recent sampling period 2001-2003.

Sampling period	Population increase	D [Individuals *generation/km^2]	*blog*	*NS* [Individuals]	σ [m/generation$^{1/2}$] (% deviation)	
1971 - 73	2 x	0.435	0.0090	111.1	4508	(*204.9*)
	3 x	0.290	0.0090	111.1	5522	(*251.0*)
1982 - 84	2 x	0.435	0.0249	40.2	2711	(*123.2*)
	3 x	0.290	0.0249	40.2	3320	(*150.9*)
2001 - 03	-	0.870*	0.0189	52.9	2200	-

* D for sampling period 2001-03 was calculated based on demographic data; Chapter 2.

Discussion

The main aim of this study was to assess the temporal and spatial population genetic structure in an Alpine red fox population following and after successful eradication of a rabies epizootic. Microsatellite data were collected from historic and recent fox samples spanning three decades. The major result of this chapter is that the observed temporal and spatial genetic population structure is likely to be the consequence of changing population density and dispersal distances. This result is discussed separately for population dynamics, temporal population genetic structure and spatial population genetic structure.

Population dynamics

According to the hunting records of the Canton Grisons, the red fox population experienced a two to three fold increase in estimated density following the eradication of rabies (Figure 2). Although the estimated population density is likely to have reached pre-rabies abundance within a decade after the first and most severe outbreak of the disease, it continued in what appears to be a long-term growth. This trend was consistent with the observation of a generally growing red fox population in Switzerland and Europe (Breitenmoser *unpublished, reviewed in* Chautan *et al.* 2000, Chapter 3). Rabies induced mortality is thought to be density dependent (*e.g.* Anderson *et al.* 1981). Because fox abundance at lower altitude is higher (Wandeler 1995; *e.g.* the Swiss plateau, Chapter 3), the mortality rate following a rabies epizootic can be expected to be considerably lower in Alpine habitat.

Average generation time for red foxes in Switzerland was estimated to be 2.75 years based on recent demographic data and assuming an equal reproduction across age classes and sex (Chapter 2). In addition, the age structure of a red fox population was found to be altered following a rabies epizootic (Chapter 3). Therefore, a shorter generation-time than 2.75 years subsequent to the rabies infection can be expected (Chapter 3). Based on these assumptions, the number of generations between the sampling periods 1971-73 and 1982-84, and 1982-84 and 2001-03 were approximated to be between four to six and six to eight generations, respectively. Overall, the population genetic structure described in this study represented ten to fourteen generations.

Temporal changes in population genetic structure

The observed allele frequencies of the red fox population changed significantly between sampling periods in the study area. The potential causes for the temporal changes in allele frequencies are random genetic drift and migration / immigration.

The red fox population described in the study area is enclosed by topographic features such as Alpine mountain ridges (Figure 1). Dispersal in red foxes is affected by the topography based on both direct, demographic methods (Zimen 1984, Funk 1994) and indirect, genetic methods (Chapter 2). Therefore the examined fox population can be assumed to be partially isolated from its surrounding populations. Nevertheless, based on an estimated N_e of 3907 individuals for the red fox population of the study area (for details see Chapter 2) and a total sampling period of ten to fourteen generations, the effect of random genetic drift might be small. Minor effects of genetic drift for the whole red fox population in the study area were reflected by two marginal pairwise F_{ST} - values computed between the three sampling periods. Despite the assumed smaller number of generations between the sampling periods 1971-73 and 1982-84 versus 1982-84 and 2001-2004, the observed genetic differentiation (F_{ST}) for the earlier time span was slightly higher. Therefore, the N_e in the 1970s and early 1980s during the rabies epizootic can be expected to be lower than in the present.

In contrast to the detected minor temporal differences in allele frequencies, the genetic diversity (estimated by H_O, H_E and A) remained constant over time (Table 2, Table 3). This result confirms previous findings (Chapter 3) where the rabies induced mortality did not affect the genetic diversity. Analogous to the study area, the control area is well surrounded by mountains, but smaller in size (Figure 1). Under these circumstances, a smaller N_e and as a consequence higher random genetic drift in the fox population could be expected. Nonetheless, no significant changes in allele frequencies were observed.

Male biased dispersal in red foxes was revealed in the study area by comparing single-locus F_{IS} - values for males and females (Chapter 2). The observed male biased dispersal not only revealed immigration into the study area but also implies a certain level of genetic differentiation between the study area and its surroundings (Chapter 2,

Goudet *et al.* 2002). The level of genetic differentiation expected between the study area and its surroundings was confirmed by the significant but minor observed genetic differentiation between the study and the control area. Although the control area represents only one of several areas from which potential immigrants might originate from (Figure 2), a similar level of genetic differentiation across the mountain ridges encompassing the study area can be expected.

The observed genetic differentiation between the study and the control area was relatively constant over the three decades examined, although the highest genetic differentiation was calculated for the second time period (1982-84) at the end of the rabies epizootic. It can be speculated whether this result reflects a lower rate of migration across the mountain ridge during rabies or increasing genetic drift due to small effective population size. Recent studies documented higher values of genetic differentiation between populations due to genetic drift (Goodman *et al.* 2001, Keller & Largiader 2003, Johnson *et al.* 2004). The latter found reduced gene flow and increased genetic drift between fragmented populations of the endangered greater prairie-chicken (*Tympanuchus cupido*) by comparing the population genetics based on historic (1950) and recent samples. The higher genetic differentiation observed between the study and control area following the rabies epizootic are therefore consistent with the expected smaller N_e for the study area based on the temporal estimates of genetic differentiation. Finally, these results are supported by the dynamics of the red fox population for the study area as described above.

Spatial genetic structure within the study area

There was clear evidence for spatial genetic structure within the study area. Analyses revealed differences for the three time periods examined. Whilst significant genic differentiation and *IBD* pattern were inferred for the two time periods at the end of the rabies epizootic (1982-84) and for recent times (2001-03), a lower level of spatial genetic structure was found for the first sampling period (1971-73).

Several methodological constraints could have affected the temporal variations of the estimated spatial genetic differentiation. As previously reported, the amount of extracted nuclear DNA from historic tooth samples in this study correlated negatively with storage time (Chapter 2). This resulted in a non-random distribution of

genotyping success among the three time periods (Table 3). The negative relationship between genotyping success-rate and storage time was further reflected by the higher variance of relatedness calculated for the five spatial distance classes in the two earlier time periods (Figure 4b). A similar pattern was revealed for the computed variance of the three global F_{ST}–values (Figure 3). Given the higher sampling variance, in particular for the earliest sampling period (1971-73), the non-random distribution of genotyping success-rate might have therefore affected the power of the applied genic differentiation and Mantel test.

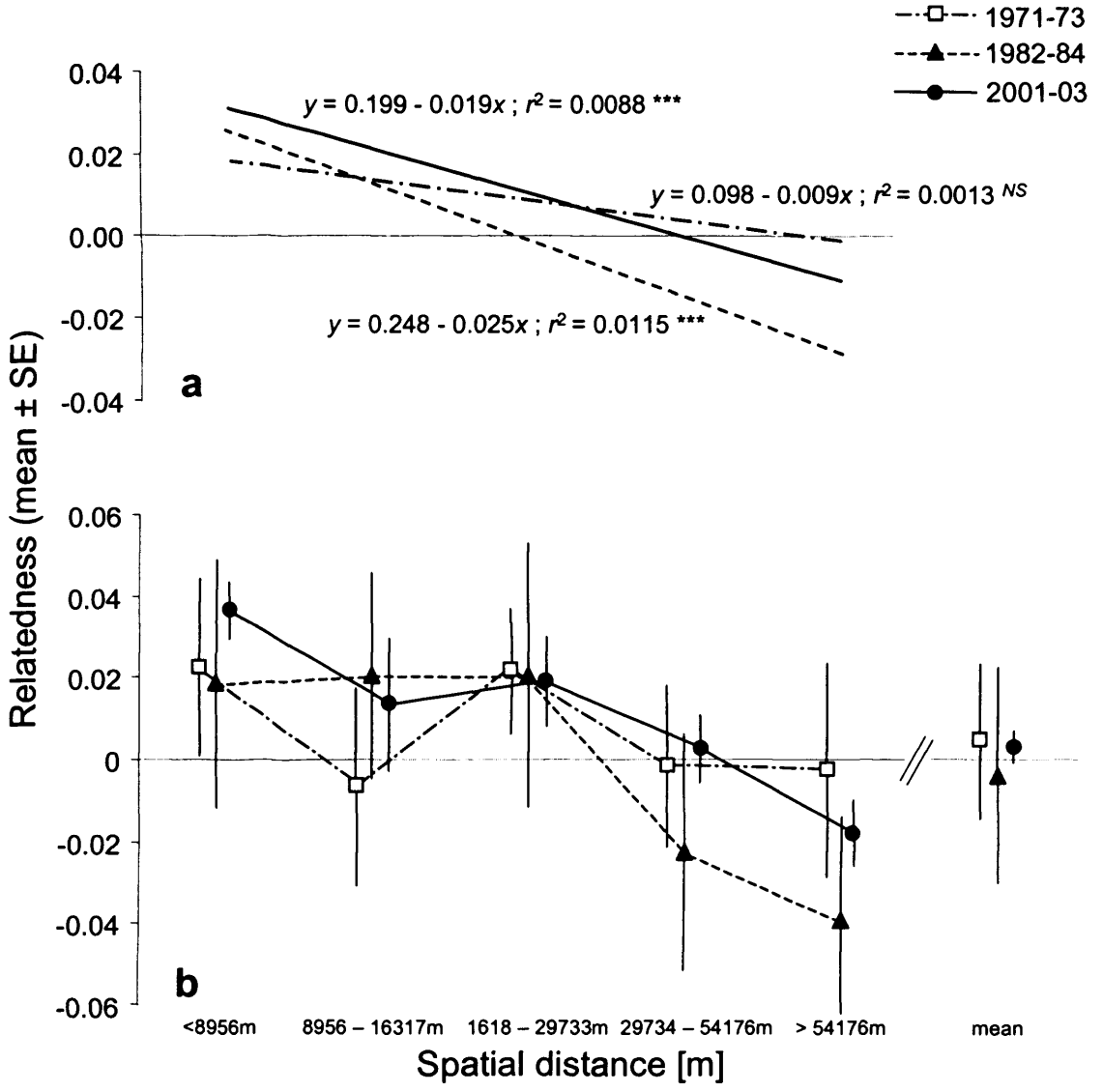

Figure 4 Isolation-by-distance for three time periods in a continuous red fox population (Canton Grisons, Switzerland) following a rabies epizootic. Spatial distances accounted for the topography of the study area. (1400m altitude threshold, see text for details) .a) Regression slopes between pairwise spatial distances and relatedness (R_W; Wang 2002) for three time periods. b) Average (± *SE*; jackknifing over loci) relatedness across all individuals for five log transformed and a priori defined distance categories (*** = $p < 0.001$; ^{NS} = not significant).

In contrast to Chapter 2, the geographic origin for individual samples was based on borough data only and was considerably less accurate. In addition, the clustered distribution of individual samples for each of the three time periods was not optimal for representing a 'continuous' population. Despite this, a significant *IBD* pattern was observed. Furthermore, the estimated slope between geographic and genetic relatedness (R_W) was considerably steeper in this study than compared to Chapter 2. This is not unexpected, based on the previously observed variance of computed single locus slopes in Chapter 2 (Table 3, Appendix) and the selection of microsatellite markers chosen for this study.

The lack of historic samples for site GR_6 for time period 1982-84 and its resulting effect on the estimated parameters was difficult to assess. However, it is interesting to note that by calculating the global F_{ST} for the latest time period (2001-03) and across all sample sites instead for GR_{1-4} only, the genetic differentiation observed was smaller (Figure 3). It can be speculated whether the lack of sampling for site GR_6 could be account for the somehow steeper slope revealed in the *IBD* analyses for the time period 1982-84.

A lower level of local genetic drift was revealed for the sampling period 2001-03 compared to the period 1982-84. This is in accordance with the theory of *IBD*, where a flatter regression slope between genetic and spatial individual distances can be expected given an increasing population density and a constant average dispersal distance. However, there was strong evidence that between 1982 and 2003 average gene dispersal decreased. Further to this, the computed dispersal distance for sampling period 1971-73 was substantially longer than for the sampling period 1982-84. Overall, this result supports the general prediction of a negative correlation between population density and gene dispersal (Table 6) and therefore is in concordance with theoretical models (Wolff 1997) and Trewhella's *et al.* (1988) empirical review of recovery distance and population density in red foxes.

It is important to point out that average gene dispersal distance per generation^{½} σ does not directly relate to average natal dispersal distance. Because measuring gene dispersal in an *IBD* context estimates the average distance a gene disperses in a population per generation, this method does not differentiate between the proportion of

juveniles dispersing and the distance of dispersal. In addition, *IBD* – models can only help to infer dispersal based on successful reproduction of a dispersed individual at its new location (Chapter 2). Finally, correlating red fox N_e with census population size or density is dependent upon the assumption that N_e increases in a linear way with red fox abundance. However, social systems in red foxes are variable, ranging from monogamous pairs to complex family groups, and are further thought to be density-dependent (*review in* Cavallini 1996). Therefore, the number of breeding individuals and thus N_e might have increased at a lower rate over the past three decades than the red fox population density.

Although density is likely to be the most important factor determining the observed discrepancy in spatial genetic structure over time, the rabies epizootic could have indirectly altered dispersal pattern. In this context, the higher mortality induced by rabies could have let to a transiently higher proportion of juveniles to disperse. Rabies is a contact transmitted disease (Macdonald 1980). Therefore, the probability of transmitting the disease between neighbours (closely related animals) can be expected to be more likely than between non-neighbours (less or none-related animals). In addition, rabies can change behaviour to increase contact rates (Blancou *et al.* 1991). As a consequence, this pattern of non-random mortality could decrease the average relatedness within a rabies-affected population compared to the level of relatedness before the outbreak of the disease. All three factors have the potential to bias the slope of the *IBD* analyses towards zero.

It is difficult to balance the importance of density and non-density dependent effects on the temporal changes of gene dispersal. Nonetheless, the rabies-related effects are temporally and spatially limited and thus only partially affect the relationship between spatial and genetic individual distances in an *IBD* context. In addition, the annual number of recorded rabies cases for the study area (Figure 2) was low, even when taking into account the small likelihood of discovery of a rabid fox (Macdonald & Voigt 1985). It can thus be hypothesized that the rabies related factors have less impact than density dependent factors in shaping the spatial genetic structure of the red fox population examined.

This study illustrates the potential of combining historic with recent molecular, demographic and geographic data in studies of individuals within populations over several generations. In the near future individual based *IBD* methods could be combined with genetic methods estimating the variance N_e from observed changes in allele frequencies of temporal samples. In this context, two of the most important demographic parameters, dispersal distance and N_e, could be estimated using genetic information only. The combination of those two methods, alongside non-invasive sampling may help to gain central information on the ecology of endangered and cryptic species.

GENERAL DISCUSSION

This study describes the first investigation into the long-term dynamics of genetic variation in red foxes following a rabies epizootic, based on microsatellites and demographic data to detail population structure over time and space. Using a large data set on historic tooth samples, genetic structure could be analysed over 35 years, representing ten to fourteen generations in red foxes. Furthermore, genetic data were completed with detailed demographic data. Comprehensive discussions of the results of this study are provided in each of the four independent chapters. I will therefore only discuss briefly the general findings of this study and will primarily focus upon further work extending from it.

Historic samples and population genetics

Using historic samples is a convincing and powerful method to infer changes in genetic structure of natural populations over time. Museums can provide reference samples for endangered and fragmented populations (Bouzat *et al.* 1998) and by comparing the genetic structure of historic and recent samples, losses of genetic diversity (*e.g.* Bouzat *et al.* 1998, Groombridge *et al.* 2000) and changes in effective population size (N_e) can be estimated (*e.g.* Miller & Waits 2003). Museum samples can further help to reveal the phylogeny of locally or globally extinct species (*e.g.* Hammond *et al.* 2001). Based on the quality and quantity of sampling and samples accessible, not only the temporal genetic structure can be assessed but also the variance in spatial genetic structure between (Johnson *et al.* 2004) and - as demonstrated in this study – even within populations. Research based on historic samples therefore augments studies that reconstruct demographic history based on the genealogy found in modern samples (*e.g.* Storz & Beaumont 2002).

Almost all genetic studies in historic samples are based on mitochondrial DNA sequences or microsatellite genotype data. Because research on historic and particularly ancient DNA poses substantial technical problems related to the highly degraded and diluted DNA extracted, guidelines for studies based on mitochondrial sequences have been established (Cooper & Poinar 2000). Yet, no such guidelines have been defined for microsatellite studies in historic samples. Whilst the authenticity of historic samples based on microsatellite can be assessed by testing for the

probability of identity (Taberlet & Luikart 1999), the likelihood of genotyping errors due to allelic dropouts and false alleles remains high (Miller & Waits 2003, Chapter 1). The bases for genotyping errors in historic and non-invasive samples are very similar and can be explained by the diminutive concentration of template DNA (Morin *et al.* 2001). This study revealed a strong negative relationship between storage time and nuclear DNA concentration measured in historic samples. Therefore, differences in the distribution of genotyping errors between non-invasive and historic samples can be expected. In addition, microsatellite studies can be biased by null alleles (Callen *et al.* 1993), homoplasy and complex mutation processes (Estoup *et al.* 2002), which have all been shown leading to ambiguity in data analyses (*reviewed in* Balloux & Lugon-Moulin 2002, Dakin & Avis 2004). Under these circumstances, studies using historic samples might benefit in the near future from applying single nucleotide polymorphisms (SNPs). SNP data can be obtained from very small PCR products (<80bps) and therefore are in particular suitable for the highly degraded DNA extracted from ancient and historic samples. Although applications using SNPs can be biased by the selection of an unrepresentative sample of loci (*i.e.* ascertainment bias; Nielsen 2000) genotyping efficiency, data quality and analytical simplicity are superior to microsatellites (Morin *et al.* 2004). Consequently, SNPs could soon become the marker of choice not only in studies based on historic samples but in the broader field of population genetics (Morin *et al.* 2004).

The importance of long-term studies in the ecology and evolution of natural systems has become widely recognized in science, since only long-term research can reveal unpredictable and slow or even cryptic evolutionary processes (Grant & Grant 2002). Long-term studies can help to associate evolutionary changes with environmental factors, rare events such as bottlenecks caused by population crashes and temporally inconsistent processes such as gene flow (Grant & Grant 2002). In this context, temporal genetic data based on neutral or selective genetic markers should significantly help to improve our understanding of the interactions between an organism and its environment over time. So far, most population genetic studies based on historic samples focused on describing the dynamic of genetic variation in relation to changes in population size only (Bouzat *et al.* 1998, Groombridge *et al.* 2000, Nielsen *et al.* 1999b, Chapter 4). Recently, Hadly *et al.* (2004) revealed genetic responses to climate changes in two small and widespread mammalian species

(*Thomomys talpoides* and *Microtus montanus*). By successfully extracting and sequencing small fragments of mitochondrial DNA from fossil records dating back over 2500 years, varying effects on the genetic structure among the two species were revealed. Nonetheless, studies combining environmental (*i.e.* climatic and habitat changes) with genetic data over time are rare.

Population genetics at an individual based level

Assessing the spatial genetic pattern at an individual level rather than using *a priori*-defined discrete populations has been proposed as a new method to infer how geographical and environmental features might shape genetic variation in natural populations (*reviewed in* Manel *et al.* 2003). This approach, landscape genetics, should help to discover discontinuities in population genetic structure by applying statistical tools such as *e.g.* Bayesian clustering methods (Prichard *et al.* 2000) or the Monmonier algorithm (Manni *et al.* 2004). The individual based isolation-by-distance (*IBD*) analysis chosen in my thesis was different in the way that the best fit between a set of geographic and genetic distance matrices was inferred rather than genetic discontinuities explored. Moreover *IBD* analyses can be easily combined with a Geographic Information System (*GIS*) one of the most compelling tools in recent ecological research. However, *IBD* analyses based on microsatellites loci and on an individual level are only applicable in smaller areas due to the high mutation rate of the genetic markers in use (Leblois *et al.* 2003). Recent studies (Sumner *et al.* 2002, Coulon *et al.* 2004, Chapter 3 and 5) demonstrated that *IBD* patterns can be observed in animals, indicating that continuous populations evolving under *IBD* might be rather common. However, if *IBD* can be expected, current clustering methods applied in population genetics are not suitable because they do not account for the continuous change in allele frequencies.

Yang (2004) demonstrated a likelihood-based approach for estimating and testing general *IBD* patterns. This method allows the user to combine several explanatory matrices (*e.g.* environmental and habitat data) within a single analyses. In addition, Yang's (2004) method can test for homogeneity between slopes of different regression lines. For example, differences in the spatial genetic structure observed between populations or within a population but estimated for different time periods (*e.g.* Chapter 5) can be assessed. Moreover, the computed likelihood values for different

IBD models can be used to select the best model based on Akaike's information criterion and for multimodel inference (Burnham & Anderson 2002). By applying this approach across the eleven altitude models in Chapter 3, the best model could be selected based on Akaike weights rather on r^2 - values. Furthermore, model averaging across all altitude models should improve the slope estimation of the regression line between genetic and spatial distances and as a consequence the inferred average gene dispersal distance σ.

Taking into account landscape structure for estimating ecological distances between individuals in a heterogeneous habitat can improve the amount of genetic variation explained in an *IBD* context (Coulon *et al.* 2004, Chapter 3). Although the principle of cost-friction analyses is straightforward, the difficulty is, however, to assess a species-specific friction value for a given type of habitat (*i.e.* the cost for an individual to cross a specific habitat type relative to all other habitat types). *IBD* analyses based on such detailed environmental data therefore require particularly good knowledge of the ecology of the species of interest.

Probably the weakest element of individual based *IBD* analyses, however, is the weak estimation of genetic distance or relatedness between a pair of individuals. In general, relatedness estimators cannot be used to make a precise statement about the degree of relatedness between two individuals (Lynch & Ritland 1999). Although a large proportion of the observed variance between genetic and spatial distances in an *IBD* context is explained by Mendelian segregation, a significant proportion of it can be attributed to the sampling variance of the applied genetic estimators (see Wang 2002 for a discussion on sampling variance in relatedness estimators). Consequently, simulations are needed to gain a better understanding of how these two parameters determine the overall variance in an individual based *IBD* analyses. Furthermore, studies comparing *IBD* in natural populations based on molecular and pedigree data would additionally help to assess the robustness of individual based *IBD* methods.

The temporal and spatial genetic structure observed in this study has been repeatedly discussed in relation to past and recent effective population size (N_e). To date, several statistical methods are available for estimating the variance N_e based on temporal sampling and neutral genetic markers (*e.g.* Wang 2001, Berthier *et al.* 2002, Beaumont

2003). Therefore, N_e estimations could have been applied in this study. However, given the complexity of these methods, such analyses could not be realized within the timeframe of this study.

I can see great potential in the application of genetic N_e estimations for each of the three empirical data chapters. In Chapter 3, the demographic estimation of N_e could be replaced by a genetic estimation of N_e based on temporal changes in allele frequencies between historic samples from 1982-84 (Chapter 5) and modern samples. Preliminary results applying Wang's 2001 pseudo-likelihood approach for the two temporal samples 1982-84 and 2001-03 using twelve microsatellites revealed a harmonic mean of 840 individuals (95%CI: 402 – 4829). This reflects a lower estimate of effective population density (D) and consequently resulted in a larger estimated effective dispersal distance σ of 7'188m (95%CI: 3'044 – 10'376m). By incorporating the computed N_e estimations into the individual based *IBD* analyses, the two important demographic population parameters N_e and dispersal distance can therefore be assessed based on population genetic data only.

Furthermore, changes in red fox population size during the rabies epizootic in Chapter 4 might be inferred using Beaumont's (2003) Bayesian approach for estimation population growth. However, because the expected dispersal rate and average dispersal distance is likely to have changed over time (Chapter 5), the effect of immigration on temporal N_e estimation has to be taken into account. Furthermore, the inferred genetic data on changes in population size could be directly compared with the detailed demographic population records based on annual roadkill and hunting statistics. Finally, the conclusions of Chapter 5 could be substantially improved by replacing the assumed ratio of population growth following rabies (2 and 3 times respectively) with N_e estimations among the three sampling periods.

Population genetics in red foxes and rabies

Infectious diseases can play a central role in natural systems (Altizer *et al.* 2003). In particular diseases can decrease the size of populations substantially and as a consequence can negatively affect the viability of populations (Woodroffe 1999). In this study, long-term effects of rabies induced mortality were revealed in population size and age structure (Chapter 4). However, demographic effects were less apparent

for the observed temporal and spatial genetic population structure. No long-term trends in temporal genetic diversity were observed (Chapter 4). More difficult was the interpretation of the observed dynamic of the fine-scale spatial genetic structure in respect to population density and rabies (Chapter 5). Rabies is though to change the behaviour of infected foxes and consequently will increase contact rates between individuals (Macdonald 1980). For example, a proportion of rabies infected animals, the so called furious form, can become highly mobile (Macdonald & Voigt 1985). Further work could therefore assess the spatial genetic structure based on rabies infected and non-infected foxes within a continuous population.

More generally, the large collection of historic samples analysed here could help to investigate sex-specific migration patterns in red fox populations with changing density. Although male biased dispersal was revealed based on autosomal genetic markers (Chapter 3), the difference in genetic variation revealed between males and females holds only for one generation. However to assess sex-specific spatial genetic patterns more in detail, sex-specific genetic markers (mitochondrial DNA and Y-chromosome) could be applied. In general, a four times smaller N_e for both types of markers compared with nuclear markers can be assumed when reproductive success among sexes is equal (Petit *et al.* 2001). Mitochondrial DNA and Y-chromosome markers are therefore very sensitive to genetic drift and could help to assess more effectively the rabies induced demographic effects on the genetic structure between and within red fox populations.

BIBLIOGRAPHY

Alexander KA, Smith JS, Macharia MJ, King AA (1993) Rabies in the Masai-Mara, Kenya - Preliminary-Report. *Onderstepoort Journal of Veterinary Research* **60**, 411-414.

Allen SH, Sargeant AB (1993) Dispersal patterns of red foxes relative to population density. *Journal of Wildlife Management* **57**, 526-533.

Altizer S, Harvell D, Friedle E (2003) Rapid evolutionary dynamics and disease threats to biodiversity. *Trends in Ecology & Evolution* **18**, 589-596.

Anderson RM, Jackson HC, May RM, Smith ADM (1981) Populations dynamics of fox rabies in Europe. *Nature* **289**, 765-771.

Artois M, Aubert M, Stahl P (1990) Organization spatiale du renard roux (*Vulpes vulpes L., 1758*) en zone d'enzootie de rage en Lorraine. *Revue d'Écologie (La Terre et la Vie)* **45**, 113-134.

Artois M, Langlais M, Suppo C (1997) Simulation of rabies control within an increasing fox population. *Ecological Modelling* **97**, 23-34.

Baker PJ, Funk SM, Bruford MW, Harris S (2004) Polygynandry in a red fox population: implications for the evolution of group living in canids? *Behavioral Ecology* **15**, 766-778.

Baker PJ, Funk SM, Harris S, White PCL (2000) Flexible spatial organisation of urban foxes (*Vulpes vulpes*) before and during an outbreak of sarcoptic mange. *Animal Behaviour* **59**, 127-146.

Baker PJ, Robertson CPJ, Funk SM, Harris S (1998) Potential fitness benefits of group living in the red fox, *Vulpes vulpes*. *Animal Behaviour* **56**, 1411-1424.

Balloux F, Lugon-Moulin N (2002) The estimation of population differentiation with microsatellite markers. *Molecular Ecology* **11**, 155-165.

Beaumont MA (1999) Detecting population expansion and decline using microsatellites. *Genetics* **153**, 2013-2029.

Beaumont MA (2003) Estimation of population growth or decline in genetically monitored populations. *Genetics* **164**, 1139-1160.

Bennetts RE, Nichols JD, Lebreton JD, *et al.* (2001) Methods for estimating dispersal probabilities and related parameters using marked animals. In: *Dispersal* (eds. Clobert J, Danchin E, Dhondt AA, Nichols JD), pp. 3-17. Oxford University Press, Oxford.

Berthier P, Beaumont MA, Cornuet JM, Luikart G (2002) Likelihood-based estimation of the effective population size using temporal changes in allele frequencies: A genealogical approach. *Genetics* **160**, 741-751.

Blancou J, Aubert MFA, Artois M (1991) Fox rabies. In: *The natural history of rabies* (ed. Baer GM), pp. 257-290. CRC Press, Boca Raton.

Bögel K, Arata AA, Moegle H, Knorpp F (1974) Recovery of reduced fox populations in rabies control. *Zentralblatt für Veterinarmedizin* **21**, 401-412.

Bouzat JL, Lewin HA, Paige KN (1998) The ghost of genetic diversity past: Historical DNA analysis of the greater prairie chicken. *American Naturalist* **152**, 1-6.

Breen M, Jouquand S, Renier C, *et al.* (2001) Chromosome-specific single-locus FISH probes allow anchorage of an 1800-marker integrated radiation-hybrid/linkage map of the domestic dog genome to all chromosomes. *Genome Research* **11**, 1784-1795.

Breitenmoser U, Muller U, Kappeler A, Zanoni RG (2000) The final phase of the rabies epizootic in Switzerland. *Schweizer Archiv für Tierheilkunde* **142**, 447-454.

Bruford MW, Beaumont MA (1999) Microsatellites in conservation genetics. In: *Microsatellites* (eds. Goldstein DB, Schlötterer C), pp. 166-180. Oxford University Press, Oxford.

Burnham KP, Anderson DR (2002) *Model selection and multimodel inference - a practical information-theoretic approach*, 2nd edn. Springer, New York.

Caizergues A, Ratti O, Helle P, *et al.* (2003) Population genetic structure of male black grouse (*Tetrao tetrix L.*) in fragmented vs. continuous landscapes. *Molecular Ecology* **12**, 2297-2305.

Callen DF, Thompson AD, Shen Y, *et al.* (1993) Incidence and origin of null alleles in the $(AC)_n$ microsatellite markers. *American Journal of Human Genetics* **52**, 922-927.

Cavallini P (1996) Variation in the social system of the red fox. *Ethology Ecology & Evolution* **8**, 323-342.

Chautan M, Pontier D, Artois M (2000) Role of rabies in recent demographic changes in red fox (Vulpes vulpes) populations in Europe. *Mammalia* **64**, 391-410.

Clobert J, Wolff JO, Nichols JD, Danchin E, Dhondt AA (2001) Introduction. In: *Dispersal* (eds. Clobert J, Danchin E, Dhondt AA, Nichols JD), p. xvii. Oxford University Press, Oxford.

Consuegra S, De Leaniz CG, Serdio A, *et al.* (2002) Mitochondrial DNA variation in pleistocene and modern Atlantic salmon from the Iberian glacial refugium. *Molecular Ecology* **11**, 2037-2048.

Cooper A, Poinar HN (2000) Ancient DNA: Do it right or not at all. *Science* **289**, 1139-1139.

Cornuet JM, Piry S, Luikart G, Estoup A, Solignac M (1999) New methods employing multilocus genotypes to select or exclude populations as origins of individuals. *Genetics* **153**, 1989-2000.

Coulon A, Cosson JF, Angibault JM, *et al.* (2004) Landscape connectivity influences gene flow in a roe deer population inhabiting a fragmented landscape: an individual-based approach. *Molecular Ecology* **13**, 2841-2850.

Crawley MJ (1993) *GLIM for Ecologist* Blackwell Scientific Publications, Oxford.

Dakin EE, Avise JC (2004) Microsatellite null alleles in parentage analysis. *Heredity* **93**, 504-509.

Daszak P, Cunningham AA, Hyatt AD (2000) Wildlife ecology - emerging infectious diseases of wildlife - threats to biodiversity and human health. *Science* **287**, 443-449.

Dickman CR, Pressey RL, Lim L, Parnaby HE (1993) Mammals of particular conservation concern in the Western division of New-South-Wales. *Biological Conservation* **65**, 219-248.

Dieckmann U, O'Hara B, Weisser W (1999) The evolutionary ecology of dispersal. *Trends in Ecology & Evolution* **14**, 88-90.

Ellegren H, Savolainen P, Rosen B (1996) The genetical history of an isolated population of the endangered grey wolf *Canis lupus*: A study of nuclear and mitochondrial polymorphisms. *Philosophical Transactions of the Royal Society of London Series B-Biological Sciences* **351**, 1661-1669.

Englund J (1980) Yearly variations of recovery and dispersal rates of fox cubs tagged in Swedish coniferous forests. In: *The red fox* (ed. Zimen E), pp. 195-208. Dr. W. Junk Publishers, The Hague.

ESRI (1996a): *Using ArcView GIS*: *User manual.* Redlands, California: Environmental Systems Research Institute.

ESRI (1996b): *Using ArcView Spatial Analyst.* Redlands, California: Environmental Systems Research Institute.

ESRI.(1996c): *Using Avenue.* Redlands, California: Environmental Systems Research Institute.

Estoup A, Jarne P, Cornuet JM (2002) Homoplasy and mutation model at microsatellite loci and their consequences for population genetics analysis. *Molecular Ecology* **11**, 1591-1604.

Falush D, Stephens M, Pritchard JK (2003) Inference of population structure using multilocus genotype data: Linked loci and correlated allele frequencies. *Genetics* **164**, 1567-1587.

Fenster CB, Vekemans X, Hardy OJ (2003) Quantifying gene flow from spatial genetic structure data in a metapopulation of *Chamaecrista fasciculata* (Leguminosae). *Evolution* **57**, 995-1007.

Francisco LV, Langston AA, Mellersh CS, Neal CL, Ostrander EA (1996) A class of highly polymorphic tetranucleotide repeats for canine genetic mapping. *Mammalian Genome* **7**, 359-362.

Funk SM (1994) *Zur Dichteabhängigkeit der räumlichen und sozialen Organsiation und der Reproduktion beim Rotfuchs (Vulpes vulpes L.): Eine Studie bei zeitlich und räumlich durch Jagd und Tollwut variierenden Populationsdichten in Südwest- Deutschland und Ost-Frankreich* Thesis, Universität des Saarlandes, Saarbrücken.

Funk SM, Fiorello CV, Cleaveland S, Gompper ME (2001) The role of disease in carnivore ecology and conservation. In: *Carnivore Conservation* (eds. Gittleman JL, Funk SM), pp. 443-466. Cambridge University Press, Cambridge.

Gagneux P, Boesch C, Woodruff DS (1997) Microsatellite scoring errors associated with noninvasive genotyping based on nuclear DNA amplified from shed hair. *Molecular Ecology* **6**, 861-868.

Garnier-Gere P, Dillmann C (1992) A computer-program for testing pairwise linkage disequilibria in subdivided populations. *Journal of Heredity* **83**, 239-239.

Goldstein H (1995) *Multilevel Statistical Models* Edward Arnold, London.

Goodman SJ, Tamate HB, Wilson R, *et al.* (2001) Bottlenecks, drift and differentiation: the population structure and demographic history of sika deer (*Cervus nippon*) in the Japanese archipelago. *Molecular Ecology* **10**, 1357-1370.

Goossens B, Waits LP, Taberlet P (1998) Plucked hair samples as a source of DNA: reliability of dinucleotide microsatellite genotyping. *Molecular Ecology* **7**, 1237-1241.

Goudet J, Perrin N, Waser P (2002) Tests for sex-biased dispersal using bi-parentally inherited genetic markers. *Molecular Ecology* **11**, 1103-1114.

Grant PR, Grant BR (2002) Unpredictable evolution in a 30-year study of Darwin's finches. *Science* **296**, 707-711.

Greenwood AD, Capelli C, Possnert G, Paabo S (1999) Nuclear DNA sequences from late Pleistocene megafauna. *Molecular Biology and Evolution* **16**, 1466-1473.

Greenwood PJ (1980) Maiting system, phylopatry, and dispersal in birds and mammals. *Animal Behaviour* **28**, 1140-1162.

Groombridge JJ, Jones CG, Bruford MW, Nichols RA (2000) 'Ghost' alleles of the Mauritius kestrel. *Nature* **403**, 616-616.

Grue H, Jensen B (1973) Annular structures in canine tooth cementum in red foxes (*Vulpes vulpes L.*) of known age. *Danish Review of Game Biology* **8**, 1-12.

Hadly EA, Ramakrishnan U, Chan YL, *et al.* (2004) Genetic response to climatic change: insights from ancient DNA and phylochronology. *PLoS Biology* **2**, e290.

Hammond RL, Macasero W, Flores B, *et al.* (2001) Phylogenetic reanalysis of the Saudi gazelle and its implications for conservation. *Conservation Biology* **15**, 1123-1133.

Hanski I (1998) Metapopulation dynamics. *Nature* **396**, 41-49.

Hardy OJ, Vekemans X (2002) SPAGEDi: a versatile computer program to analyse spatial genetic structure at the individual or population levels. *Molecular Ecology Notes* **2**, 618-620.

Harris S (1977) Distribution, habitat utilization and age structure of a suburban fox (Vulpes vulpes) population. *Mammal Review* **7**, 25-39.

Harris S, Smith GC (1987) Demography of two urban fox (Vulpes vulpes) populations. *Journal of Applied Ecology* **24**, 75-86.

Harris S, Trewhella WJ (1988) An analysis of some of the factors affecting dispersal in an urban fox (*Vulpes vulpes*) population. *Journal of Applied Ecology* **25**, 409-422.

Hartl DL, Clark AG (1997) *Principels of Population Genetics*, 3rd edn. Sinauer Associates, Inc., Massachusetts.

Heath DD, Busch C, Kelly J, Atagi DY (2002) Temporal change in genetic structure and effective population size in steelhead trout (*Oncorhynchus mykiss*). *Molecular Ecology* **11**, 197-214.

Heuertz M, Vekemans X, Hausman JF, Palada M, Hardy OJ (2003) Estimating seed vs. pollen dispersal from spatial genetic structure in the common ash. *Molecular Ecology* **12**, 2483-2495.

Hofreiter M, Serre D, Poinar HN, Kuch M, Paabo S (2001) Ancient DNA. *Nature Reviews Genetics* **2**, 353-359.

Holmes NG, Dickens HF, Parker HL, *et al.* (1995) 18 Canine microsatellites. *Animal Genetics* **26**, 132-133.

Höss M (2000) Ancient DNA - Neanderthal population genetics. *Nature* **404**, 453-454.

Hummel S, Schultes T, Bramanti B, Herrmann B (1999) Ancient DNA profiling by megaplex amplications. *Electrophoresis* **20**, 1717-1721.

Ims RA, Hjermann DO (2001) Condition-dependent dispersal. In: *Dispersal* (eds. Clobert J, Danchin E, Dhondt AA, Nichols JD), pp. 203-216. Oxford University Press, Oxford.

Johnson DL (1977) Inbreeding in populations with overlapping generations. *Genetics* **87**, 581-591.

Johnson JA, Bellinger MR, Toepfer JE, Dunn P (2004) Temporal changes in allele frequencies and low effective population size in greater prairie-chickens. *Molecular Ecology* **13**, 2617-2630.

Kappeler A (1985) *Untersuchungen zur Altersbestimmung und zur Altersstruktur verschiedener Stichproben am Rotfuchs (Vulpes vulpes L.) in der Schweiz.* MSc, University of Bern.

Kappeler A (1991) *Die orale Immunisierung von Füchsen gegen Tollwut in der Schweiz.* Thesis, University of Bern.

Keller I, Largiader CR (2003) Recent habitat fragmentation caused by major roads leads to reduction of gene flow and loss of genetic variability in ground beetles. *Proceedings of the Royal Society of London Series B-Biological Sciences* **270**, 417-423.

Keller LF, Jeffery KJ, Arcese P, *et al.* (2001) Immigration and the ephemerality of a natural population bottleneck: evidence from molecular markers. *Proceedings of the Royal Society of London Series B-Biological Sciences* **268**, 1387-1394.

Keller LF, Waller DM (2002) Inbreeding effects in wild populations. *Trends in Ecology & Evolution* **17**, 230-241.

Koenig WD, VanVuren D, Hooge PN (1996) Detectability, philopatry, and the distribution of dispersal distances in vertebrates. *Trends in Ecology & Evolution* **11**, 514-517.

Kolb HH (1986) Some Observations on the Home Ranges of Vixens (*Vulpes Vulpes*) in the Suburbs of Edinburgh. *Journal of Zoology* **210**, 636-639.

Lade JA, Murray ND, Marks CA, Robinson NA (1996) Microsatellite differentiation between Phillip island and mainland Australian populations of the red fox *Vulpes vulpes*. *Molecular Ecology* **5**, 81-87.

Lande R (1988) Genetics and demography in biological conservation. *Science* **241**, 1455-1460.

Larson S, Jameson R, Etnier M, Fleming M, Bentzen P (2002) Loss of genetic diversity in sea otters (*Enhydra lutris*) associated with the fur trade of the 18th and 19th centuries. *Molecular Ecology* **11**, 1899-1903.

Leblois R, Estoup A, Rousset F (2003) Influence of mutational and sampling factors on the estimation of demographic parameters in a "continuous" population under isolation by distance. *Molecular Biology and Evolution* **20**, 491-502.

Leblois R, Rousset F, Estoup A (2004) Influence of spatial and temporal heterogeneities on the estimation of demographic parameters in a continuous population using individual microsatellite data. *Genetics* **166**, 1081-1092.

Leblois R, Rousset F, Tikel D, Moritz C, Estoup A (2000) Absence of evidence for isolation by distance in an expanding cane toad (*Bufo marinus*) population: an individual-based analysis of microsatellite genotypes. *Molecular Ecology* **9**, 1905-1909.

Leonard JA, Wayne RK, Cooper A (2000) Population genetics of Ice age brown bears. *Proceedings of the National Academy of Sciences of the United States of America* **97**, 1651-1654.

Lindahl T (1993) Instability and decay of the primary structure of DNA. *Nature* **362**, 709-715.

Lindström E, Andrén H, Angelstam P, *et al.* (1994) Disease reveals the predator: sarcoptic mange, red fox predation, and prey populations. *Ecology* **75**, 1042-1049.

Longford NT (1993) *Random Coefficient Models* Clarendon Press, Oxford.

Luikart G, Cornuet JM (1998) Empirical evaluation of a test for identifying recently bottlenecked populations from allele frequency data. *Conservation Biology* **12**, 228-237.

Lynch M, Ritland K (1999) Estimation of pairwise relatedness with molecular markers. *Genetics* **152**, 1753-1766.

Macdonald DW (1979) 'Helpers' in fox society. *Nature* **282**, 69-71.

Macdonald DW (1980) *Rabies and Wildlife. A biologist's perspective* Oxford University Press, Oxford.

Macdonald DW, Bacon PJ (1982) Fox society, contact rate and rabies epizootiology. *Comparative Immunology, Microbiology and Infectious Diseases* **5**, 247-256.

Macdonald DW, Voigt DR (1985) The biological basis of rabies models. In: *Population Dynamics of Rabies in Wildlife* (ed. Bacon PJ), pp. 71-108. Academic Press, London.

Manel S, Bellemain E, Swenson JE, Francois O (2004) Assumed and inferred spatial structure of populations: the Scandinavian brown bears revisited. *Molecular Ecology* **13**, 1327-1331.

Manel S, Schwartz MK, Luikart G, Taberlet P (2003) Landscape genetics: combining landscape ecology and population genetics. *Trends in Ecology & Evolution* **18**, 189-197.

Manni F, Guerard E, Heyer E (2004) Geographic patterns of (genetic, morphologic, linguistic) variation: how barriers can be detected by using Monmonier's algorithm. *Human Biology* **76**, 173-190.

Matocq MD, Villablanca FX (2001) Low genetic diversity in an endangered species: recent or historic pattern? *Biological Conservation* **98**, 61-68.

May RM (1988) Conservation and disease. *Conservation Biology* **2**, 28-30.

McCallum H (2000) *Population parameters - Estimation for Ecological Models* Blackwell Science, Oxford.

Meldgaard T, Nielsen EE, Loeschcke V (2003) Fragmentation by weirs in a riverine system: A study of genetic variation in time and space among populations of European grayling (*Thymallus thymallus*) in a Danish river system. *Conservation Genetics* **4**, 735-747.

Miller CR, Waits LP (2003) The history of effective population size and genetic diversity in the Yellowstone grizzly (*Ursus arctos*): implications for conservation. *Proceedings of the National Academy of Sciences of the United States of America* **100**, 4334-4339.

Morin PA, Chambers KE, Boesch C, Vigilant L (2001) Quantitative polymerase chain reaction analysis of DNA from noninvasive samples for accurate microsatellite genotyping of wild chimpanzees (*Pan troglodytes verus*). *Molecular Ecology* **10**, 1835-1844.

Morin PA, Luikart G, Wayne RK (2004) SNPs in ecology, evolution and conservation. *Trends in Ecology & Evolution* **19**, 208-216.

Murakami H, Yamamoto Y, Yoshitome K, *et al.* (2000) Forensic study of sex determination using PCR on teeth samples. *Acta Medica Okayama* **54**, 21-32.

Navidi W, Arnheim N, Waterman MS (1992) A multiple-tubes approach for accurate genotyping of very small DNA samples by using PCR - statistical considerations. *American Journal of Human Genetics* **50**, 347-359.

Nei M (1987) *Molecular Evolutionary Genetics* Columbia University Press, New York.

Nei M, Maruyama T, Chakraborty R (1975) The bottleneck effect and genetic variability in populations. *Evolution* **29**, 1-10.

Neigel JE (1997) A comparison of alternative strategies for estimating gene flow from genetic markers. *Annual Review of Ecology and Systematics* **28**, 105-128.

Neigel JE (2002) Is F_{ST} obsolete? *Conservation Genetics* **3**, 167-173.

Nielsen EE, Hansen MM, Loeschcke V (1999a) Genetic variation in time and space: Microsatellite analysis of extinct and extant populations of Atlantic salmon. *Evolution* **53**, 261-268.

Nielsen EE, Hansen MM, Loeschcke V (1999b) Analysis of DNA from old scale samples: technical aspects, applications and perspectives for conservation. *Hereditas* **130**, 265-276.

O'Brien SJ, Evermann JF (1988) Interactive influence of infectious-disease and genetic diversity in natural-populations. *Trends in Ecology & Evolution* **3**, 254-259.

O'Brien SJ, Wildt DE, Goldman D, Merril CR, Bush M (1983) The cheetah is depauperate in genetic-variation. *Science* **221**, 459-462.

Ostrander EA, Mapa FA, Yee M, Rine J (1995) 101 New simple sequence repeat-based markers for the Canine genome. *Mammalian Genome* **6**, 192-195.

Ostrander EA, Sprague GF, Rine J (1993) Identification and characterization of dinucleotide repeat (CA)n markers for genetic-mapping in dog. *Genomics* **16**, 207-213.

Paetkau D, Calvert W, Stirling I, Strobeck C (1995) Microsatellite analysis of population-structure in Canadian Polar bears. *Molecular Ecology* **4**, 347-354.

Peakall R, Ruibal M, Lindenmayer DB (2003) Spatial autocorrelation analysis offers new insights into gene flow in the Australian bush rat, *Rattus fuscipes*. *Evolution* **57**, 1182-1195.

Pertoldi C, Hansen MM, Loeschcke V, *et al.* (2001) Genetic consequences of population decline in the European otter (Lutra lutra): an assessment of microsatellite DNA variation in Danish otters from 1883 to 1993. *Proceedings of the Royal Society of London Series B-Biological Sciences* **268**, 1775-1781.

Petit E, Balloux F, Excoffier L (2002) Mammalian population genetics: why not Y? *Trends in Ecology & Evolution* **17**, 28-33.

Pichler FB, Baker CS (2000) Loss of genetic diversity in the endemic Hector's dolphin due to fisheries-related mortality. *Proceedings of the Royal Society of London Series B-Biological Sciences* **267**, 97-102.

Piechocki R (1979) *Makroskopische Präparationstechnik. Leitfaden für das Sammeln, Präparieren und Konservieren, Teil I, Wirbeltiere*, 3rd edn. Gustave Fischer Verlag, Stuttgart.

Piry S, Alapetite A, Cornuet JM, *et al.* (2004) GENECLASS2: A software for genetic assignment and first-generation migrant detection. *Journal of Heredity* **95**, 536-539.

Pritchard JK, Stephens M, Donnelly P (2000) Inference of population structure using multilocus genotype data. *Genetics* **155**, 945-959.

Prugnolle F, de Meeus T (2002) Inferring sex-biased dispersal from population genetic tools: a review. *Heredity* **88**, 161-165.

Queller DC, Goodnight KF (1989) Estimating relatedness using genetic markers. *Evolution* **43**, 258-275.

Queney G, Ferrand N, Marchandeau S, *et al.* (2000) Absence of a genetic bottleneck in a wild rabbit (*Oryctolagus cuniculus*) population exposed to a severe viral epizootic. *Molecular Ecology* **9**, 1253-1264.

Rasbash J, Browne WJ, Healy M, Cameron B, Charlton C (2000) The MLwiN software package version 1.10. Institute of Education, University of London, London.

Raymond M, Rousset F (1995a) An exact test for population differentiation. *Evolution* **49**, 1280-1283.

Raymond M, Rousset F (1995b) Genepop (Version-1.2) - Population-genetics software for exact tests and ecumenicism. *Journal of Heredity* **86**, 248-249.

Rey N (2002) Cost Distance Matrix, Anthropology and Ecology Departement, Genetics and Biometry Laboratory, University of Geneva (ArcView extension). URL: http://arcscripts.esri.com/details.asp?dbid=11192

Rice WR (1989) Analysing tables of statistical tests. *Evolution* **43**, 223-225.

Robinson NA, Marks CA (2001) Genetic structure and dispersal of red foxes (*Vulpes vulpes*) in urban Melbourne. *Australian Journal of Zoology* **49**, 589-601.

Rosatte RC (2002) Long distance movement by a coyote, *Canis latrans*, and red fox, *Vulpes vulpes*, in Ontario: Implications for disease-spread. *Canadian Field-Naturalist* **116**, 129-131.

Rousset F (1997) Genetic differentiation and estimation of gene flow from *F*-statistics under isolation by distance. *Genetics* **145**, 1219-1228.

Rousset F (2000) Genetic differentiation between individuals. *Journal of Evolutionary Biology* **13**, 58-62.

Rousset F (2001) Genetic approaches to the estimation of dispersal rates. In: *Dispersal* (eds. Clobert J, Danchin E, Dhondt AA, Nichols JD), pp. 18-29. Oxford University Press, Oxford.

Rousset F, Gandon S (2002) Evolution of the distribution of dispersal distance under distance-dependent cost of dispersal. *Journal of Evolutionary Biology* **15**, 515-523.

Rozen S, Skaletsky HJ (2000) Primer3 on the WWW for general users and for biologist programmers. In: *Bioinformatics Methods and Protocols: Methods in Molecular Biology* (eds. Krawetz S, Misener S), pp. 365-386. Humana Press, Totowa, NJ.

Rueness EK, Jorde PE, Hellborg L, *et al.* (2003) Cryptic population structure in a large, mobile mammalian predator: the Scandinavian lynx. *Molecular Ecology* **12**, 2623-2633.

Sacks BN, Brown SK, Ernest HB (2004) Population structure of California coyotes corresponds to habitat-specific breaks and illuminates species history. *Molecular Ecology* **13**, 1265-1275.

Schwartz MK, Tallmon DA, Luikart G (1999) Using genetics to estimate the size of wild populations: many methods, much potential, uncertain utility. *Animal Conservation* **2**, 321-323.

Shapiro B, Sibthorpe D, Rambaut A, *et al.* (2002) Flight of the dodo. *Science* **295**, 1683-1683.

Sillero-Zubiri C, King AA, Macdonald DW (1996) Rabies and mortality in Ethiopian wolves (*Canis simensis*). *Journal of Wildlife Diseases* **32**, 80-86.

Smith GR (1982) Animal-disease and conservation. *Nature* **295**, 16-16.

Smith S, Vigilant L, Morin PA (2002) The effects of sequence length and oligonucleotide mismatches on 5 ' exonuclease assay efficiency. *Nucleic Acids Research* **30**, e111.

Sokal RR, Rohlf FJ (1995) *Biometry*, 3rd edn. W.H. Freeman and Company, New York.

Spong G, Creel S (2001) Deriving dispersal distances from genetic data. *Proceedings of the Royal Society of London Series B-Biological Sciences* **268**, 2571-2574.

Steck F, Wandeler A (1980) The epidemiology of fox rabies in Europe. *Epidemiologic Reviews* **2**, 71-96.

Stöhr K, Meslin FM (1996) Progress and setbacks in the oral immunisation of foxes against rabies in Europe. *Veterinary Record* **139**, 32-35.

Storz JF, Beaumont MA (2002) Testing for genetic evidence of population expansion and contraction: An empirical analysis of microsatellite DNA variation using a hierarchical Bayesian model. *Evolution* **56**, 154-166.

Sugg DW, Chesser RK, Dobson FS, Hoogland JL (1996) Population genetics meets behavioral ecology. *Trends in Ecology & Evolution* **11**, 338-342.

Sumner J, Rousset F, Estoup A, Moritz C (2001) 'Neighbourhood' size, dispersal and density estimates in the prickly forest skink (Gnypetoscincus queenslandiae) using individual genetic and demographic methods. *Molecular Ecology* **10**, 1917-1927.

Swanson BJ, Fuhrmann RT, Crabtree RL (2005) Elevational isolation of red fox populations in the Greater Yellowstone Ecosystem. *Conservation Genetics* **6**, 123-131.

Taberlet P, Griffin S, Goossens B, *et al.* (1996) Reliable genotyping of samples with very low DNA quantities using PCR. *Nucleic Acids Research* **24**, 3189-3194.

Taberlet P, Luikart G (1999) Non-invasive genetic sampling and individual identification. *Biological Journal of the Linnean Society* **68**, 41-55.

Tallmon DA, Luikart G, Beaumont MA (2004) Comparative evaluation of a new effective population size estimator based on approximate Bayesian computation. *Genetics* **167**, 977-988.

Teagle WG (1967) The red fox in the London suburbs. *The London Naturalist* **46**, 44-68.

Tessier N, Bernatchez L (1999) Stability of population structure and genetic diversity across generations assessed by microsatellites among sympatric populations of landlocked Atlantic salmon (*Salmo salar L.*). *Molecular Ecology* **8**, 169-179.

Thompson PM, Goodman S (1997) Direct and indirect estimates of dispersal distances. *Trends in Ecology & Evolution* **12**, 195-196.

Tischendorf L, Thulke HH, Staubach C, *et al.* (1998) Chance and risk of controlling rabies in large-scale and long-term immunized fox populations. *Proceedings of the Royal Society of London Series B-Biological Sciences* **265**, 839-846.

Travis JMJ, Murrell DJ, Dytham C (1999) The evolution of density-dependent dispersal. *Proceedings of the Royal Society of London Series B-Biological Sciences* **266**, 1837-1842.

Trewhella WJ, Harris S (1988) A simulation model of the pattern of dispersal in urban fox (*Vulpes vulpes*) populations and its application for rabies control. *Journal of Applied Ecology* **25**, 435-450.

Trewhella WJ, Harris S, McAllister FE (1988) Dispersal distance, home-range size and population density in the red fox (*Vulpes vulpes*): a quantitaive analysis. *Journal of Applied Ecology* **25**, 423-434.

Valiere N, Berthier P, Mouchiroud D, Pontier D (2002) GEMINI: software for testing the effects of genotyping errors and multitubes approach for individual identification. *Molecular Ecology Notes* **2**, 83-86.

Vekemans X, Hardy OJ (2004) New insights from fine-scale spatial genetic structure analyses in plant populations. *Molecular Ecology* **13**, 921-935.

Vila C, Sundqvist AK, Flagstad O, *et al.* (2003) Rescue of a severely bottlenecked wolf (*Canis lupus*) population by a single immigrant. *Proceedings of the Royal Society of London Series B-Biological Sciences* **270**, 91-97.

Vitasek J (2004) A review of rabies elimination in Europe. *Veterinarni Medicina* **49**, 171-185.

Voigt DR, Macdonald DW (1984) Variation in the spatial and social behaviour of the red fox, *Vulpes vulpes*. *Acta Zoologica Fennica*, 261-265.

Vos AC (1994) Reproductive performance of the Red fox, *Vulpes vulpes*, in Garmisch-Partenkirchen, Germany, 1987-1992. *Zeitschrift für Saugetierkunde - International Journal of Mammalian Biology* **59**, 326-331.

Vrana P, Wheeler W (1992) Individual Organisms as terminal entities - laying the species problem to rest. *Cladistics - the International Journal of the Willi Hennig Society* **8**, 67-72.

Wakelin D, Apanius V (1997) Immune defence: genetic control. In: *Host-Parasite Evolution - General Principles & Avian Models* (eds. Clayton DH, Moore J), pp. 30-58. Oxford University Press, Oxford.

Walker CW, Vila C, Landa A, Linden M, Ellegren H (2001) Genetic variation and population structure in Scandinavian wolverine (*Gulo gulo*) populations. *Molecular Ecology* **10**, 53-63.

Wandeler A (1995) Vulpes vulpes (L., 1758). In: *Säugetiere der Schweiz* (ed. Hausser J), pp. 407-411. Birkhäuser Verlag, Basel.

Wandeler A, Müller J, Wachendörfer G, *et al.* (1974) Rabies in wild carnivores in central Europe. III. Ecology and biology of the fox in relation to control operations. *Zentralblatt für Veterinärmedizin* **21**, 765-773.

Wandeler AI (2000) Oral immunization against rabies: afterthoughts and foresight. *Schweizer Archiv für Tierheilkunde* **142**, 455-462.

Wandeler P, Smith S, Morin PA, Pettifor RA, Funk SM (2003a) Patterns of nuclear DNA degeneration over time-a case study in historic teeth samples. *Molecular Ecology* **12**, 1087-1093.

Wandeler P, Funk SM, Largiader CR, Gloor S, Breitenmoser U (2003b) The city-fox phenomenon: genetic consequences of a recent colonization of urban habitat. *Molecular Ecology* **12**, 647-656.

Wang JL (2001) A pseudo-likelihood method for estimating effective population size from temporally spaced samples. *Genetical Research* **78**, 243-257.

Wang JL (2002) An estimator for pairwise relatedness using molecular markers. *Genetics* **160**, 1203-1215.

Wang JL, Whitlock MC (2003) Estimating effective population size and migration rates from genetic samples over space and time. *Genetics* **163**, 429-446.

Waser PM (1996) Patterns and consequences of dispersal in gregarious carnivores. In: *Carnivore Behavior, Ecology, and Evolution* (ed. Gittleman JL), pp. 267-295. Cornell University Press, Ithaca.

Waser PM, Elliott LF (1991) Dispersal and genetic-structure in kangaroo rats. *Evolution* **45**, 935-943.

Waser PM, Strobeck C (1998) Genetic signatures of interpopulation dispersal. *Trends in Ecology & Evolution* **13**, 43-44.

Weir BS, Cockerham CC (1984) Estimating *F*-statistics for the analysis of population structure. *Evolution* **38**, 1358-1370.

White PCL, Harris S, Smith GC (1995) Fox contact behaviour and rabies spread: a model for the estimation of contact probabilities between urban foxes at different population densities and its implications for rabies control in Britain. *Journal of Applied Ecology* **32**, 693-706.

Wolff JO (1997) Population regulation in mammals: an evolutionary perspective. *Journal of Animal Ecology* **66**, 1-13.

Woodroffe R (1999) Managing disease threats to wild mammals. *Animal Conservation* **2**, 185-193.

Woollard T, Harris S (1990) A behavioural comparision of dispersing and non-dispersing foxes (*Vulpes vulpes*) and an evaluation of some dispersal hypotheses. *Journal of Animal Ecology* **59**, 709-722.

Wright S (1943) Isolation by distance. *Genetics* **28**, 114-138.

Wright S (1946) Isolation by distance under diverse systems of mating. *Genetics*, 39-59.

Wright S (1977) *Evolution and the Genetics of Populations: Experimental Results and Evolutionary Deductions.* The University of Chicago Press, Chicago.

Yang DY, Eng B, Waye JS, Dudar JC, Saunders SR (1998) Technical note: improved DNA extraction from ancient bones using silica-based spin columns. *American Journal of Physical Anthropology* **105**, 539-543.

Yang RC (2004) A likelihood-based approach to estimating and testing for isolation by distance. *Evolution* **58**, 1839-1845.

Young TP (1994) Natural Die-Offs of Large Mammals - Implications for Conservation. *Conservation Biology* **8**, 410-418.

Zanoni RG, Kappeler A, Muller UM, *et al.* (2000) Rabies free status of Switzerland after 30 years of fox rabies. *Schweizer Archiv Für Tierheilkunde* **142**, 423-429.

Zimen E (1982) Tollwut, Fuchs und Mensch. *Die Pirsch* **34**, 352-357,432-435,516-519.

Zimen E (1984) Long range movements of the red fox *Vulpes vulpes L. Acta Zoologica Fennica* **171**, 267-270.

APPENDICES

A1: Demographic N_e estimation in populations with overlapping generations.

To investigate the effective dispersal distance in an isolation-by-distance context in Chapter 2, an estimate of the effective population size (N_e) for the study area was needed. Based on Wright's infinite island model without overlapping generations, N_e was calculated from demographic data assuming constant population size, sex ratio and age distribution. In brief, N_e can be estimated in terms of two matrices specifying the passage of genes between different age groups (and sexes) and the number of individuals in each age group (Equation 10; Johnson 1977). This model was then further simplified by assuming a balanced sex ratio and that the reproductive success for each age group was equal for both sexes. If individuals are retained in the population for n mating seasons, the population can be divided into i age classes if $n \geq i \geq 1$. Because reproduction in red foxes occurs once a year, the unit of time and age classes are based on years. Let N_i be the number of individuals of age class i and p_i be the probability that a gene in a newborn individual came from a parent of age class i. Under these assumptions the effective population size can be derived as

$$\frac{1}{N_e} = \frac{1}{2L}\left[\frac{1}{0.5N_1} + \sum_{i=2}^{n}(0.5q_i)^2\left(\frac{1}{0.5N_i} - \frac{1}{0.5N_{i-1}}\right)\right]$$

where N_1 equals the number of newborn individuals while the generation interval L is given by

$$L = \sum_{i=1}^{n} ip_i = \sum_{i=1}^{n} q_i \,.$$

To calculate N_e, the red fox abundance was assumed to be constant and that mortality was human induced only (hunting or roadkill). Consequently, the average recorded number of foxes killed in the study site in 2001 and 2002 (n = 2412) represents N_1 as the total annual number of newborn individuals. Because accurate age data were not available for this part of Switzerland, the expected age distribution in the study site was derived as follows: First, the total number of adult individuals $\left(\sum_{i=1}^{n} N_i\right)$ was calculated from N_1 given the total ratio of recorded juvenile and adult foxes in the

Swiss rabies data base from 1995 onwards (1:1.343; n=4122). Second, the proportion of adult individuals for each age class i was computed based on the observed age distribution of 160 accurately aged adult individuals from the canton of Aargau collected from 1995 onwards (Table A1, for details see Chapter 3). To account for sampling error in age classes with small samples size (*i.e.* for $i > 3$), the proportion for a given age class i was described using an exponential function ($y = 0.5483e^{-0.44495i}$), which was extrapolated based on the observed age data distribution using S-plus 2000 (Mathsoft). Finally, a second estimate of N_{e_mod} was calculated assuming a 50% reduced reproduction (p_{i_mod}) in age class $i = 1$.

Table A1 Summary of the parameters needed to calculate N_e from demographic data (Johnson 1977). Shown are the age classes i, the expected number of individuals for each class N_i, the probability p_i and p_{i_mod} that a gene in a newborn individual derived from a parent of age class i. and the observed age data for a sample from the Canton of Aargau (for details see text).

Age Class i	N_i *	p_i	$p_{i\ mod}$	Observed data
1	1168	0.360	0.180	73
2	748	0.231	0.296	30
3	480	0.148	0.190	14
4	308	0.095	0.122	12
5	196	0.060	0.077	12
6	126	0.039	0.050	8
7	80	0.025	0.032	7
8	52	0.016	0.021	2
9	34	0.010	0.013	1
10	22	0.007	0.009	1
11	14	0.004	0.006	-
12	8	0.002	0.003	-

A2: Performance of Di - vs. tetranucleotide microsatellite loci under *IBD.*

In Chapter 2, additional analyses revealed a significant difference for the *blog* – values between di – and tetranucleotide microsatellite loci (a_r: $n_{di} = 13$, $m_{tetra} = 4$, $W = 140$, $p < 0.006$; R_W: $W = 99$, $p < 0.05$; Wilcoxon rank sum tests, Table 3). Although there is a significant difference, the reason is not clear. It is likely to be a sampling error, considering the small sample size (n = 4). Therefore, calculations were conducted using the total data set.

Based on dinucleotide loci only, the regression between pairwise genetic distance a_r and relatedness R_W with Euclidian distance remained significant (a_r: $p < 0.0001$, $r^2 = 0.0098$; R_W: *blog* = - 0.0130, $p < 0.0001$, $r^2 = 0.0050$; Mantel test) and further resulted in steeper multilocus regression slopes (a_r: *blog* = 0.0113; R_W: *blog* = - 0.01230). Hence, the overall *blog* value calculated on individual genetic distance (a_r) revealed a smaller *NS* of 88.9 individuals (95% confidence interval = 60.0 – 171.2 individuals) compared with the mean *NS* of 135.1 individuals computed across all seventeen microsatellites. Finally, the computed measure of fit (r^2) for dinucleotide loci between individual genetic and spatial matrices were consistently higher compared to r^2 - values calculated across all loci (*e.g.* a_r for 1400m altitude threshold: $r^2 = 0.016$).

Given the wide range of single locus H_E – values for both tetra – and dinucleotides (Table 2), the dissimilarity between the observed *blog* - values, was unlikely to be caused by differences in mutation rates between the two types of microsatellites as emphasized by Leblois *et al.'s* (2003) simulation study. Furthermore, an unintended swap of individual samples during genotyping of tetranucleotide loci can be ruled out, because both types of micosatellites were co-amplified within the same PCR reaction. Based on the small sample size of loci compared in these analyses, the observed differences between tetra– and dinucleotide loci in relation to *IBD*, should be thus interpreted with caution. Nevertheless, comparing different types of microsatellites in an *IBD* context might help to improve our understanding of the mutation process in microsatellites.